Active Fault Tolerant Control of Livestock Stable Ventilation System

Gholami, Mehdi

Publication date:
2011

Document Version
Early version, also known as pre-print

[Link to publication from Aalborg University](#)

Citation for published version (APA):
Gholami, M. (2011). *Active Fault Tolerant Control of Livestock Stable Ventilation System.*

Mehdi Gholami

Active Fault Tolerant Control of Livestock Stable Ventilation System

AALBORG UNIVERSITY

Active Fault Tolerant Control of Livestock Stable Ventilation Systems
Ph.D. thesis

Contents

Contents

Preface and Acknowledgments

This thesis is submitted as partly fulfillment of the requirement for the Doctor of Philosophy at Center for Embedded Software System (CISS), Automation and Control, Department of Electronic System at Aalborg University, Denmark. The work has been carried out in the period of March 2008 to March 2011 under supervision of Associate Professor Henrik Schiøler and Professor Thomas Bak.

The aim of the thesis is to derive new methodologies for fault detection, isolation, and control reconfiguration in the climate control system of a pig stable such that a comfortable climate environment is satisfied for the animal in normal situation as well as in faulty case.

I am grateful to Henrik Schiøler. He was always available for discussion, and ready to open the problems and discover new ideas. His knowledge and creativity guided me over the project, and helped me toward my achievement. I would also like to thank Thomas Bak. He managed me in the project to improve my English competency, and to cope with the time line of the project.

I would like to thank CISS, Professor Kim Guldstrand Larsen, and Anders Peter Ravn to support my research. Many thanks go to my friends and staff in CISS and the Automation section which provided nice environment for my research.

I would like to thank also Roozbeh Izadi Zamanabadi for helping me to find a relevant research center for my external visit. I was at the Laboratoire d'Automatique, Gnie Informatique et Signal LAGIS - Lille from March 2010 to August 2010. I would like to show my gratitude to professor Vincent Cocquempot who was so kind during my stay at the Lab, and he dedicated much time to discuss the research which undoubtedly was very fruitful to my research achievement.

Many thanks go to my friends specially Mojtaba Tabatabaei-pour, and Hamrid Reza Shaker for their support during my research.

At the end, I feel grateful to my parents who always encouraged and enthused me to determinedly pursue my aim in life, which indeed resulted in my accomplishment.

Abstract

Modern stables and greenhouses are equipped with different components for providing a comfortable climate for animals and plant. A component malfunction may result in loss of production. Therefore, it is desirable to design a control system, which is stable, and is able to provide an acceptable degraded performance even in the faulty case.

In this thesis, we have designed such controllers for climate control systems for live-stock buildings in three steps:

- Deriving a model for the climate control system of a pig-stable.

- Designing a active fault diagnosis (AFD) algorithm for different kinds of fault.

- Designing a fault tolerant control scheme for the climate control system.

In the first step, a conceptual multi-zone model for climate control of a live-stock building is derived. The model is a nonlinear hybrid model. Hybrid systems contain both discrete and continuous components. The parameters of the hybrid model are estimated by a recursive estimation algorithm, the Extended Kalman Filter (EKF), using experimental data which was provided by an equipped laboratory.

Two methods for active fault diagnosis are proposed. The AFD methods excite the system by injecting a so-called excitation input. In both methods, the input is designed off-line based on a sensitivity analysis in order to improve the precision of estimation of parameters associated with faults. Two different algorithm, the EKF and a new adaptive filter, are used to estimate the parameters of the system. The fault is detected and isolated by comparing the nominal parameters with those estimated. The performance of AFD methods depend on model accuracy, hence, the nonlinear model for the climate control of the stable is used.

For the reconfiguration scheme, the nonlinear model is approximated to a piecewise affine (PWA) model. The advantages of PWA modeling for controlling schemes are: most complex industrial systems either show nonlinear behavior or contain both discrete and continuous components which is called hybrid systems. PWA models are a relevant modeling framework for such systems. Some industrial systems may also contain piecewise affine (PWA) components such as dead-zones, saturation, etc or contain piecewise nonlinear models which is the case for the climate control systems of the stables.

Fault tolerant controller (FTC) is based on a switching scheme between a set of predefined passive fault tolerant controller (PFTC). In the FTC part of the thesis, first a passive fault tolerant controller (PFTC) based on state feed-back is proposed for discrete-time PWA systems. only actuator faults are considered. By dissipativity theory and H_∞ analysis, the problem is cast as a set of linear matrix inequalities (LMIs). In the next

contribution, the problem of reconfigurability of PWA systems is evaluated. A system subject to a fault is considered as reconfigurable if it can be stabilized by a state feedback controller and the optimal cost of the performance of the systems is admissible. In the previous methods the input constraints are not included, while due to the physical limitation, the input signal can not have any value. In continuing, a passive fault tolerant controller (PFTC) based on state feedback is proposed to track a reference signal while the control inputs are bounded.

Synopsis

Moderne stalde og drivhuse er udstyret med forskellige komponenter, som skal sikre et komfortabelt klima for dyr og planter. En funktionsfejl på en komponent kan resultere i et tab af produktion. Derfor er det ønskeligt at designe et kontrol system, som er stabilt, og som er i stand til at give en acceptabel ydelse selv i fejlramt tilstand.

I denne afhandling har vi designet sådanne kontrolenheder til klima kontrol systemer til bygninger med husdyrhold i tre trin:

- Udlede en model for klima kontrol systemet til en svinestald.

- Designe en aktiv fejl diagnose (AFD) algoritme til forskellige typer af fejl.

- Designe et fejl tolerant kontrol system til klima kontrol systemet.

I første trin bliver en konceptuel multi-zone model til klima kontrol af en bygning med husdyrhold udledt. Modellen er en ulineær hybrid model. Hybride systemer indeholder både diskrete og kontinuerlige bestanddele. Parametrene i den hybride model er estimeret med en rekursiv estimerings algoritme, et Extended Kalman Filter (EKF), ved brug af empiriske data fra en laboratorie opstilling.

To metoder til aktiv fejl diagnose foreslås. Disse AFD metoder eksiterer systemet ved at påtrykke et såkaldt eksiterings input. I begge metoder er inputtet designet off-line baseret på en sensitivitets analyse for at forbedre præcisionen af estimeringen af parametrene forbundet med funktionsfejl. To forskellige metoder, EKF og et nyt adaptivt filter, er anvendt til at estimere systemets parametre. Funktionsfejlen er detekteret og isoleret ved at sammenligne nominelle parametre med de estimerede. Ydelsen af AFD metoderne afhænger af modellens nøjagtighed, derfor anvendes den ulineære model af staldens klima kontrol.

Til brug i rekonfigurations systemet bliver den ulineære model approximeret med en stykvis affin (PWA) model. Fordelene ved PWA modellering i kontrol systemer er: de fleste komplekse industrielle systemer udviser enten ulineære egenskaber eller indeholder både diskrete og kontinuerlige bestanddele, også kaldet hybride systemer. PWA modeller er et relevant modellerings regi for disse systemer. Visse industrielle systemer kan også indeholde stykvis affine (PWA) bestanddele sådan som dead-zones, saturation, osv, eller indeholde stykvis ulineære modeller, hvilket er tilfældet med kontrol systemet til staldene.

Det fejl tolerante kontrol system (FTC) er baseret på skift mellem et sæt af prædefinerede passive fejl tolerante kontrol systemer (PFTC). I FTC delen af afhandlingen bliver først et passivt fejl tolerant kontrol system (PFTC) baseret på tilstands tilbage kobling foreslået for diskret tids PWA systemer. Kun fejl på aktuatorer bliver betragtet. Ved hjælp

af dissipativitets teori og H_∞ analyse bliver problemet formuleret som et sæt lineære matrix uligheder (LMIs). I det næste bidrag bliver problemet med rekonfigurerbarhed af PWA systemer evalueret. Et system udsat for funktionsfejl er anset som værende rekonfigurerbart hvis det kan stabiliseres med et tilstands tilbagekoblings kontrol system og den optimale omkostning påsystemets ydelse er acceptabel. I de foregående metoder er begrænsninger påinputtet ikke inkluderet, pågrund af fysiske begræsninger, kan input signalet ikke antage alle værdier. Fremadrettet foreslås et passivt fejl tolerant kontrol system (PFTC) baseret påtilstands tilbagekobling, til at følge et reference signal mens kontrol inputs er begrænsede.

1 | Introduction

1.1 Motivation

The indoor climate of livestock buildings and greenhouses is of crucial importance for the well being of animals and plants, and thus for farming efficient production. The comfortable climate livestock building is the one that is closed, insulated and operated in a way that keeps inside temperatures relevant for the animal and independent of outside temperature. These requirements are provided by climate control systems, ventilation systems. In fact, a good climate control system must:

- Provide fresh air for respiration needs of animals.

- Control the moisture build-up within the structure.

- circulate fresh air to dilute any airborne disease organisms produced within the housing unit.

- Control and moderate the temperature.

To provide these provisions, the air exchange should have some optimum rate. In the modern stables, the climate control systems provide a convenient fresh air exchange with an optimum rate.

This modernization sometimes causes contradictory results, for example malfunction behavior of a component in the system may result in degradation of overall performance of the system or result in loss of system reliability or safety. In more details, malfunction of a component of the ventilation system may result in suffering of animals. Sometimes, it may lead to catastrophic consequence, such as the death of animals.

Also all European countries have implemented laws and regulations that aim to ensure that mechanical climate control systems must have backup systems ensuring ventilation is adequate to maintain animal health and welfare even in the case of failures. The regulations also require alarm systems and alerts of system failure. Air circulation, dust levels, temperature, relative humidity and concentration of gases are to be maintained at a level which is not harmful to animals. Therefore, it is desirable to develop the climate control systems such that they are capable of tolerating component malfunctions while still maintaining desirable performance and stability properties. These control systems are named fault tolerant control systems. Fault tolerant control (FTC) is divided generally into passive (PFTC) and active (AFTC) approaches. In AFTC, the control structure is changed with respect to the information provided by a fault detection and isolation (FDI) scheme.

As in [BKLS06], in general, AFTC systems are divided into three layers. The first layer is related to the control loop, the second layer corresponds to the FDI and accommodation scheme, and the last layer corresponds to the supervisory system. In PFTC, there is no FDI or supervisor layer. In this technique, the control laws are redesigned and fixed such that the control system is capable of tolerating a set of known faults. In fact, the fault is assumed as an external disturbance to the system, and the control system is designed to be robust against such disturbances.

Due to no on-line fault detection, the PFTC has less computation efforts. However this technique has some disadvantages:

- The system is made robust to very restricted subset of the possible faults, perhaps when a fault has a small effect on the system.

- In order to make the system insensitive to certain faults, the nominal performance of the system must be degraded. According to rare occurrence of faults, it is not reasonable to considerably degrade the fault-free performance of the system.

As is obvious from the definition, the performance of AFTC systems is related to the fault diagnosis scheme which detects and isolates the faults. Fault detection and isolation (diagnosis) means observing the input output of the system and distinguishing if a problem has occurred and what is its exact cause and where is the location of the problem. In general, there are two methods for fault diagnosis. Passive and active, the first one does not act upon the system, and it is based on monitoring input and output set of the system. In contrary with passive methods, active fault diagnosis (AFD) acts upon the system with exerting an auxiliary signal to the system. The reason for excitation is to observe the faults which are hidden during the normal operation of the system or to isolate the faults more precisely and faster. For example, the stable and greenhouse systems have a slow dynamic and there is a long delay to observe the existence of a fault in the systems. This fact may yield catastrophic results when a failure component is urgently required. Model based AFD is preferred due to fault or failure detection is reliant on comparing the faulty system with the fault-free model. In general, there are two methods for modeling. The first one relies on analyzing the input and output data (black box modeling) and the second one is mathematical modeling which uses physical laws of the system (white box modeling). There is actually also an other modeling method which is called gray-box models, and it is combination of the two previous methods.

In the large scale stables, the indoor climate is incompletely mixed and the system outputs such as temperature, humidity, etc change along the stable. This fact fostered the idea of multi-zone climate modeling. Where, the indoor space of the stable is conceptually divided into multi-zones. This modeling framework is called multi-zone modeling.

As it was mentioned before, the performance of AFD methods depend on model accuracy and small improvement on an absolute linear scale may reduce the detection error rate by orders of magnitude. Hence, the nonlinear model for the climate control of the stable is used for AFD method. However, for the reconfiguration scheme, the nonlinear model is approximated to piecewise affine (PWA) model. The advantages of PWA modeling for controlling scheme are given as follows:

- Standard control designed tools are restricted to the model domain. Also, control designs allow for less precise model.

- Most complex industrial systems either show nonlinear behavior or contain both discrete and continuous components which called hybrid systems. PWA models are a relevant modeling framework for such systems.

- Some industrial systems may also contain piecewise affine (PWA) components such as dead-zones, saturation, etc or contain piecewise nonlinear model such as climate control systems of the stables.

1.2 State of the Art and Background

1.2.1 Indoor Climate Control of the Stables

The quality of the indoor climate of the live-stock building plays a crucial role on breeding, well-being of the animals and also improving the farming productions. Poor climate condition may result in animals suffering, less weight and morality problems. It is common to regulate the temperature and humidity to control the quality of indoor climate of the stables. However, there are different parameters which affect the climate, for example, the content of gases in the air which are produced by the animals, or other factors inside the stable, such as ammonia, hydrogen sulphide and carbon monoxide. High density of these gases have lethal influence on animals and may suffocate them. A schematic of the control algorithm for providing a convenient climate for the stable is shown in Fig. 1.1. The control system measures the indoor temperature and humidity and regulates the ventilation system such that temperature and humidity are sufficiently close to a reference points. The value of the reference is assumed as a prior knowledge about the stable, which is changed with respect to the season. Regulation of temperature and humidity depends on a broad range of internal and external elements which make that a complex problem. For example, the ambient temperature, humidity and wind vary with a large magnitude, which make a substantial disturbance on the control system. Sometimes different types of failure occur on sensors, actuators and components of the system.

1.2.2 Ventilation Systems

There are many different kinds of ventilation systems, and their application depend on number, type of live-stock, location of the stable and the type of the live-stock building. Ventilation systems provide a comfortable environment inside the stable from the thermal and the quality of the air point of view. Ventilation systems are divided into three categories which have their pros and cons: In normal ventilation systems, the natural driving forces such as wind effects and thermal buoyancy are used to force fresh air from outside the building circulate inside. The performance of the system relies on the architecture of the building and natural factors, such as ambient temperature and humidity and the season. In more details, in summer, it is hard to provide a thermal comfort inside the stable, and it needs to open wide windows to cool the indoor air and remove the high rate of humidity. With a large chimney, it is also possible to create more kinetic energy and consequently to exchange more air.

Mechanical ventilation systems are not concerned about the natural factors and building architecture. In fact, it is possible to construct the building and then install the ventilation systems. This system which provide low pressure inside the building in comparison
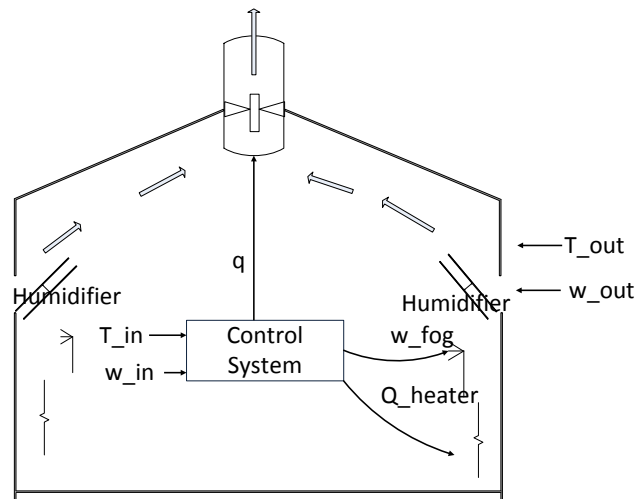
Figure 1.1: General schematic of a control algorithm for providing a convenient climate in a stable.

with the outside lets the air come in from inlets and go out through the outlets. These systems consume considerable amount of the overall electrical energy in Denmark.

It is more useful to combine both previous ventilation systems, and utilize one or both of them with respect to seasons, individual days and the external environment. These systems are assumed as hybrid ventilation systems. The hybrid systems contain both type of ventilation systems and switch automatically between them in order to create a convenient climate inside the building, and at same time use an optimal energy [Per2006]. Different ventilation systems are shown in Fig. 1.2. A key factor to use them is their location and the type of live-stock. In Danish mechanical ventilation systems of pig stable, wall inlets are the most common type of ventilation systems [Jes07].

1.2.3 Modeling of the Ventilation Systems

Overall, there are two methods for modeling. The first one relies on mathematical modeling, where the classical conservation laws of physics such as heat or mass transfer laws are used to derive a relevant model. Basically, these models are sophisticated and accurate for simulation; however, their complexity is an obstacle for control applications. The second one, which leads to simpler model, is based on statistics or data. In fact, the model is derived by analyzing the input and output data. This modeling method is meaningless in physics. In [CCR97], it is discussed how to perform a dynamic temperature modeling based on input and output data. In [SPP00], a steady state indoor climate model for pig stable is presented. [JSB06],[WSH08] shows a third method which is a combination of the two main ideas such that at first physical laws is utilized to derive a model and thereafter its parameters are estimated by analyzing the input and output data. This is known as gray box modeling in the literature [LHD97].
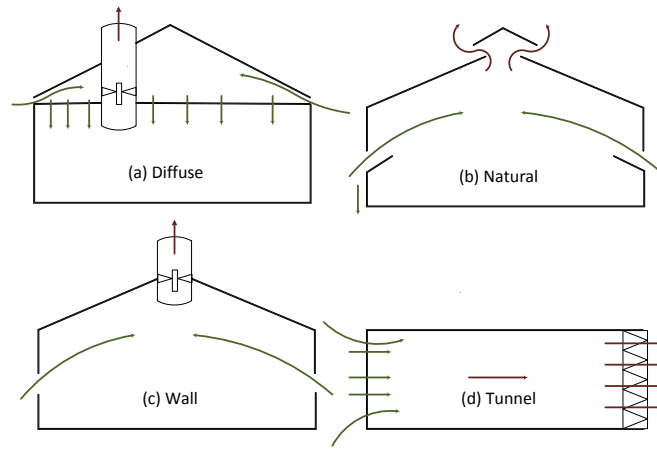
Figure 1.2: Figures of different types of ventilation systems.

There is other modeling classification for climate control systems of the stable besides the previous modeling framework. This classification consists of single-zone and multi-zone modeling. In single zone modeling, it is assumed that the indoor climate is completely mixed and there is no gradient for the air parameters. In fact, the average of temperature and humidity from the sensors are considered as temperature or humidity of the stable as in Fig 1.3. While in the large-scale stables, the indoor air is incompletely mixed and there is a gradient on the temperature and humidity over the stable. To redeem this problem, it is assumed that the inside space of the stables is conceptually divided into multi-zone. Each zone is actuated separately and can have a different set point. Multi-zone modeling let a failure actuator or sensor only affects its own zone when it yields to easier fault detection and also fault tolerant. For example, when a temperature of one zone is quite different from the adjacent zone, it shows a malfunction behavior on the component of the related zone. Figure 1.4 illustrates the general schematic of multi-zone modeling. For such modeling framework, it is referred to [JVBZD+04] and [CFN+00] where models separate into non-interacting [JVBZD+04] or interacting zone models [CFN+00].

1.2.4 Fault Detection

A fault is an unexpected change in components of a system, or is an event, which result in degradation of performance of the system, or cause the system not to satisfy its purpose, such as a leakage in a pipe, sticking an actuator etc. It is possible to prevent a fault from contributing to a severe consequence, but a failure is assumed as complete breakdown of system component or function.

Classification of faults

- **Parameter changes in a model:** parameter fault is occurred when a disturbance from the environment enters the system. For example, the change in the heat transfer coefficient due to fouling in a heat exchange as in Fig. 1.5.
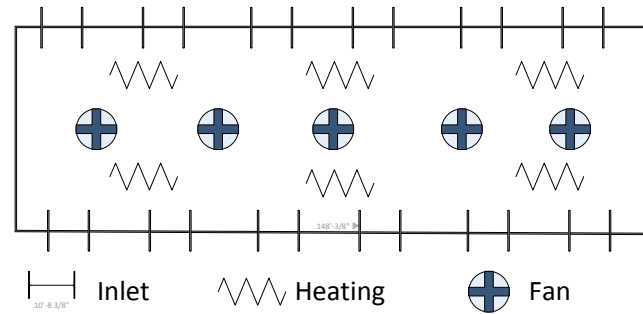
Figure 1.3: General top view of a stable.
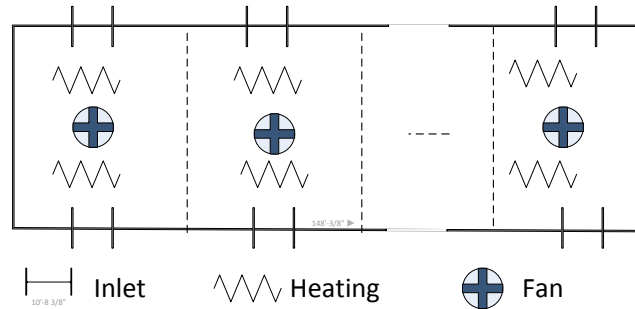
Figure 1.4: General top view of a nulti-zone stable.

- **Structural changes:** structure fault is happened due to fault in the components of the system, such as failure of a controller.

- **Malfunctioning sensors and actuators:** The sensor reading has considerable errors, such as drift, dead zone, hysteresis, etc. Effects of actuators on the process is modified or interrupted, such as deficiencies in the gears, valves, a jammed winch motor in the climate control system, etc.

Figure 1.5 shows three different kinds of fault.

There are different kinds of faults in the climate control system of the stable while some of them are more common than others: for example, the farmers forget to close the stable door which leads to the structure fault, Sensor faults in temperature and humidity sensors, actuator faults in outlets and inlets. To clarify actuator faults, it is referred to:

- The winch motor of the inlet sometimes jams.

- The wire which connects winch motor to the inlets is torn.

- The fan inside the outlet is jammed.

- The damper of the outlet is stuck.

Figure 1.6 shows these kinds of fault in the ventilation system of the stable.
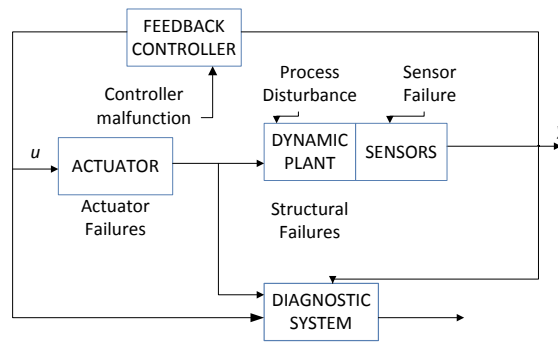
Figure 1.5: Three different kinds of fault [VRYK03].
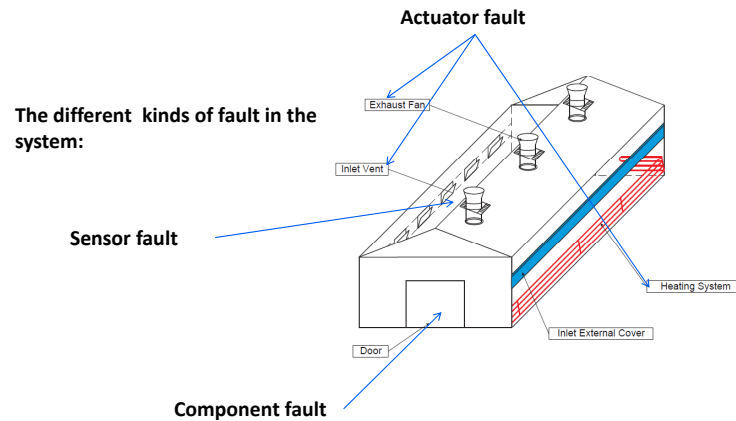
Figure 1.6: Different kinds of fault in the ventilation system of a stable.

1.2.5 Fault Diagnosis systems

An observing system which detects a fault, identifies its location and measures its influence on a process is called a fault diagnosis system and consists of the following stages:

- **Fault detection:** Detection of the time of the occurrence of faults in the process.

- **Fault isolation:** Classification of different faults.

- **Fault identification:** Identification of the type, magnitude and cause of the fault.

Fault diagnosis methods are divided into two major groups: model based and model free (process history based method). Model based is divided into quantitative and qualitative methods. In the model based method, the model is designed based on some basic knowledge about the physics of the process. In quantitative method, the model is based on some mathematical equations which describe the relation between inputs and outputs of the system. While in qualitative method, the equations are expressed in terms of qualitative functions. In more details, the qualitative model based method consists of a set

of if-then-else rules and inference engine to search through the knowledge and define a conclusion. In contrast to model based methods, the process history based methods use a large number of process data in order to extract a feature for fault diagnosis. This extraction can be divided into qualitative or quantitative. Figure 1.7 illustrates the methods for fault diagnosis. Here, it is focused on quantitative model based method. The readers are referred to good survey papers as [VRK03],[VRKY03],[VRYK03], and [FD97], and books as [BKLS06] and [CP99].
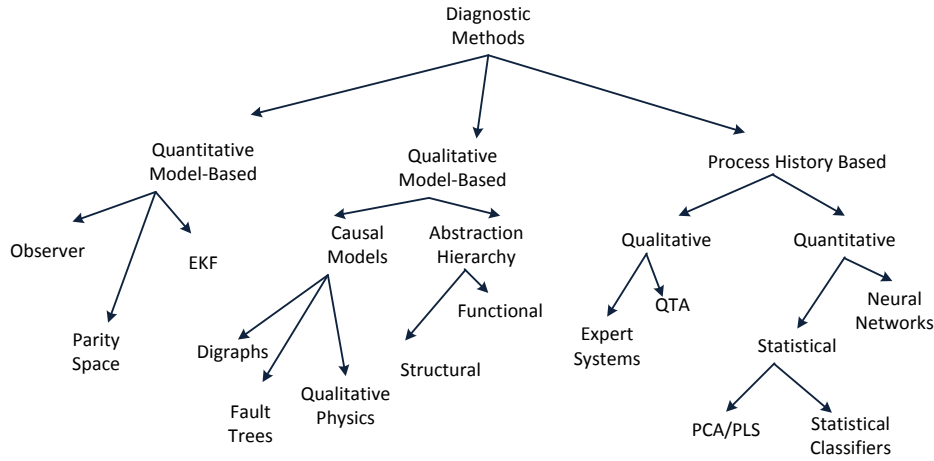
Figure 1.7: Classification of diagnostic algorithms [VRYK03].

All quantitative model based methods are based on two steps. The first step is generating inconsistencies between the actual and expected behavior of the system. These inconsistencies called residual signals specify the faults in the system. The second step is residual evaluation. The residual is evaluated to detect, isolate and identify faults. In order to evaluate the inconsistency, some form of redundancy is required. This redundancy can be hardware or analytical. Hardware redundancy can be a redundant sensor or a control system, etc. Analytical redundancy is providing by estimating the process variables using the relation between input and output of the system [BN93], [FD97]. Figure 1.8 shows a schematic of an analytical redundancy. The residual signal is sensitive to fault and insensitive to uncertainties. For example, it is close to zero when there is no fault in the system and is considerable when the system is subjected to a fault. With using disturbance decoupling methods, it is possible to design a residual signal which is not sensitive to uncertainties [PFC89].

All quantitative model based fault diagnosis methods are divided in three major categories:

- **Diagnostic observer**

- **Kalman filters**

- **Parity relations**
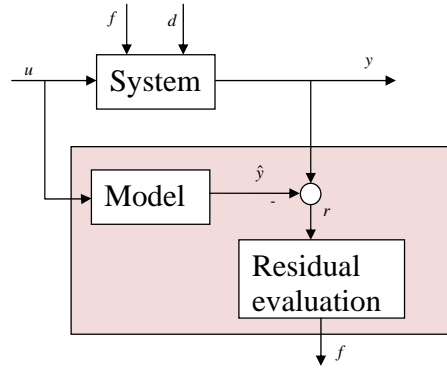
Figure 1.8: Structure of fault diagnoser.

The observer based diagnosis is based on creating a set of residuals which are insensitive to model uncertainties and the process disturbance. With evaluating the set of residual, different faults are detected and identified. In more details, a set of observers, where each of them is sensitive to a subset of faults and insensitive to the other faults are designed. When a fault occur in the system, the observer sensitive to that fault generates a significant residual while the other observers generate small residuals due to uncertainties. These observers generate small residuals for the fault-free case. For more details about the observer methods, the readers are referred to [Cla79], [PFC89], and [Fra90].

The environmental or plant disturbances are unknown at every moment and only their statistics properties are known. The method for fault diagnosis is to design a state estimator with minimum estimation error. The Kalman filter is the appropriate estimator which is based on the system model in its normal operating mode. [Wil76] are pioneered in Kalman filter, and more studies have done by [Wil86], [BN93],[BN93], and [CH98].

The parity relation method is based on rearranging the model structure such that the best fault isolation is obtained. In general, the model structure is the state space model of the system. The parity relation was introduced by [Wil76] and more studies were conducted by [GCF+95]. It is straightforward to show that parity equation and observer based method yield equivalent residual [Ger91].

There is limited literature on fault diagnosis (FD) of climate control systems for the stables; however there are more literature on greenhouses. In [KAR07] and [VF05], parity equations based on the state space model of the system is used for fault diagnosis in a climate control systems of the pig stable. The parity equation method is the same as the method developed by [WDC75]. In [LGS02], an observer-based robust failure detection and isolation in a greenhouse is presented. A fuzzy neural method for fault diagnosis of actuators and sensors in greenhouses is given in [ERH05]. A FD method based on parity relation for fault detection in the greenhouses subject to sensor and actuator faults is presented in [KRD+03].

There is intensive literature on fault diagnosis of hybrid systems. Hybrid systems contain continuous components and discrete components. Therefore, the methodologies from discrete systems, continuous systems or both are used for FD of such systems. The most common discrete event frameworks for hybrid systems are Petri-nets, hybrid bond

graphs, and finite state automata.

State and mode estimation for observer and Kalman filter based FD methods in hybrid system is a major challenge, because it is required to estimate the mode and the state of the system at the same time. Providing a remedy for such problems attracts substantially attention. For example, in [AC01], an observer based FD method for hybrid systems is proposed. A bank of Luenberger observers for state estimation in hybrid linear system is presented. In the method, both time and mode of the switching is assumed known a priori. With help of a common Lyapunov function the problem turns out as a solution of a set of LMIs. In [BBBSV02], a hybrid observer for location estimation of the plant and continuous state estimation is suggested. The aim of the hybrid observer is to design the complete state using the discrete input/output data of the plant. The method does not consider any extra assumption about the time and mode of the switching. In a networked embedded system which consist of a significant number of discrete and continuous components, particle filtering may be an appropriate observer for mode and state estimation.

In the above methods, model uncertainties and unknown disturbance are not considered; while they effect the mode transition as the fault. In order to solve this problem, a Kalman filter based FD method for hybrid nonlinear systems is presented in [WLZL07]. Here, the model uncertainties and unknown disturbance are assumed bounded, and no knowledge about the mode transition is assumed. Using an unknown input extended Kalman filter, the state and the mode of the system from input/output information are estimated. The correctness of mode estimation and stability of the continuous state estimation is guaranteed.

There is some research on parity relation FD methods for hybrid systems. For example, in [CEMS04], the authors use parity relation methods to check inconsistency between the input/output information of the plan and the model. Based on the parity residual, the potential faults in the plant are detected and isolated.

For fault diagnosis methodologies based on a discrete event framework refer to [Lun08]. The model based FD method is applied on a system which switches between its operations modes by a feedback controller. In order to show the inconsistencies between the system and the model behavior, the model is abbreviated into four categories as embedded maps, semi-Markov processes, timed automata and nondeterministic automata. [NB07] proposes a qualitative model based FD for hybrid systems subject to parametric faults. The hybrid system is simulated based on bond graphs. In [DKB09] a qualitative model based FD approach for both parametric and discrete faults in hybrid systems is presented. The hybrid modeling framework is based on hybrid bond graphs.

1.2.5.1 Passive and Active Fault Diagnoser

In general, the fault diagnosers are divided in two major groups: Passive fault diagnosis (PFD) and active fault diagnosis (AFD). In the passive method as in Fig. 1.8, the diagnoser does not act upon the system and only observes the input/output data of the system to detect any abnormal behavior of the system. For passive diagnosis, refer to the previous section.

Active fault diagnostic

In the active fault diagnosis (AFD), at first the system is excited by exerting an auxiliary signal, and then the fault is observed by PFD approaches as in Fig. 1.9. The reason for excitation is to uncover faults which are hidden during normal operation of the system.

In this case, the input-output (I/O) set of the system is in the intersection area of normal and faulty I/O sets. In more details, assume A_0 in Fig. 1.10, represents the input-output set of the normal system for a finite time interval. The same definition is also used for A_1 and A_2 which represent two different faults in the system. It is obvious that the perfect fault detection is obtained when $A_0 \cap A_1 \cap A_2 = 0$, while sometimes the observed input-output set of the system belongs to the area, where the three sets A_0, A_1 and A_2 overlap. As the result, the diagnoser is unable to decide whether the system is in normal operation or subject to a fault. In order to detect the faulty behaviour of the system, a sequential input signal over a finite time interval is applied to the system as indicated in Fig. 1.10. The input moves the sets in the direction of the arrows such that they are disjoint and fault detection is possible. At the end of the time interval, the fault isolation algorithm is executed to isolate the different faults.
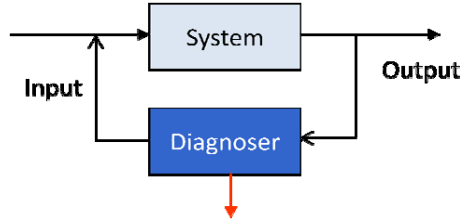
Figure 1.9: Active fault diagnosis diagram.
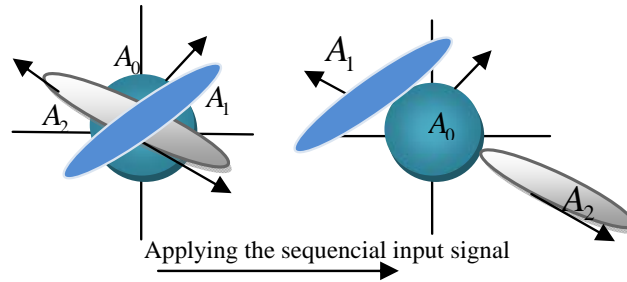
Figure 1.10: Applying test signal.

Here, the auxiliary signal should be sufficiently large such that the fault would be observable from I/O set of the system; on the other hand, it should not result in instability of the system.

Active fault diagnosis is useful for faster fault diagnostic, and detection of the hidden fault during normal operation of the system. It is also useful for sanity check, and better fault isolation in systems with slow response. Let us assume that some components of the system such as actuators are used rarely during normal operation. Consequently, these actuators do not affect on the system response efficiently such that it is not possible to distinguish their sanity from observing the I/O set of the system. Here, the remedy is to excite the system such that the actuators are forced to participate more efficiently in the system, and their sanity is distinguishable by observing the I/O data.

Although fault diagnosis has attracted attention for decades, active fault diagnosis is a quite new issue. For a study of AFD for linear systems refer to [Nik98].Here a sequential excitation signal is designed off-line over a horizon,the detection horizon, based on a recursive linear equation. After real-time implementation of the signal in open-loop mode, the input-output set of the system is observed and matched with a set of polyhedrons to detect the abnormal behavior of the system. The uncertainties are formulated as inequality constraints. In [NCD00], it is tried to define a minimum energy for the excitation signal. Also the uncertainties are assumed as a limited energy signal. The fault diagnosis is done by inconsistency checks between the I/O set of the system with the I/O set of the normal and faulty models using a hyper-plane test. [NC06] proposed a different method for design of excitation signal which is based on a multi-model formulation of the systems. Here, a priori knowledge about the initial conditions is required. The initial conditions are not restricted, and it is assumed to be in a known region. This assumption leads to detection of more different kinds of fault, such as a jump in the state of the system or bias failures. An AFD approach for model identification and failure detection in the presence of quadratic bounded uncertainty is presented in [NC06]. In [CHN02], the auxiliary signal design is obtained for rapid multi-model fault identification using optimization.

The previous AFD methods were suggested for linear system; while [ASC08], and [CDA$^+$06], [CCN09] and [And08] propose the AFD method for nonlinear systems. For example in [CDA$^+$06], the excitation signal from a linear model is tested and validated on the nonlinear problem where the uncertainties and noise as a bounded signal is also considered. [CDA$^+$06] changes the nonlinear optimization problem setup in order to find the minimum excitation signal by the linear methods.

The above approaches are proposed for open-loop system. AFD for a closed loop system with a linear feedback is presented in [ANC09]. Here, the optimization problem for designing excitation signal is not trivial, because the signal depends on the noise and changes with respect to the output. The optimization problem is restructured as a Min-Max problem, and an efficient algorithm for solving is given. [FC09] suggests a method for design of the signal for detection of incipient fault. The method is based on multi-model approach for detection of two faults.

The AFD framework in [PN08] is quite different from the previous works. The authors design a sinusoidal signal for excitation of the system and insert it through the closed loop system with a feedback controller. It turns out that the transfer function from the signal to the residual is equal to the dual Youla-Jabr-Bongiorno-Kucera (YJBK). The signal does not generate any extra term in the residual for the fault free system; however, it changes the residual when the system is subject to a fault. The fault diagnosis is done by the classical cumulative sum (CUSUM). The same AFD setup was considered in [PN09] for stochastic change detection. The aim is fast fault detection and isolation based on residual output direction. In [NP09], the AFD is based on the residual evaluation in a dedicated frequency with respect to the excitation signal. Since only the system information on that frequency is required, it is possible to use simple reduced model information. [GB09] uses the active fault diagnosis idea to isolate the faults which could be detectable but not isolable. The method embarks from the structural analysis approach.

In the previous AFD methods, the excitation signal is assumed as an external signal which is injected through the system, while there is no external signal in [Sto09]. In fact, the system switches cyclically between some observers which are sensitive for a set of faults such that the faults are detectable and the closed loop system is stable.

There are few works on active fault diagnosis for hybrid systems. The readers are referred to [TRIZB10], where the AFD approach is based on generating the excitation inputs, on-line and using a model predictive control (MPC). In order to guarantee the stability of the closed loop system, the sufficient stability conditions are considered on the problem. The mixed logical dynamical (MLD) framework is used for modeling of the hybrid system. [DKB09] uses a qualitative event-based AFD approach for better fault detection and isolation. In the method, the controller tries to execute or block the controllable event such that the fault is detectable faster and more precise in the hybrid system. In [BTMO09], the problem is addressed as a discrete event system. A finite state machine is used to guide the system from its operating point where the fault is not distinguishable to an operating point when the fault is distinguishable. Of course, the safety properties of the system are also considered. An active fault diagnosis method in [Jan09] is based on equivalent automaton states such that the faults are distinguishable from the output of the system.

1.2.6 Fault Tolerant Control Systems

Fault tolerant control systems (FTCS) are capable of tolerating component faults while preserving the reliability, maintainability and survivability of the system. In more details, a closed loop control system which maintains stability and a graceful degradation of the performance of the overall system at the presence of component faults is called FTCS.

Fault tolerant control systems are classified into two broad categories; passive fault tolerant control systems (PFTCS) and active fault tolerant control systems (AFTCS). In continuing, the required details of these two categories are given.

1.2.6.1 Passive fault tolerant control systems

In PFTCS, the control law is fixed and does not change when a fault occurs. In fact, the control system is designed to be robust against a set of limited faults. The method for designing of such control systems is embarked from robust control, where the controller is designed to be insensitive to system uncertainties and disturbances. When the effects of faults are similar to those of uncertainties or disturbance, it can be assured that the robust controller are insensitive to the faults. One of disadvantages of PFTCS is that sometimes the fault is not incipient and has significant effect on the performance of the system, or it is not possible to design a controller to be robust to set of faults. Hence, a fault estimation scheme is needed to detect and identify the fault.

State of the art

The research in the FTC of live-stock buildings and greenhouse is quite new. In [KAR07] and [VF05] an algorithm for FTCS is proposed, where the results are verified in simulation environments. However, there is an intensive body of literature in PFTCS of linear systems. In [Vei95], the author proposes a PFTCS method for a system to be tolerable against actuator faults. The fault tolerant controller also provides an acceptable performance of the system subjected to actuator faults. The fault tolerant control method is based on linear-quadratic state-feedback controllers. A reliable controller for a system subject to sensor and actuator faults is presented in [YWS01]. The controller preserves the stability and H infinity performance of the system in normal case as well as faulty case. A bounded disturbance is also considered. [NS05] presents a PFTC method

based on feedback controller using Yola-Jabr-Bomgiorno-Kucera (YJBK) parameterization. The method is a multi objective optimization design, where the parameters of the YJBK controller are optimized such that the performance and stability of the closed-loop system subjected to a fault is preserved.

Most complex industrial systems either show nonlinear behavior or contain both discrete and continuous components. A PFTC approach for nonlinear systems is presented in [BL10]. The approach is based on feedback controller which is insensitive to a set of actuator faults. The actuator fault is assumed as a bounded periodic unknown signal, likewise the model uncertainties. In [LXJ$^+$] a PFTC method for uncertain non-linear stochastic systems with distributed delays is given. The closed-loop system based on a state feedback controller is robust against a set of actuator failure. The stability analysis is done using the Lyapunov-Krasovskii function, and the sufficient condition is derived in terms of linear inequality matrices (LMIs).

For PFTCS of hybrid systems, the reader is referred to [WLZ07]. Here an H infinity state feedback controller is proposed for a class of continuous time switched nonlinear systems subjected to actuator fault. The sufficient condition for asymptotically stability of the closed-loop system using the multiple Lyapunov function is given. In [NRZ09], a state feedback controller is designed for continuous-time piecewise affine (PWA) systems while an upper bound of cost function is minimized. Design of the controller which is robust to actuator faults is cast as a set of linear matrix inequalities (LMIs). In [TIZBR10], a new method for passive fault tolerant control of discrete time PWA systems is presented. The approach is based on a reliable piecewise linear quadratic regulator (LQR) state feedback control that is tolerant against actuator faults. Here, also the upper bound of performance cost is minimized, and the control design problem is transformed into a convex optimization problem with LMI constraints. The PWA systems switch arbitrary due to state variables.

As was mentioned, the passive fault tolerant control framework is similar to design the controllers to be insensitive and robust to uncertainties and disturbance. Therefore, in the following a literature survey on robust control design is given. The author of [Fen02] proposes a piecewise-continuous controller for uncertain piecewise-linear systems based on a piecewise-smooth Lyapunov function. The sufficient conditions for guarantee of the stability and H infinity performance of the closed loop system is given in the terms of LMIs. A dynamic output feedback controller for an uncertain piecewise Lyapunov function is designed in [ZT09]. It is assumed that the uncertainties do not exceed an admissible boundary. The stability of the closed loop systems with minimization of the upper bound of the cost function is taken into account. Design of the controller is cast as a bilinear matrix inequality (BMI), and with using genetic algorithm (GA) it transformed to a semidefinite programming (SDP), which can be solved numerically efficiently. In [GLC09], a novel H infinity controller is suggested for discrete-time PWA systems when time-varying uncertainties, external disturbances and physical constraints on the states and inputs are considered. Stability guarantee of the closed loop system based on a state feedback controller is investigated through a dissipativity inequality, and it cast as feasibility of a set of LMIs.

1.2.6.2 Active fault tolerant control systems (AFTCS)

When severe faults such as the complete failure of actuators or sensors breaks the control loops, it is necessary to use a different set of inputs or outputs for the control task. Active fault tolerant control consists of finding and implementing a new control structure in response to the occurrence of a severe fault. After selecting the new control configuration new controller parameters would be found. The redesign of controller is carried out automatically during the operation of the system [ZJ08]. Active fault tolerant control system (AFTCS) is able to accommodate faults such that stability and performance of the system are preserved. Also AFTCS prevent faults in subsystems from developing into failures of the system.

A general schematic that appropriate to many fault tolerant control systems is illustrated in Fig. 1.11. The plant in the figure contains sensor and actuator that can be subjected to a fault. The fault detection and isolation (FDI) block in the figure provide the required information about the location and effect of the fault on performance of the system for the supervision block. The supervision block reconfigures the sensors and actuators to isolate the faults, and adapt the controller to accommodate the fault effect [Pat97].
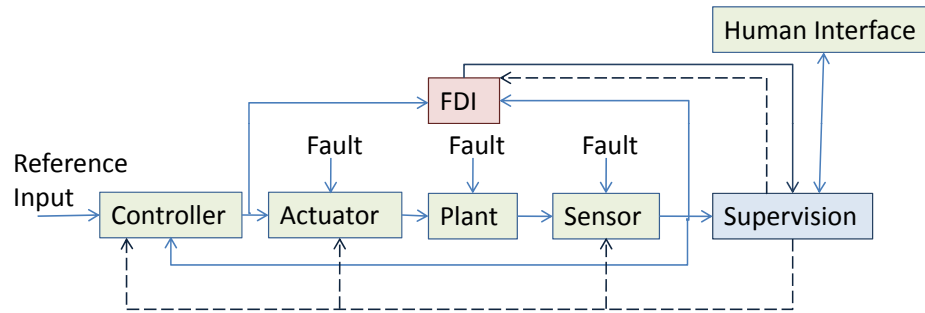
Figure 1.11: General structure of fault-tolerant control system with supervision scheme [Pat97].

There are different classifications for active fault tolerant control methods in the literature. According to [Pat97], active methods are classified into four major groups: physical redundancy, learning control, projection-based methods and on-line automatic controller redesign methods as in Fig 1.12. The latter method is concerned with defining new controller parameters or control law, known as a reconfigurable controller. In the projection based method, a set of controller are designed in advance and the system switches automatically between them such that a sacrificed degree of performance of the system at the presence of faults are preserved. As is illustrated in the figure, the reconfigurable controller methods are divided into many different methods [LRM08]. In safety-critical applications, the actuators and sensors are duplicated. When a fault happens, a simple decision algorithm switches the controller from a faulty component to a healthy one. This fault tolerant control method is known as physical redundancy. In the learning control method, the classical control techniques are combined with learning control method. Basically, a fast component, e.g. Kalman filter is used to estimate a changing condition

quickly, then a slower learning component is employed to store previous knowledge to use it again in the future.
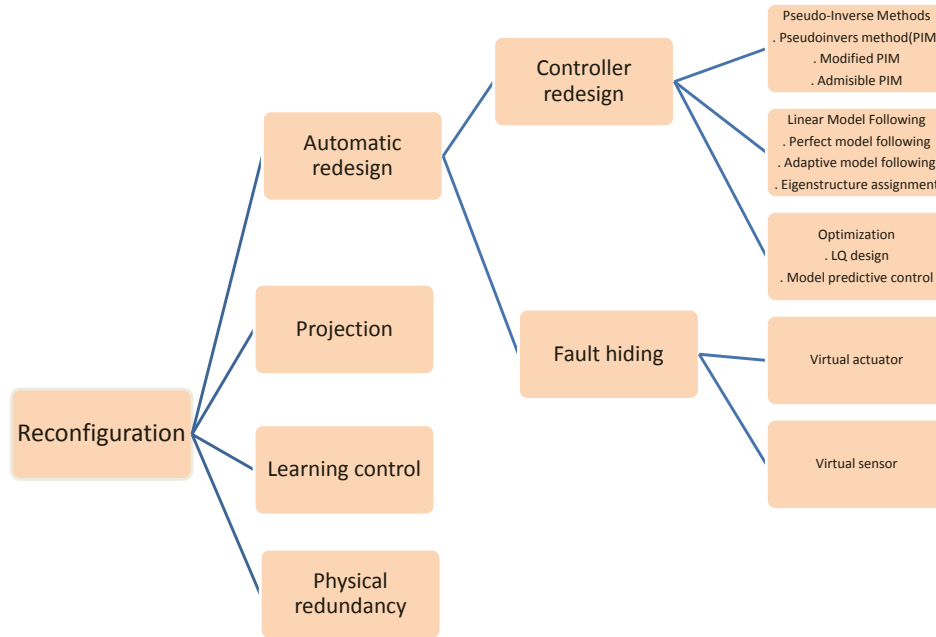
Figure 1.12: Classification of control reconfiguration merhods [LRM08].

There is an intensive literature review on AFTC of linear, nonlinear and hybrid systems; however, we focus only on literature on nonlinear and hybrid systems. For nonlinear systems, the reader is referred to [DGM$^+$02], where a hierarchical fault detection, isolation and recovery method is discussed and applied to automated transfer vehicle (ATV). In the case of severe fault, for example failure of an actuator, the controller must be redesigned completely in order to achieve a tolerable performance [KV02]. The AFTC scheme of [YJC09a] contains a fault diagnosis block and a control reconfiguration block. First, the process fault is diagnosed with an adaptive observer, then the parameters of the faulty system is identified, and controller is restructured such that the closed-loop system is stable. Sensor fault is considered in [QIJS03], where the fault tolerant controller switches between two controllers. The one is designed to be robust against bounded uncertainties in normal system, and the one is designed to be robust against sensor fault. The sensor fault is detected by an observer. The overall stability conditions of the closed-loop system is done based on input to state stability.

In [YJC09b], a brief survey on fault tolerant control of hybrid systems is presented. For AFTC of hybrid systems, the reader is referred to [OMP08]. Where the system inherently contains some modes, and also the faults are considered as new modes. The AFTC is implemented based on a model predictive control (MPC) scheme and a real-time FDI scheme. Mixed logical dynamical (MLD) framework is used for model of the overall hybrid systems.

In [RTAS07], the authors design a linear output feedback controller against multiple actuator failures for discrete-time switched linear systems. It is assumed that a FDI block detects and isolates the fault on-line. Authors modified the method for polytopic linear parameter varying (LPV) systems in [RTAS07]. The approach is based on a static output feedback controller, and the stability guarantee of the closed loop system is preserved by using LMIs. The idea of [Sta02] is the same as AFTC of switched linear systems employing LMIs, where the system switches to a new system due to actuator failure such that the overall stability and performance of the system are held. Here, the fault is detected by an adaptive filter, and it is assumed that always the system is controllable with the healthy actuators. [YJC09a] presents a AFTC method for a class of periodic switched nonlinear systems subjected to both continuous and discrete faults. The continuous fault is diagnosed by an adaptive filter and discrete fault is diagnosed by a sliding mode observer.

In [RHvdWL10], an AFTC approach based on virtual sensors and actuators for continuous-time PWA system subject to actuator and sensor faults is proposed. The basic idea is that the faults are hidden from the normal controller of the system. Sufficient conditions for stability and performance of the closed loop system are given as a solution of a set of linear inequalities matrices (LIMs). The controller is designed to be insensitive to model uncertainties.

1.3 Objective

The main goal of the research is to design an active fault tolerant control (AFTC) scheme for the climate control systems of live-stock buildings such that the AFTC is able to maintain the stability and acceptable degree of the performance of the system subjected to actuator faults. The AFTC switches between different controllers based on the information provided by an active fault diagnosis (AFD) scheme. It is important that the information of the AFD block should be precise enough to avoid having false alarm and wrong switching sequence which may yield instability of the system. Here, active fault diagnosis method is utilized to excite the system a little to isolate and identify the faults more accurately. The active fault diagnosis scheme is a quantitative model based method. In this AFD method, analytical redundancy is used to derive the residual, which is the discrepancy between the output of the model and output of the system. Analytical redundancy is a mathematical or graphical model of the system which has significant effect on the performance of the AFD, and small improvement on an absolute linear scale of the model may reduce the detection error rate by orders of magnitude. To achieve a precise model for the climate control systems of live-stock buildings, we modified a conceptual multi-zone model. Since the live-stock buildings are big, the indoor climate properties such as temperature and humidity are not constant and change along the buildings. Therefore the indoor space is divided into conceptual multi-zones, and climate properties for each zone are considered separately. Finally this conceptual multi-zone model was validated through a laboratory as typical pig stable in Denmark.

1.4 Outline of the Thesis

The remaining of this thesis is structured as follows:

- **Chapter 2 - Climate Modeling and Validation for Livestock Stable** In this chapter a conceptual multi-zone model for climate control of a live-stock building is derived. The model is a nonlinear hybrid system, and in the continuing, it is discussed how to estimate the coefficient of the model. The results are validated based on the measurements.

- **Chapter 3 - Active Fault Detection** In this chapter an method for active fault diagnostic (AFD) of a piecewise nonlinear model of the stable climate control system subjected to actuator fault is proposed. Fault diagnosis is based on comparing the nominal parameter of the model with those estimated by two adaptive filter. EKF and an other adaptive filter is used for parameter estimation.

- **Chapter 4 - Fault Tolerant Control** The aim of this chapter is to design a active fault tolerant control (AFTC) law for climate control systems of the livestock buildings. Only actuator faults are considered. The AFTC framework is based on a switching scheme which switches between a set of predefined controllers such that the stability and a sacrificed degraded performance of the faulty system is held.

- **Chapter 5 - Conclusion** Conclusion and future works are discussed here.

- **Chapter 6 - Paper A** This paper proposes a multi-zone model for climate control systems of a livestock building. The parameters of the model are estimated using extended Kalman filter and measurement data provided by a equipped laboratory.

- **Chapter 7 - Paper B** An active fault diagnosis approach for different kinds of faults is proposed in the paper. The AFD approach excites the system by injecting a so-called excitation input, which is designed off-line based on sensitivity analysis. The fault detection and isolation is done by comparing the nominal parameters with those estimated by extended Kalman filter (EKF).

- **Chapter 8 - Paper C** This paper also proposes another active fault diagnosis technique which is relevant for actuator fault detection. The inputs are defined also using sensitivity analysis, and the parameters of the system are estimated by a new adaptive filter.

- **Chapter 9 - Paper D** In this paper, the problem of reconfigurability of piecewise affine (PWA) systems is investigated. Actuator faults are considered. Sufficient conditions for reconfigurability are cast as a feasibility of a set of linear matrix inequalities (LMIs).

- **Chapter 10 - Paper E** In this paper we design a passive fault tolerant controller (PFTC) against actuator faults for discrete-time piecewise affine (PWA) systems. The PFTC technique is based on dissipativity theory and H_∞ analysis. The problem is structured as as a set of Linear Matrix Inequalities (LMIs).

- **Chapter 11 - Paper F** A passive fault tolerant controller (PFTC) based on state feedback is proposed for discrete-time piecewise affine (PWA) systems. The controller is tolerant against actuator faults and is able to track the reference signal while the control inputs are bounded.

2 | Climate Modeling and Validation for Livestock Stable

The aim of this chapter is to derive a model for the climate control systems of live-stock buildings. In reality the air inside the large stable is not uniformly distributed. It means that the climate properties change along the stable, and it is not a good approximation to assume the climate properties in one point as the properties of the whole stable. This concept has fostered the idea of multi-zone climate modeling, where indoor space of the stable is divided into conceptual multi-zones, and climate properties in each zone is considered separately. Here, a conceptual multi-zone model for climate control of a live stock building is elaborated. The main challenge of this research is to estimate the parameters of this nonlinear hybrid model. A recursive estimation algorithm, the Extended Kalman Filter (EKF) is implemented for estimation. The results are validated based on a laboratory as a typical equipped stable. A brief description of the laboratory is given.

2.1 Laboratory System Description

The laboratory is an old broiler house located in Syvsten, Denmark. It has made of concrete with the following specifications; the length is $64.15\ m$, the floor area is $753\ m^2$, the width is $11.95\ m$, and the total volume is $2890\ m^2$, the figure of the stable is given in Fig. 2.1.

The laboratory is equipped with a ventilation control system made by SKOV company to control temperature and humidity of the air inside the stable. The ventilation system is installed for three zone modeling and its specification is illustrated in Fig 2.2 and given as follows:

1-Outlets Five outlet are installed on the ridge of the roof as in Fig. 2.2. The outlet is a chimney with an electrically controlled fan and adjustable shuttle inside.

2-Inlets 62 inlets mounted on the side wall of the stable are divided into six group; 12 inlets in the vest side and 14 inlets in east side of the first zone, 6 inlets in the vest and east side of the second zone, and 12 inlets in vest and east side of the third zones. Each group of the inlets are connected to a winch motor. An inlet consists of a hinged flap for adjusting amount and direction of the incoming air.

Figure 2.1: The equiped laboratory as a climate control system of live-stock buildings.
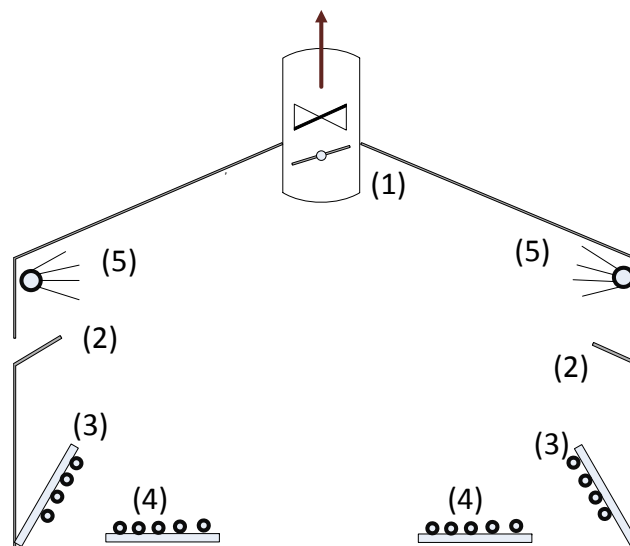
Figure 2.2: The cross section of the stable which shows the ventilation system.

3-Stable Heating System It consists of steel pipes mounted along the walls under the

Figure 2.3: The heating system for the stable which is installed on the west and east indoor space of the stable.

inlets to warm the ventilated air before reaching animals, see Fig. 2.3. The pipes are connected to an oil furnace which provide hot water ranging 15^oC to 55^oC. The general schematic of the heating system is shown in Fig. 2.4. The hot water from oil furnace enter the stable heating system with temperature of $T_{stableH,in}$, and enter the animal heating system, which stimulate the propagated heat by the animal, with temperature of $T_{animalH,in}$. $V_{stableH}$ and $V_{animalH}$ stand for two 3-way valves for two stable and animal heating system. $P_1 - P_3$ stand for the heating pumps in the stable.
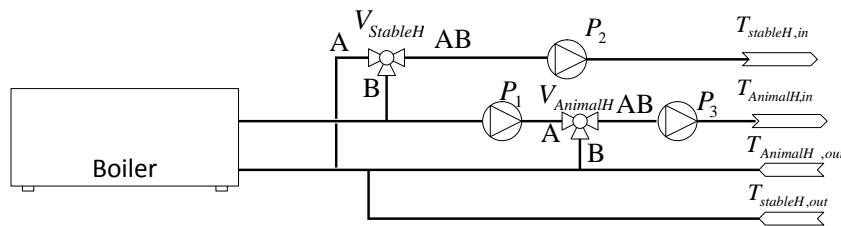
Figure 2.4: The schematic of the heating system, which contains animal and stable heating system, inside the stable.

4-Animal Heating System There are six radiator made of Spiraflex pipes, two radiators for each zone as a simulation of the animal heating production. These radiator also coupled with stable heating system to the oil furnace, see Fig. 2.5.

5-Humidifier The Humidifier system consists of pipes installed top of the inlets along the walls, and includes 10 sprinklers for each zone. They spread the water into the air. They are the simulation of the production of water vapor by the animals, se Fig. 2.6.

Figure 2.5: The heating system for the animal which is installed $10\ cm$ top of the floor for each zone of the stable.
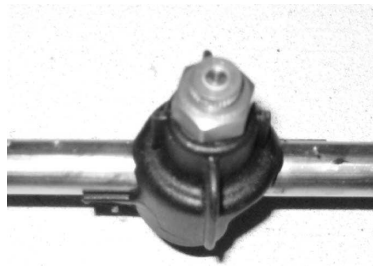
Figure 2.6: The sprinkler which is intalled on top of the wall close to the roof.

Next, it is described how the climate control mechanism in the stable maintain a convenient environment such as climate comfort for the animal. The ventilation system play a significant rule in providing a convenient climate, it produces a low pressure inside the stable and let the fresh air enter the stable and mix with indoor air. With speed of the fan propeller and swivel of the shuttle of the chimney and flap of the inlet , the amount of airflow capacity is controlled. In order to avoid cold ambient air directly to reach the livestock, the hanged flap of the inlet is open with a small angle to guide the airflow toward the ceiling, and then it drops down and mixes slowly with the air to create a comfortable environment.

In the case that the ventilation system can not provide a convenient climate for the animal, for example if the ambient air is too cold, then the heating system warm the indoor air.

A humidifier is required in the summer when the ambient air is too warm, and the ventilation system can not create a qualified climate for the animal. In this case, the sprinkler of the humidifier pour out water on the animals to let them feel more comfortable.

The airflow follows different patterns in winter and summer according to the environmental element such as ambient temperature and wind speed; however, here a general pattern for air flow is considered as Fig. 2.7.
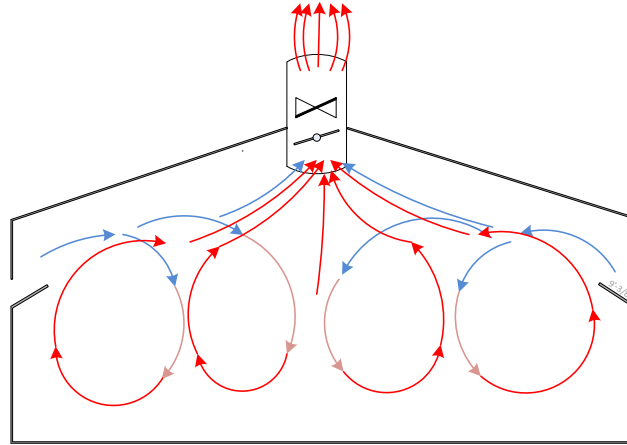
Figure 2.7: The illustration of the aif-flow patter inside the stable in general.

The stable is equipped with a number of sensors to measure the climate properties and regulate them. The sensors are connect to interface hardware and a PC which is located in the control room. The are different kinds of sensor; 18 temperature and 6 humidity sensors located 1 meter above the floor, 5 flow sensors for measuring the exhaust flow rate, 6 position sensors for measuring the angle of the inlet flaps, and 6 pressure sensors for pressure difference cross the inlet. The general view of the sensors in the stable is given in Fig. 2.8, and their details are given in Table 8.2.
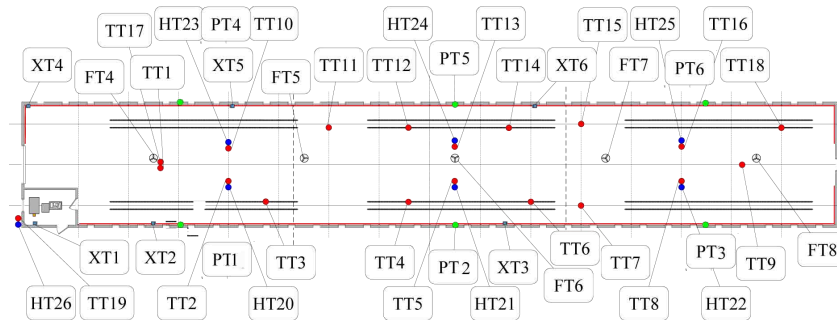
Figure 2.8: A schematic drawing with the positioning, numbering and function of the various sensors mounted in the test stable.

The control computer is a commercial off-the shelf system (COTS) developed by [Jes07]. The server is a standard computer with operational system, Linux, with a PCI I/O cards from National Instruments which is used to connect PC through the sensors and

Table 2.1: Sensor functions

Sensors	Function
$FT4 - FT8$	Flow sensor (outlet)
$HT20 - HT26$	Humidity sensor
$PT1 - PT6$	Pressure difference sensor
$TT1 - TT19$	Temperature sensor
$XT1 - XT6$	Position sensor (inlet)

actuators inside the stable. A open source library such as Comedi is used to connect the PC to the I/O cards. It is possible to connect remotely to the control system of the stable. The procedure is as follows; the control program is defined in the Simulink environment, and it is transferred to C-code and compiled by Real-Time Workshop. The client uploads the compiled file to the server through the Internet and execute it. The data acquisition of the sensors is saved in the data-base of the server, and extracted through the Internet by the user. The general scheme of the connection is shown in Fig. 2.9.
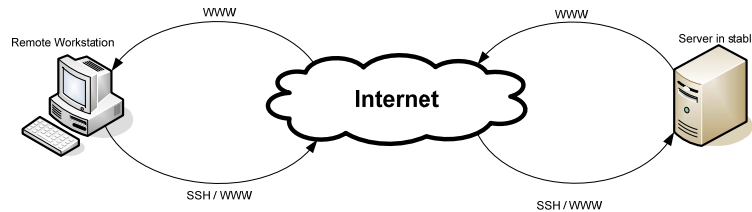
Figure 2.9: Schematic of the remote communication with the stable in Syvsten

In order to upload and run programs remotely, a SSH server is running. The client access to the sensor data and actuator commands through a network interface card (NIC) over the Internet or a local area network (LAN) to a web browser. More details of the stable descriptions is given in [KAR07] and [Jes07].

2.2   Model Description

The airspace inside the stable is incompletely mixed, and is divided into three conceptually homogeneous parts which is called multi-zone climate modeling. The reason of dividing the airspace inside the stable into three zone is because of the ventilation system which is installed separately for three zone. Due to the indoor and outdoor conditions, the airflow direction varies between adjacent zones. Therefore, the system behavior is represented with different discrete dynamic equations. In more details, each flow direction depends on its relevant condition (invariant condition), and as long as the condition is met by the states, the system behavior is expressed according to the appropriate dynamic equations. Once the states violates the invariant condition and satisfies a new one, the sys-

tem behavior is defined with a new equation. A general overview of airflow circulation in the stable is illustrated in Fig 2.10.
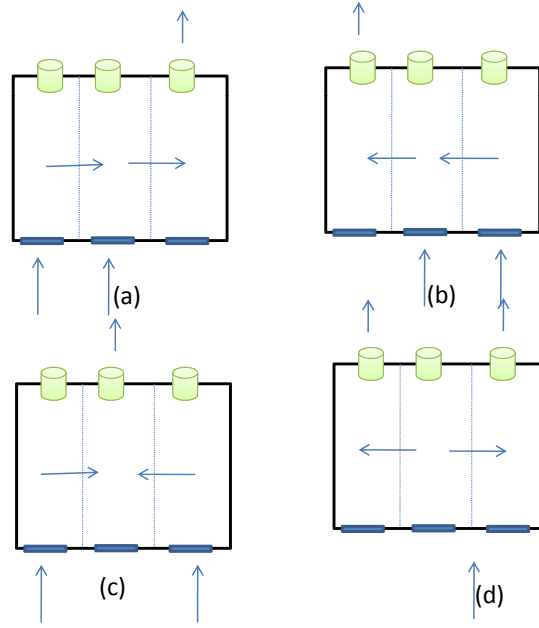
Figure 2.10: Four piecewise nonlinear models defined by different direction of the flow based on indoor pressure.

In the current research some assumption are made to derive an appropriate model:

1. Airflow properties such as density do not change.

2. Due to the humidifier facility of the laboratory was not ready at the time of data acquisition, the humidity model has not been validated.

3. Pressure coefficient C_p is assumed the same for all inlets.

4. Solar radiation is neglected as there is only a small window on the control room.

2.2.1 Inlet Model

An inlet is built into an opening in the wall, and it consists of a hanged flap for adjusting amount and direction of incoming air. In [Jes07], the following approximated model is suggested for airflow q_i^{in} into the zone i

$$q_i^{in} = k_i(\alpha_i + leak)\Delta P_{inlet}^i \qquad (2.1)$$

This model presents enough precision and is used in the research ; however, there is more complex model in according to [Hei04] and [WSH08]:

$$q_i^{in} = C_d A_{inlet}^i \sqrt{\frac{\Delta P_{inlet}^i}{\rho}} \qquad (2.2)$$

$$\Delta P_{inlet}^i = 0.5 C_P V_{ref}^2 - P_i + \rho g (1 - \frac{T_o}{T_i})(H_{NLP} - H_{inlet}) \qquad (2.3)$$

where P_i is the pressure inside zone i, k_i and $leak$ are constants, a_i is the opening angle of the inlets, ΔP_{inlet}^i is the pressure difference across the opening area and wind effect, ρ is the outside air density, V_{ref} is the wind speed, C_p stands for the wind pressure coefficient. H stands for height and H_{NLP} is the neutral pressure level which is calculated from mass balance equation. T_i and T_o are temperature inside and outside the stable, A_{inlet} is the geometrical opening area, C_d is the discharge coefficient and g is gravity constant.

2.2.2 Outlet Model

The outlet is a chimney with an electrically controlled fan and plate inside. A simple linear model for the airflow out of zone i is given by:

$$q_i^{out} = V_{fan}^i c_i - d_i \Delta P_{outlet}^i \qquad (2.4)$$

This model presents enough precision and is used in the research, however, a complex airflow model is given as in [Hei04]:

$$\Delta P_{fan}^i = a_0 (V_{fan}^i)^2 + a_1 q_i^{out} V_{fan}^i + a_2 (q_i^{out})^2 \qquad (2.5)$$

$$\Delta P_{damper}^i = (q_i^{out})^2 (a_0 + a_1 \theta + a_2 \theta^2) \qquad (2.6)$$

$$\Delta P_{outlet}^i = \Delta P_{fan}^i + \Delta P_{loss}^i + \Delta P_{damper}^i \qquad (2.7)$$

$$\Delta P_{outlet}^i = 0.5 C_P V_{ref}^2 - P_i + \rho g (1 - \frac{T_i}{T_o})(H_{NLP} - H_{outlet}) \qquad (2.8)$$

$$\sum_{i=1}^{3} q_i^{in} \rho \frac{\Delta P_{inlet}^i}{|\Delta P_{inlet}^i|} + \sum_{i=1}^{3} q_i^{out} \rho = 0 \qquad (2.9)$$

where c_i and d_i are constants, V_{fan}^i is fan voltage and the number of zones is 3. Here, ΔP_{loss}^i is neglected, $\Delta P_{loss}^i = 0$, however, ΔP_{loss}^i is defined by the chimney factory, ΔP_{damper}^i is the difference pressure across damper inside the chimney, and θ is the angle of the damper. In the meantime, it must be noted that the entire space of stable is divided into three conceptual zones where P_i corresponded to each zone can be calculated from applying equation (2.5-2.9) for each zone.

More details about the relevant condition for the airflow direction are illustrated in Fig. 2.11.

The stationary flows, $q_{i-1,i}^{st}$ and $q_{i,i+1}^{st}$, which moves through the zonal border of two adjacent zones is given by:

$$q_{i-1,i}^{st} = m_1 (P_{i-1} - P_i) \qquad (2.10)$$

$$q_{i,i+1}^{st} = m_2 (P_i - P_{i+1}) \qquad (2.11)$$

$$q_{i-1,i}^{st} = \{q_{i-1,i}^{st}\}^+ - \{q_{i-1,i}^{st}\}^- \qquad (2.12)$$
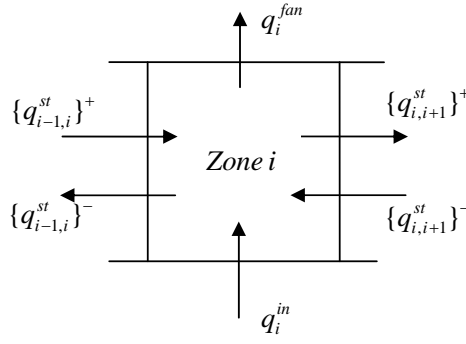
Figure 2.11: Illustration flow for zone i

where m_1 and m_2 are constants coefficients. The use of curly brackets is defined as:

$$\left\{q_{i-1,i}^{st}\right\}^{+} = max(0, q_{i-1,i}^{st}), \quad \left\{q_{i-1,i}^{st}\right\}^{-} = min(0, q_{i-1,i}^{st}) \tag{2.13}$$

2.2.3 Stable Heating Model

The following model as in [KAR07] is used to represent heating:

$$Q_{heater}^i = C_1(T_i - T_{win}^i)C_2 \tag{2.14}$$

$$C_1 = \dot{m}_{heater}C_{pwater} \tag{2.15}$$

$$C_2 = exp\left[\frac{-U_{heater}A_{pipe}}{\dot{m}_{heater}C_{pwater}}\right] - 1 \tag{2.16}$$

where $\dot{m}_{heater}$ is the mass flow rate of heating system, heat capacity is presented by C_{pwater}, T_{win} is temperature of incoming flow of heating system, U_{heater} is the overall average heat transfer coefficient, and A_{pipe} is the cross are of the pipe in the heating system. In order to derive more precise stable heating model, C_2 is estimated from the laboratory experiments.

2.2.4 Animal Heating Model

According to the principle of heat exchange: $Q = mc_p\Delta T$ the following model is derived directly:

$$Q_{animal}^i = \dot{m}_w C_{pwater} k_1 \left(\frac{T_{ain}^i + T_{out}^i}{2} - T_i\right) \tag{2.17}$$

where m_w is the heating mass flow rate, k_1 is constant; while T_{ain}^i, T_{out}^i and T_i are temperature of incoming and out coming flow of heating system and inside the stable respectively.

2.2.5 Modeling Climate Dynamics

The following formulation for the dynamical model of the temperature for each zone inside the stable is driven by thermodynamic laws. The dynamical model includes four

piecewise nonlinear models which describe the heat exchange between adjacent zones:

$$M_i c_i \frac{\partial T_i}{\partial t} = Q_{i-1,i} + Q_{i,i-1} + Q_{i,i+1} + Q_{i+1,i} + Q_{in,i} \tag{2.18}$$

$$+ Q_{out,i} + Q_{conv,i} + Q_{source,i}$$

$$Q = \dot{m} c_p T_i, \quad Q_{i-1,i} = \left\{ q_{i-1,i}^{st} \right\}^+ \rho c_p T_{i-1}, \tag{2.19}$$

$$Q_{i,i-1} = \left\{ q_{i-1,i}^{st} \right\}^- \rho c_p T_i$$

where $Q_{in,i}$, and $Q_{out,i}$ represent the heat transfer by mass flow through inlet and outlet, $Q_{i-1,i}$ denotes heat exchange from zone $i-1$ to zone i which cause by stationary flow between zones. $Q_{conv} = U A_{wall}(T_i - T_o)$ is the convective heat loss through the building envelope, $Q_{source,i}$ is the heat source, $\dot{m}$ is the mass flow rate, c_i is the heat capacity and M_i is the mass of the air inside zone i.

The state space model is given by

$$\dot{T} = f_j(T, U, q) \quad for \quad \begin{bmatrix} T \\ U \end{bmatrix} \in \mathfrak{X}_j, \quad j = 1, \ldots, 4 \tag{2.20}$$

$$q = h_3(T, P, U) = \left[q_i^{in}, q_{1,2}^{st}, q_{2,3}^{st}, q_i^{out} \right]^T, \quad i = 1, \ldots, 3 \tag{2.21}$$

$$h_2(P, T, U) = 0, \quad U = \left[\alpha_i, V_{fan}^i, Q_{source,i} \right]^T \tag{2.22}$$

$$y = CT \tag{2.23}$$

where f_j is dedicated to each piecewise state space model, h_2 denotes the mass balance equation (2.9) for obtaining the indoor pressure in each zone and U is the system inputs.

2.2.6 Parameter Estimation

An extended Kalman filter is used to estimate the parameters of the system. The state vector of the system is hence augmented with the parameters of the system resulting in:

$$\dot{X} = \begin{bmatrix} \dot{T} \\ \dot{\theta} \end{bmatrix} = \begin{bmatrix} f_j(T, U, q) + v \\ 0_{l \times 1} \end{bmatrix} \quad for \quad \begin{bmatrix} T \\ U \end{bmatrix} \in \mathfrak{X}_j \tag{2.24}$$

$$q = h_3(X, P, U) \tag{2.25}$$

$$h_2(P, X, U) = 0, \quad y = CX \tag{2.26}$$

where θ is the coefficient vector with zero dynamics, $\theta = [m_1, m_2, U A_{wall,i}, k_{1,i}, C_{1,i}, V_i]$, w is the measurement noise, and v is the process moise.

The discrete extended Kalman algorithm which consists of two steps is presented as follows:

1. Prediction stage:

$$\hat{X}_k(-) = f_{j,k-1}(\hat{X}_{k-1}(+)) \tag{2.27}$$

$$P_k(-) = \varphi_{k-1} P_{k-1}(+) \varphi_{k-1}^T + Q_{k-1} \tag{2.28}$$

2. Update stage

$$\bar{K}_k = P_k(-)C_k^T[C_kP_k(-)C_k^T + R_k]^{-1} \tag{2.29}$$

$$\hat{X}_k(+) = \hat{X}_k(-) + \bar{K}_k(y_k - \hat{y}_k) \tag{2.30}$$

$$P_k(+) = \{1 - \bar{K}_kC_k\}P_k(-) \tag{2.31}$$

where $Q = E(\begin{bmatrix} v_{k-1} \\ 0_{l\times 1} \end{bmatrix}\begin{bmatrix} v_{k-1} \\ 0_{l\times 1} \end{bmatrix}^T)$ is the covariance matrix of the process noise, and $R = E[w_{k-1} \ w_{k-1}^T]$ is the covariance matrix of the measurement noise. $\bar{K}_k$ is the Kalman gain at time t_k, $\hat{X}_k(+)$ the expected value of X_k given the k measurements, $\hat{X}_k(-)$ is the predicted state estimate.

$$X_k(+) = E(X_k/y_i, \ i = 1, \ldots, k+1), \tag{2.32}$$

$P_k(-)$ is the covariance matrix of the prediction error

$$P_k(-) = E[(X_k - X_k(-))(X_k - X_k(-))^T/y_i, \ i = 1, \ldots, k+1)], \tag{2.33}$$

$P_k(+)$ is the covariance matrix of the estimation error

$$P_k(+) = E[(X_k - X_k(+))(X_k - X_k(+))^T/y_i, \ i = 1, \ldots, k+1)], \tag{2.34}$$

The state and measurement for the EKF are:

$$X = [T_i, m_1, m_2, UA_{wall,i}, k_{1,i}, C_{1,i}, V_i] \tag{2.35}$$

$$y = [T_i, q_{out}^i, \Delta P_{inlet}^i], \quad i = 1, \ldots, 3 \tag{2.36}$$

Note that the parameters of the inlets and outlets, $[k_i, leak_i, c_i, d_i]$, are estimated by standard least square (LS) method.

2.2.7 Experimental Setup and Model Validation

The experimental data were collected from the live-stock building with slow dynamic behavior with time constants around 10 minutes, more details about the experimental setup is described in [GSS10]. In continuing, different sub-models of the climate control model of the stable are validated.

First, we validate the out-coming and in-coming air flow model for the outlet and inlet respectively. The real value of the flow and predicted value of the flow from the outlet by both linear model (2.4) and nonlinear model (2.5) are illustrated in Figure (2.12). The real and predicted data graphs are matched well; however, there are some discrepancies between the real and predicted data. These discrepancies are acceptable as they have small effect on the value of the indoor temperature of the stable. In the current research the linear model is considered. Also the graphs for real and prediction flow from the outlet by linear and nonlinear model are given separately in Figures (2.13, 2.14, and 2.15) separately.

The characteristic of the inlet are given in Fig. (2.16, 2.17, 2.18 and 2.19) as incoming flow (m^3/s) from the inlet with respect to angle of the inlet and difference pressure across
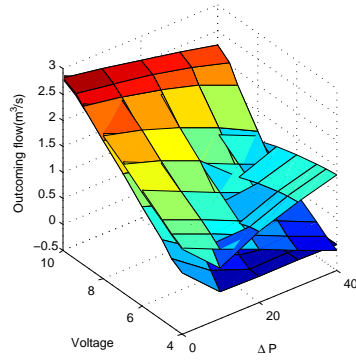
Figure 2.12: The real out-coming flow and predicted out-coming flow by linear and nonlinear models
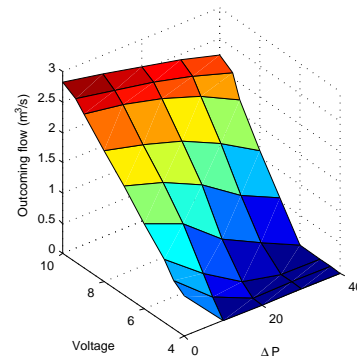
Figure 2.13: The real value of the out-coming flow.
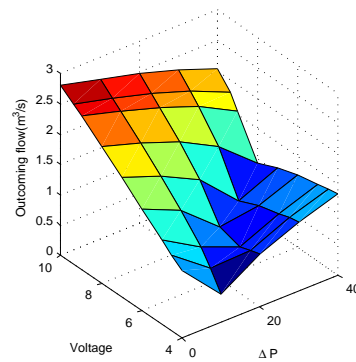
Figure 2.14: The predicted value of out-coming flow by the nonlinear model (2.5).
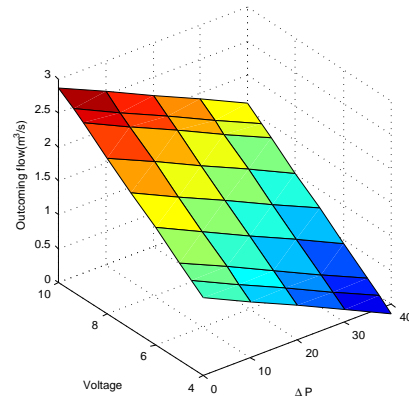
Figure 2.15: The predicted value of out-coming flow by the linear model (2.4).

the inlet. The graphs show that the prediction data represent well the measurement data with a small difference which is assumed to be acceptable.

Here, we validate the animal heating system. To achieve this aim, the inlets, outlets and stable heating source are closed and animal heating source is turn on , and has a small mass flow rate deviation. Figure 2.20 shows the measurement and prediction temperatures inside the stable. The graph confirm that the animal model is designed well due to the measurement and model output are well fitted. In the next step the stable heating system is validated. We consider the same scenario for the inputs except that the animal heating source is closed and the stable hating system is turn on. Figure 2.21 illustrates the measurement and prediction temperature inside the stable. It is obvious that the prediction output track well the measurement.

In order to validate the temperature dynamical model of the stable, the following
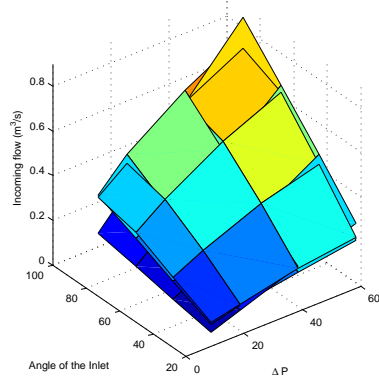
Figure 2.16: The real value of incoming flow, and the predicted value of incoming flow with respect to angle and difference pressure across the inlet by the linear and nonlinear model (2.1) and (2.2).
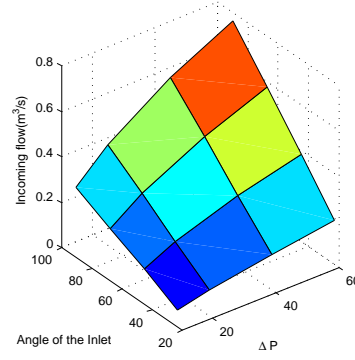
Figure 2.17: The real value of incoming flow with respect to angle and difference pressure across the inlet.
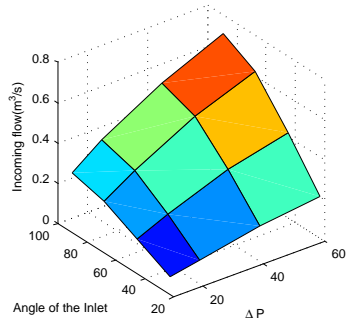
Figure 2.18: The predicted value of incoming flow with respect to angle and difference pressure across the inlet by the nonlinear model (2.2).
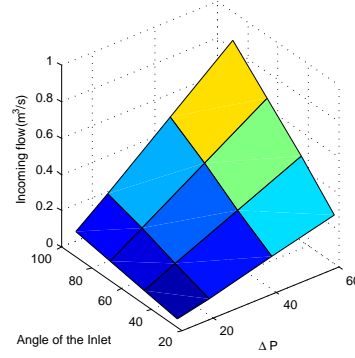
Figure 2.19: The predicted value of incoming flow with respect to angle and difference pressure across the inlet by the linear model (2.1).

scenario on the inputs is considered. The actuator settings (control signals) for ventilation systems are a Pseudo-Random Digital Signal (PRDS) with time granularity of 10 minutes and an amplitude variation. Temperature of the stable and animal heating systems are held at 40 degrees with small oscillation; while, the flow of the heating system is fixed. For further information about the experiment design; see [GSS10].

The validation of the indoor temperature of the stable is carried out for an open loop system. The prediction output is compared with the measurements in Fig. (2.22). Where the graph presents the measurement and predicted temperature for each zone of the stable. It illustrates that there is a non negligible discrepancy attributed to a modeling error. The
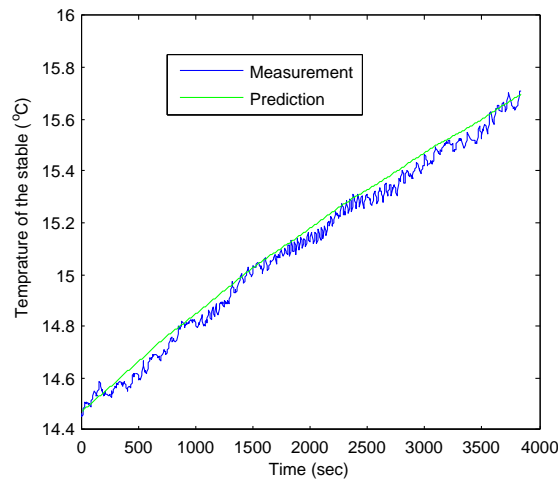
Figure 2.20: The real and prediction temperature inside the stable while all inputs are considered zero except animal heating source which has small deviation.
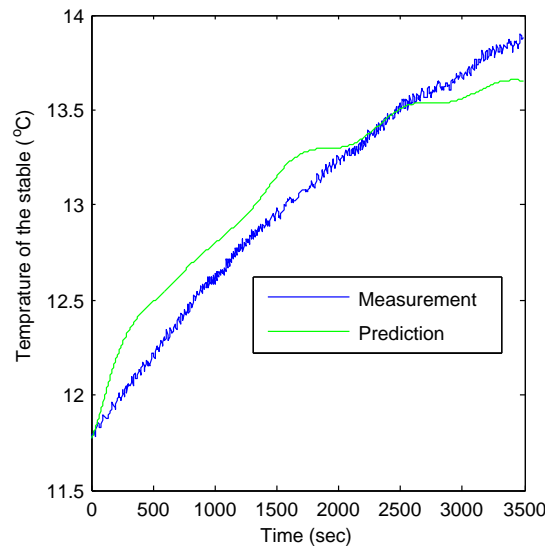
Figure 2.21: The real and prediction temperature inside the stable while all inputs are considered zero except stable heating source which has small deviation.

modeling error is due to several factors such as sharp deviation of wind which mentioned before, heat capacity of the construction material, the latent heat loss through evaporation, the degree of air mixing, building leakage, and large scale livestock building which cause high uncertainty.
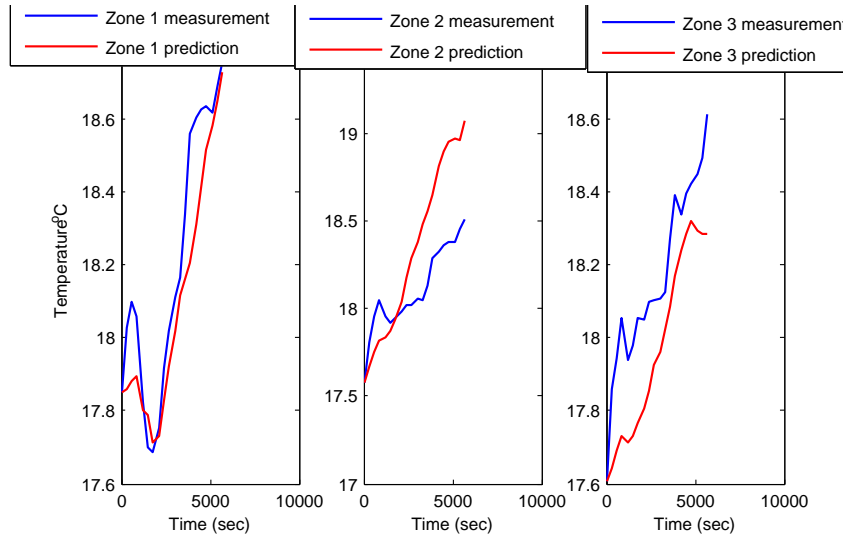
Figure 2.22: The real and prediction temperature for each zone of the stable

2.2.8 Conclusion

The graphs for simulation and measurement data demonstrate a good performance of the designed models and estimation of their coefficient by LS and EKF. In outlet sub-model, there is a difference between the measurement and simulation data of the linear and nonlinear models, which shows that the outlet has a highly nonlinear characteristic. Inlet has a less nonlinear characteristics in comparison with outlet and the graphs also demonstrate that there is a small difference between measurement and prediction data by both linear and nonlinear model. The temperature dynamical model based on the conceptual multi-zone modeling has a good performance, as the result is relevant for the indoor climate of large-scale live-stock building. The difference of real and prediction temperature is attributed to undesirable environmental disturbance. In fact, the model uncertainty is an unavoidable aspect of model identification.

3 | Active Fault Detection

In this chapter two methods for active fault diagnostic (AFD) of a piecewise nonlinear system subjected to actuator fault are discussed and compared. The AFD approaches are based on excitation of the system by a so-called excitation input and a passive fault diagnosis methods to detect and identify the fault. In both AFD methods, the excitation input is designed off-line based on a sensitivity analysis such that the maximum sensitivity for each parameter of the system is obtained. Maximum sensitivity yields better precision of the corresponding parameter estimation. Fault diagnosis is based on comparing the nominal parameter of the system with the those estimated by two adaptive filters. In two AFD methods, two different filters; EKF and an new adaptive filter are used for parameter estimation. The fault diagnosis analysis and simulation is done on the climate control system of the live-stock building which was designed in the modeling chapter.

3.1 Model Reformulation and General AFD Framework

3.1.1 Model Reformulation

The state space model of the climate control system of the stable is transformed into discrete-time switching model as follows:

$$x(k+1) = f_i(x(k), u(k), k, \theta, F_A, v(k)), \; for \; \begin{bmatrix} x(k) \\ u(k) \end{bmatrix} \in \mathfrak{X}_i \tag{3.1}$$

$$y_m(k) = Cx(k) + w(k) \tag{3.2}$$

where F_A is actuator fault, $u(k) \in \mathbb{R}^m$ is the control input and $x(k) \in \mathbb{R}^n$ is the state, and $y_m(k) \in \mathbb{R}^p$ is the output. All variables are at time k, the set

$$\mathfrak{X}_i \underline{\Delta} \{ \begin{bmatrix} x(k)^T u(k)^T \end{bmatrix}^T | \mathfrak{g}_i(x, u) \le K_i, i = 1, \dots, s \} \tag{3.3}$$

are manifolds (possibly un-bounded) in the state-input space $\theta \in \mathcal{R}^l$ is the parameter vector, $v(k)$ and $w(k)$ are disturbance and measurement noise respectively, f_i is vector fields of the state space description, $\mathfrak{g}_i$ is a known function.

3.1.2 The AFD Framework

The main idea of AFD approach is to excite the system response by the so-called excitation input such that the parameters of the system are estimated with better precision and

---

probably the fault is observable. Here, the parameters are related to the actuators as only the actuator fault is considered. Inserting the excitation input to the system also contribute to excitation of the actuators, and in fact excitation of the system response is attributed to a excitation of the actuators. As the result an estimation algorithm is able to estimate the parameter of the actuators from the response of the system more precisely. The main work is divided into two parts:

1. Design of the excitation input, off-line and relying on the so-called sensitivity analysis such that the maximum sensitivity for each individual system parameter is obtained.

2. Deriving the fault isolation algorithm, based on estimation of the system parameters with an adaptive filter and EKF and comparing those of parameters with the normal values that are considered known.

3.2   Design of The Excitation Input

The goal is to design the excitation input using sensitivity analysis for more precise parameter estimation and consequently a better fault isolation. To achieve this goal, first we describe the sensitivity analysis, then show how sensitivity analysis improve the parameter estimation. Finally, the excitation input signal is designed using genetic algorithm (GA) such that the maximum sensitivity for each parameter is obtained.

Let us assume that the problem is to estimate the system parameters through the following LMS approach

$$\hat{\theta} = \operatorname*{argmin}_{\theta} P(u, y, \theta, \xi) \tag{3.4}$$

where the performance function P is given by:

$$P(u, y, \theta, \xi) = \frac{1}{2N} \sum_{k=1}^{N} \epsilon^2(k, u, y, \theta, \xi) \tag{3.5}$$

$$\epsilon(k, \theta, \xi) = y_m(k, \theta) - y(k, \xi), \tag{3.6}$$

where ξ is the noise signal, $y(k, \xi)$ is the measurement signal approximated as $y(k, \xi) = y_m(k, \theta^*, \xi)$, $y_m(k, \theta^*, \xi)$ is the output of the model when it depends on the noise signal ξ, and $y_m(k, \theta)$ is the output of the model when it does not depend on the noise signal ξ, we assume ξ is zero. Estimated, running and true parameter vectors are presented by $\hat{\theta}$, θ, θ^*. In the following we omit u and y from the notation. Consider the following definitions:

$$\theta^* = \operatorname*{argmin}_{\theta} P(\theta^*, 0) \Rightarrow [D_\theta P](\theta^*, 0) = 0 \tag{3.7}$$

$$\hat{\theta} = \operatorname*{argmin}_{\theta} P(\hat{\theta}, \xi) \Rightarrow [D_\theta P](\hat{\theta}, \xi) = 0. \tag{3.8}$$

Here, we specify the definition of the sensitivity analysis. In order to present the sensitivity principle according to [Knu03], the error is reformulated as:

$$\epsilon_{RMS}(\theta) = \sqrt{\frac{1}{N}\sum_{k=1}^{N}\epsilon^2(k,\theta)} \approx \sqrt{(\theta-\theta^*)^T\widetilde{H}(\theta)(\theta-\theta^*)} \qquad (3.9)$$

where H is the Hessian matrix. The relative parameter is defined as:

$$\theta_r = L^{-1}\theta, \quad L = diag(\theta^*) \qquad (3.10)$$

Consider the normed error

$$\epsilon_{RMSn} = y_{RMS}^{-1}\epsilon_{RMS}, \;\; y_{RMS} = \sqrt{\frac{1}{N}\sum_{k=1}^{N}y^2(k)} \qquad (3.11)$$

The sensitivity with respect to one relative parameter θ_{ri} is:

$$S_i = \frac{\partial \epsilon_{RMSn}}{\partial \theta_{ri}} \qquad (3.12)$$

An illustration of the sensitivity in one dimension is shown in Fig 3.1. The graph of RMS error with respect to the individual parameter θ_i demonstrates how a large sensitivity implies that a small deviation of θ_i from the true value θ^* generates considerable deviation in the value of $\epsilon_{P,RMS}(\theta)$. Which result in more precise parameter estimation, as it is obvious from (3.5) to (3.8).
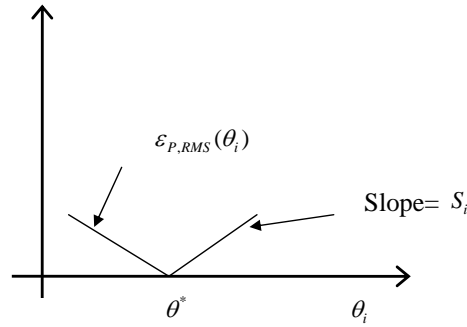
Figure 3.1: RMS parameter dependent error $\epsilon_{P,RMS}(\theta_i)$ as a function of parameter θ_i

For obtaining high sensitivity for the entire system parameters, the ratio of maximum to minimum sensitivity should be small

$$R = \frac{S_{max}}{S_{min}} = \frac{\sqrt{\lambda_{max}}}{\sqrt{\lambda_{min}}} = \frac{\sigma_{max}(H)}{\sigma_{min}(H)} \qquad (3.13)$$

where σ_{max} and σ_{min} are maximum and minimum of singular value of the Hessian matrix H, and λ is eigenvalue of the Hessian matrix of H.

Table 3.1: Fault Isolation Algorithm

Algorithm 1
For $i = 0 \ to \ l$
    IF $r_i = \left| \hat{\theta}_i - \theta_{Ni} \right| > \delta$
        $F = F_i$
    End IF
End For

In the following, we assume the excitation input as a sinusoidal signal and its amplitude α and frequency $\mathfrak{f}$ is designed such that the minimum R is obtained:

$$U = \alpha sin(2\pi \mathfrak{f} t) \qquad (3.14)$$

$$(\alpha, \mathfrak{f}) = \underset{\alpha, \mathfrak{f}}{\mathrm{argmin}} R \qquad (3.15)$$

$$s.t. \begin{cases} (3.1) \\ \alpha_{min} \leqslant \alpha \leqslant \alpha_{max} \\ \mathfrak{f}_{min} \leqslant \mathfrak{f} \leqslant \mathfrak{f}_{max} \end{cases}$$

where α_{min} and α_{max} are minimum and maximum values of α, and $\mathfrak{f}_{min}$ and $\mathfrak{f}_{max}$ are minimum and maximum values of $\mathfrak{f}$. In some cases, it may be necessary to consider more than one periodic signal in U for estimation of different parameters.

Equation (3.15) is non-convex and non-differentiable. To solve the problem with classical approaches, the problem must be changed to a convex problem by defining some constraints. Obtaining these constraints is not always feasible and is considered an open issue in the literature; see [MWL09]. Using evolutional search algorithms such as GA, avoids having to change the problem to a convex one. As the optimization problem is calculated off-line, the computational effort is not important. The reader is referred to [CFPF94] for more details of the GA.

3.3   Fault Detection and Isolation

Here, the EKF and an new adaptive filter are used to estimate the parameters after exciting the system by exerting the inputs. The abnormal behaviour of the system is detected from the estimated parameters. In [GSB11a] and [GSB11b] the required setup for the EKF and the new adaptive filter is given.

Fault detection and isolation relies on a simple algorithm. The algorithm isolate the fault F_i according to the residual generator $r_i = \hat{\theta}_i - \theta_{Ni}$, where θ_{Ni} is the nominal value of ith parameter of the system which is assumed as the prior knowledge of the system and $\hat{\theta}_i$ is the estimated parameter by the adaptive filter and EKF. The fault isolation algorithm is given as Table 3.1. If r_i is greater than a predefined threshold δ, the system is subject to the fault F_i.

3.4   Simulation and Results

Here, the AFD approach is used for sanity check of actuators, such as the inlets, fans and heating system in the stable. In the winter due to the cold weather there is no need for full time ventilation mechanism, therefore the controller closes the inlets and turns off the fans or excites them very slowly, and without AFD, it may take a long time to detect the abnormal behavior of the actuators. In the following, the algorithm is applied to detection/isolation of fault in the fans. The procedure consists of two parts. First, the input designed off-line using sensitivity analysis is applied to the system over a time horizon h as; $U = \{U(0), \dots, U(h)\}$, and the parameters of the system are estimated by the adaptive filter and EKF. Then, the residual which is the discrepancy between the normal and estimated parameters is examined at the end of the time horizon h.

The results of the AFD algorithm are illustrated in the following graphs. In Fig. 3.2, the temperature of each zone and the real and estimated parameters of the fans are illustrated. The estimation is done by both the adaptive filter and EKF. The illustration shows that both filter track the fans parameter correctly before occurrence of any fault. After 3.5 hours, it is assumed that the fan 1 and fan 3 are stuck, and they are turned off. As shown, the adaptive filter is able to detect that the fan 2 is in healthy condition and the other fans are faulty after few steps; while the EKF has a delay to detect the faults. Note that since the adaptive filter is sensitive to the measurement, as a result it is also sensitive to the measurement noise. Large noise may degrades the filter performance.

It is obvious from Fig. 3.2, that there is a small discrepancy between the estimated and real value of the parameter of the second fan. We assume this discrepancy as an admissible boundary. It means that if the difference of a estimated and real parameter is less than this boundary then the fan is in healthy condition otherwise the fan is faulty. In the following, the simulation is executed with an arbitrary input which was not designed by sensitivity analysis. Fig. 3.3, shows that there is a large discrepancy between the simulated and real parameters; in which it is not possible to infer if the fan is in a faulty or healthy condition.

3.5   Conclusion

In this chapter, a method for active fault detection and isolation in hybrid systems, which is based on off-line design of the excitation signal using sensitivity analysis, is proposed. Deriving the signals off-line reduces the computational efforts for the AFD algorithm. The problem of designing the inputs is formulated as a non-convex optimization problem for obtaining the maximum sensitivity for each individual system parameter and it was solved by genetic algorithm (GA). Simulation results illustrate that an adaptive filter is able to detect actuator faults of the system faster than the EKF.

The required assumption for the ADF method is that the value of the system parameters is known and the system is only subjected to actuator fault. This method is more beneficial in comparison to a bank of EKFs where an prior knowledge about the system faults and a model for each individual fault are required. Dedicating a model for each fault is computationally expensive for a system with large number of sensors and actuators which can also be subjected to different kinds of faults.
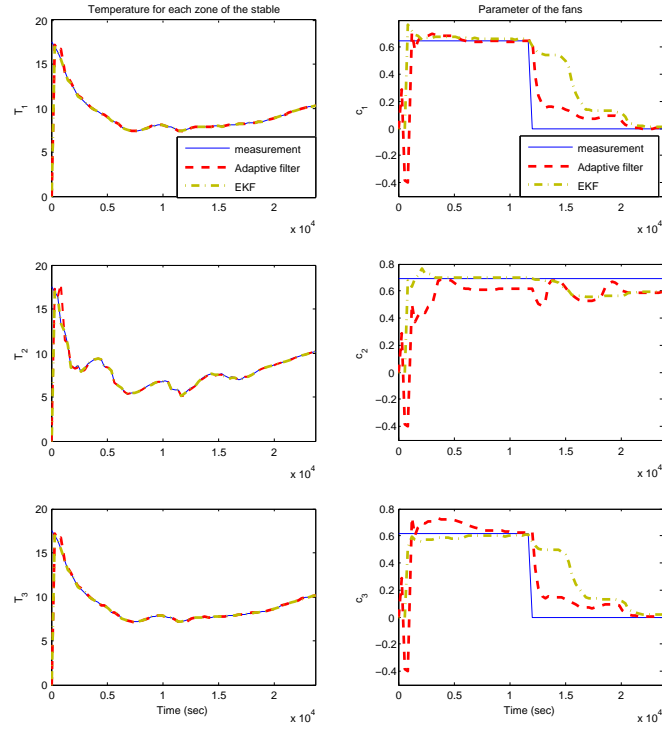
Figure 3.2: The real and estimated values by adaptive filter and EKF for indoor temperature and parameter of the fan for each zone of the stable. The excitation input is designed by sensitivity analysis.
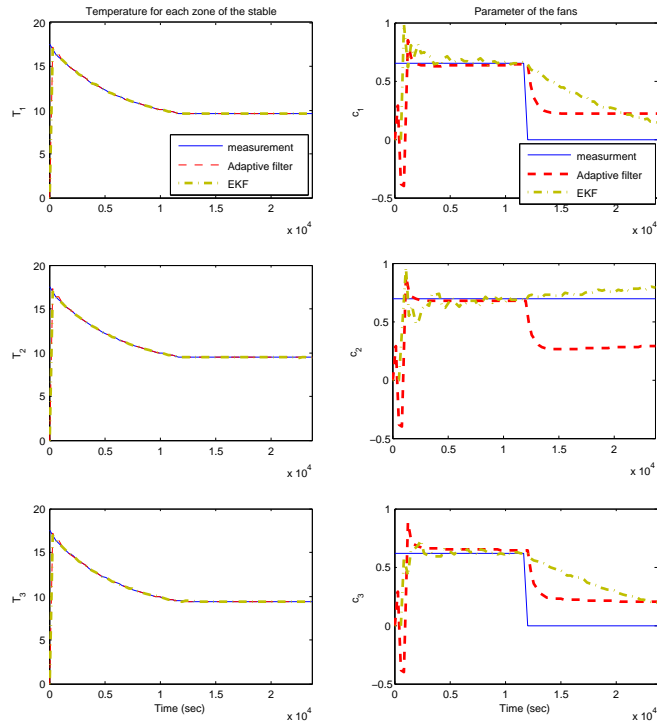
Figure 3.3: The real and estimated values by adaptive filter and EKF for indoor temperature and parameter of the fan for each zone of the stable. The excitation input is chosen arbitrary without sensitivity analysis.

4 | Fault Tolerant Control

The aim of this chapter is design of an active fault tolerant control (AFTC) law for climate control systems of live-stock buildings. Only actuator faults are considered. The AFTC framework contains a supervisory scheme which switches between a set of controllers such that the stability and a degraded performance of the faulty system is held. Design of the supervisory scheme is not considered here. The set of controllers consist of a normal controller for the fault free case, an active FDI controller for isolation and identification of the faults, and a set of passive fault tolerant controllers (PFTCs) designed to be robust against a set of actuator faults. In this research, the piecewise nonlinear model is approximated to a piecewise affine (PWA) system to design PFTCs. We pursue this chapter as following: first, the general schematic of the AFTC is discussed. Second, preliminaries and PWA model approximation are presented, then different PFTCs are elaborated, and finally simulation, result and conclusion are given.

4.1 Active Fault Tolerant Control Framework

Climate control systems of the stable consists of a large number of actuators and sensors which can be subjected to different kinds of fault. Therefore, it may be impossible to design a single controller to be robust against a wide range of faults. Here, the AFTC scheme includes a family of control laws and a switching mechanism to switch between the control laws, which is done by by the supervision scheme as in Fig. 4.1. The control objective is to stabilize and provide a acceptable performance of the system in normal situation as well as in faulty cases. The AFTC procedure is as follows:

- **Normal Control law:** when no fault in the system is detected, the supervisor uses this control law in the closed loop system to satisfies the control objective.

- **FD block:** the fault diagnosis (FD) block is an observer which estimate the output of the system in every sample instant in order to detect an abnormal behaviour of the system and inform the supervisor.

- **AFDI Controller:** once, after the supervisor receives a message from FD block denoting an abnormal behaviour of the system, the supervisor uses the active fault diagnosis control law in order to isolate and identify the current faults in the system. When the AFDI controller isolates and identifies the faults, it informs the supervisor. Note that here, AFDI is applied in open-loop due to the climate control system is stable, and it will not be destabilized by the AFDI controller; however,

the AFDI controller should be implemented in closed-loop system with considering the stability guarantees of the overall system as in [TIZRB10]. As is obvious, this controller deteriorate the performance of the system due to excitation of the system by exerting a test signal. This excitation is only on a short period of time to identify the fault faster.

- **Family of PFTC:** it consists of a family of passive fault tolerant controllers designed to be robust to a specific set of faults. Once, the fault is isolated and identified by AFDI block, the supervisory switches to a appropriate passive fault tolerant controller such that the stability and acceptable performance of the closed loop system is satisfied.

Design of the normal control law is similar to those of passive fault tolerant control law, and its details is postpone to PFTC section.

Most complex industrial systems either show nonlinear behavior or contain both discrete and continuous components. Industrial systems may also contain piecewise affine (PWA) components such as dead-zones, saturation, etc. One of the modeling frameworks which is relevant for such systems is PWA. This framework has been applied in several areas, such as switched system, [RB06], etc. In the following, it is described how to approximate the nonlinear piecewise model to piecewise affine systems, thereafter the preliminaries and the required details about the passive fault tolerant controller for PWA systems are given.
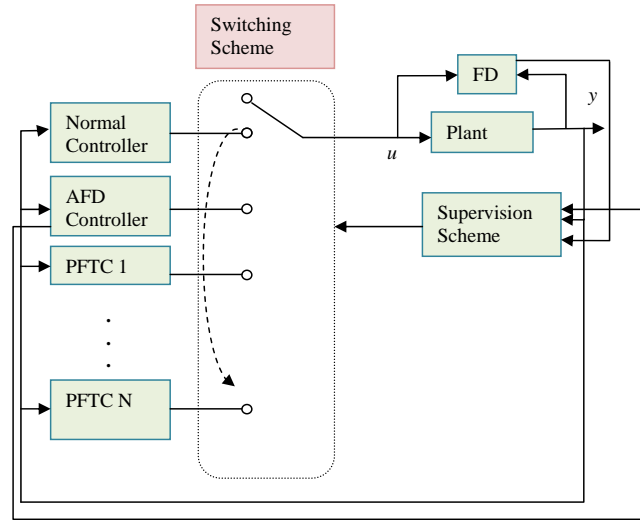
Figure 4.1: The general schematic of the active fault tolerant control scheme

4.2 Model Approximation and Preliminaries

4.2.1 Model Approximation Into PWA Systems

In the following, the procedure to transform the nonlinear model into PWA model is given.

Consider the climate control system of the stable as a discrete-time piecewise nonlinear model of the form

$$x(k+1) = f_i(x(k), u(k), k), \ for \ \begin{bmatrix} x(k) \\ u(k) \end{bmatrix} \in \mathfrak{X}_i \tag{4.1}$$

$$y_m(k) = Cx(k) \tag{4.2}$$

where $u(k) \in \mathbb{R}^m$ is the control input and $x(k) \in \mathbb{R}^n$ is the state, and $y_m(k) \in \mathbb{R}^p$ is the output. All variables are at time k, the set

$$\mathfrak{X}_i \underline{\underline{\Delta}} \{ \begin{bmatrix} x(k)^T u(k)^T \end{bmatrix}^T | \mathfrak{g}_i(x, u) \leq K_i, i = 1, \ldots, s \} \tag{4.3}$$

are manifolds (possibly un-bounded) in the state-input space, f_i is vector fields of the state space description, and $\mathfrak{g}_i$ is a known function.

The piecewise nonlinear model is approximated into a piecewise affine model as with the following form:

$$x(k+1) = A_i x(k) + B_i u(k) + a_i \quad for \ \begin{bmatrix} x(k) \\ u(k) \end{bmatrix} \in \mathcal{X}_i, \tag{4.4}$$

$$y_m(k) = Cx(k) \tag{4.5}$$

where A_i, B_i and a_i are affine matrix which are obtained from the nonlinear model f_i. The set $\mathbb{X} \subseteq \mathbb{R}^{n+m}$ represents every possible vector $\begin{bmatrix} x(k)^T u(k)^T \end{bmatrix}^T$, $\{\mathcal{X}_i\}_{i=1}^s$ denotes polyhedral regions of $\mathbb{X}$ which is obtained from $\mathfrak{g}_i$ and $a_i \in \mathbb{R}^n$. Each polyhedral region is represented by:

$$\mathcal{X}_i = \{ \begin{bmatrix} x(k)^T u(k)^T \end{bmatrix}^T \mid F_i^x x + F_i^u u \leq f_i^{xu} \} \tag{4.6}$$

It is assumed that the regions are defined with known matrices F_i^x, F_i^u, f_i^{xu}. $\mathscr{I} = \{1, \cdots, s\}$ is the set of indices of regions $\mathcal{X}_i$. All possible switchings from region $\mathcal{X}_i$ to $\mathcal{X}_j$ are defined by the set $\mathcal{S}$:

$$\mathcal{S} = \{(i, j): \ i, j \in \mathscr{I} \ and \ \exists \begin{bmatrix} x(k) \\ u(k) \end{bmatrix}, \begin{bmatrix} x(k+1) \\ u(k+1) \end{bmatrix} \in \mathbb{X} \tag{4.7}$$

$$\mid \begin{bmatrix} x(k) \\ u(k) \end{bmatrix} \in \mathcal{X}_i \ and \ \begin{bmatrix} x(k+1) \\ u(k+1) \end{bmatrix} \in \mathcal{X}_j \}$$

$\mathscr{I}$ is divided in two partitions. First partition is $\mathscr{I}_0$, which is the index set of the regions that contain the origin and $a_i = 0$. The second partition is $\mathscr{I}_1$ which is the index set of the regions that do not contain the origin.

In order to obtain the PWA model (4.4) two steps should be carried out:

1. The polyhedral region $\mathcal{X}_i$ (4.6) is obtained by approximation of the manifold $\mathfrak{X}_i$ (4.3).

2. The state space description of (4.4) is obtained by approximation of the state space description of (4.1).

Two steps are carried out as two next problems.

Problem 1. The matrices F_i^x, F_i^u, f_i^{xu} which specify the polyhedral region $\mathcal{X}_i$ are obtained as follows:

$$\mathfrak{g}_i(x, u) - k_i \approx F_i^x x + F_i^u u - f^{xu} \tag{4.8}$$

which will be reformulate as convex optimization problem [LR08]:

$$\min_{F_i^x, F_i^u, f_i^{xu}} \sum_{k=1}^{N_s} e^T(x_k) e(x_k)) \tag{4.9}$$

$$s.t. \begin{cases} e(x_k) = \mathfrak{g}_i(x, u) - k_i - F_i^x x - F_i^u u + f^{xu} \\ (F_i^x - F_j^x)x_k^* + (F_i^u - F_j^u)u_k^* + (f_i^{xu} - f_j^{xu}) = 0, \\ \quad i = 1, \ldots, s, \; j \in \mathcal{N}_i, \\ \quad k = 1, \ldots, N_s, \end{cases}$$

where x_k is the sampling points, s is the number of the polyhedral regions, x_k^* are the sampling points corresponding to the boundary between two neighboring regions and N_i is the regions neighboring region i.

Problem 2. The matrices A_i, B_i, a_i which specify the state space description of of (4.4) are obtained as follows:

$$f_i(x(k), u(k), k) \approx A_i x + B_i u + a_i \tag{4.10}$$

which will be reformulate as a convex optimization problem:

$$\min_{A_i, B_i, a_i} \sum_{k=1}^{N_s} e^T(x_k) e(x_k)) \tag{4.11}$$

$$s.t. \begin{cases} e(x_k) = f_i(x(k), u(k), k) - A_i x - B_i u - a_i \\ (A_i - A_j)x_k^* + (B_i - B_j)u_k^* + (a_i - a_j) = 0, \\ \quad i = 1, \ldots, s, \; j \in \mathcal{N}_i, \\ \quad k = 1, \ldots, N_s, \end{cases}$$

4.2.2 Preliminaries

In this section, the stability of the PWA systems in terms of some Theorems is explained and the required definitions are given [SW].

Definition 1. Let $\phi : T \times T \times \chi$ be flow and suppose that $T = (R)$ and χ is a normed vector space. The fixed ponit x^* is said to be

- **Stable** if given any $\varepsilon > 0$ and $t_0 \in T$, there exists $\varrho = \varrho(\varepsilon, t_0) > 0$ such that

$$\|x_0 - x^*\| \leq \varrho \Rightarrow \|\phi(t, t_0, x_0) - x^*\| \leq \varepsilon \ \ for \ \ all \ \ t \geq t_0. \qquad (4.12)$$

- **Attractive** If for all $t_0 \in T$ there exists $\varrho = \varrho(t_0) >$ with the property that

$$\|x_0 - x^*\| \leq \varrho \Rightarrow \lim_{t \to \infty} \|\phi(t, t_0, x_0) - x^*\| = 0. \qquad (4.13)$$

- **Exponentially Stable** If for all $t_0 \in T$ there exists $\varrho = \varrho(t_0), \mathfrak{d} = \mathfrak{d}(t_0) > 0$ and $\beta = \beta(t_0) > 0$ such that

$$\|x_0 - x^*\| \leq \varrho \Rightarrow \|\phi(t, t_0, x_0) - x^*\| \leq \beta \|x_0 - x^*\| e^{-\mathfrak{d}(t-t_0)} \ for \ all \ t \geq t_0. \qquad (4.14)$$

- **Asymtotically Stable** If it is both stable and attractive.

Definition 2. The system (4.4) with supply function $\mathfrak{d} : \mathbb{R}^m \times \mathbb{R}^p \to \mathbb{R}$ is said to be dissipative if there exists a function $V : \mathbb{R}^n \to \mathbb{R}$ such that

$$V(x(t_0)) + \int_{t_0}^{t_1} \mathfrak{d}(u(t), y_m(t)) dt \geq V(x(t_1)) \qquad (4.15)$$

for all $t_0 \leq t_1$ and all signals (u, x, y_m) which satisfy (4.4).

4.2.2.1 Quadratic Lyapunov function

Lyapunov function can be defined in terms of common or piecewise for PWA systems as:

- **Common Lyapunov Function:** $V(x(k)) = x(k)^T P x(k)$, where P is positive definite matrix of appropriate dimension, and it is the same for all regions $\mathcal{X}_i$.

- **Piecewise Lyapunov Function:** $V(x(k)) = x(k)^T P_i x(k) \ for \ x(k) \in \mathcal{X}_i$, where P_i is positive definite matrix of appropriate dimension, and it is different for each region $\mathcal{X}_i$.

The following theorem gives the sufficient conditions for stability of a piecewise affine systems.

Theorem 1. *([CM01]) The system of (4.4) is asymptotically stable if there exist matrices $P_i = P_i^T > 0$ or $P = P^T > 0$, $\forall i \in \mathscr{I}$, such that the positive definite function $V(x(k)), \forall x \in \mathcal{X}_i$, satisfies $V(x(k+1)) - V(x(k)) < 0$.*

Lemma 1. *([CM01]) Let us $V : \mathcal{R}^n \to \mathcal{R}$ terms storage function, $\gamma^2 \|w\|^2 - |y\|^2, \gamma > 0$ terms the supply rate. The system of (4.4) with disturbance is as:*

$$x(k+1) = A_i x(k) + B_i u(k) + B_i^w w(k) a_i \quad for \quad \begin{bmatrix} x(k) \\ u(k) \end{bmatrix} \in \mathcal{X}_i, \qquad (4.16)$$

$$y_m(k) = C x(k) + D_i^w w(k) \qquad (4.17)$$

where $w(k) \in \mathcal{R}^r$ is a disturbance signal and initial condition is zero $x_0 = 0$. If there exist a function $V(x)$ for $[x^T \ u^T]^T \in \mathcal{X}_i$ satisfying the dissipativity inequality as

$$\forall k, V(x(k+1)) - V(x(k)) < (\gamma^2 \|w\|^2 - \|y\|^2), \qquad (4.18)$$

then, the H_∞ performance condition $\sum_{k=0}^{N} \|y(k)\|^2 < \gamma \sum_{k=0}^{N} \|w(k)\|^2$ is satisfied and system (4.16) is stable.

4.3   Passive Fault Tolerant Control

In this section the faulty model of (4.4) is introduced and a state feedback fault tolerant controller for stabilizing and satisfying a acceptable performance of the faulty system is given. For more details about the design of the passive fault tolerant controller and how to transform it into feasibility of a set of LMIs, the readers are referred to [GCSB11a] and [GCSB11b].

4.3.1   Fault Model

Actuator faults are considered. u_j is the actuator output. The partial loss of actuator can be formulated as

$$u_j^F = (1 - \alpha_j)u_j, \quad 0 \leq \alpha_j \leq \alpha_{Mj}, \qquad (4.19)$$

where α_j is the percentage of efficiency loss of the actuator j and α_{Mj} is the maximum loss. $\alpha_j = 0$ corresponds to the nominal system, $\alpha_j = 1$ corresponds to 100% loss of the actuator and $0 \leq \alpha_j \leq 1$ corresponds to partial loss. Let us define α as

$$\alpha = diag\{\alpha_1, \alpha_2, \ldots, \alpha_m\}. \qquad (4.20)$$

Then

$$u^F = \Gamma u, \qquad (4.21)$$

where $\Gamma = (I_{m \times m} - \alpha)$, I is a identity matrix. Thus u^F represents the control signal that is applied in normal or faulty situation. The PWA model of the system with the fault F_i is

$$x(k+1) = A_i x(k) + B_i \Gamma u(k) + a_i \quad for \quad \begin{bmatrix} x(k) \\ u(k) \end{bmatrix} \in \mathcal{X}_i \qquad (4.22)$$

4.3.2   State Feedback Control Design

The piecewise linear state feedback control can be specified as:

$$u(k) = K_i x(k) \ for \ \begin{bmatrix} x(k) \\ u(k) \end{bmatrix} \in \mathcal{X}_i \qquad (4.23)$$

where K_i is controller gain designed to stabilize asymptotically the closed loop PWA system. Since the index i is not a priori known, it is not possible to calculate $u(k)$. Hence, the problem is changed to the following structure

$$u(k) = K x(k) \quad for \quad \begin{bmatrix} x(k) \\ u(k) \end{bmatrix} \in \mathcal{X}_i. \qquad (4.24)$$

It means that we are positive; that we consider the same controller in all regions $\mathcal{X}_i$ with $i \in \mathscr{I}$.

Considering the piecewise affine faulty model of (4.22) and applying the control law (4.24) the following closed loop system is obtained:

$$x(k+1) = \mathcal{A}_i x(k) + a_i \tag{4.25}$$
$$for\ \in \mathcal{X}_i,$$

where $\mathcal{A}_i = A_i + B_i \Gamma K$.

4.3.3 Passive Fault Tolerant Control of PWA Systems

The pasive fault tolerant control design through the following definition is obtained.

Definition 3. The control law (4.24) is a passive fault-tolerant control if the closed loop system (4.25), which is subject to fault F_i, is asymptotically stable i.e. the following inequality for system (4.25) is satisfied: $V(x(k+1)) - V(x(k)) < 0 \ \forall (i,j) \in \mathcal{S}$.

4.4 Simulation and Results

The method is applied to a climate control systems of a live-stock building, the PFTC objective is to tolerate actuator faults. The climate control system contains 10 actuators, 6 inlets, 3 fans and a heating system. Each of inlets consists of 6 or 12 connected inlets. In order to show the performance of the PFTC, 3 of the 6 inlets and 1 of the 3 fans are assumed to be faulty with 95% efficiency loss. $x(0) = 20°C$ and the aim is to regulate the temperature of each zone around $10°C$. The PFTC based on Definition 3 is designed for temperature regulation while the control inputs due to the physical restrictions are bounded. Here $\mathscr{I}_0 = 1$ and $\mathscr{I}_1 = 2, 3, 4$. The LMIs problem is solved with the YALMIP/SeDuMi solver.

Fig. 4.2 shows the temperature of each zone, the fault tolerant controller is able to track the reference signal after $1500\ s$ when there is no fault in the system. 3 of 6 inlets and 1 of 3 fans lose 95% of their efficiency at time 900 second. Fig. 4.3 shows that the controller with a small oscillation is still able to track precisely the reference signal after $2000\ s$. The bounded control signal for the faulty system is illustrated in Fig. 4.4.

4.5 Conclusion

Here, an active fault tolerant control (AFTC) scheme based on a switching mechanism between a set of predefined passive fault tolerant controllers (PFTC) is given. For design of the controllers, the nonlinear model of the system is approximated into piecewise affine (PWA) model. Each predefined controller is a passive fault tolerant controller which is robust to the actuator loss. The PWA model switches not only due to the state but also due to the control input. By using a common Lyapunov function for stability analysis, a state feedback controller is design such that the closed-loop system is able to track the reference signal in healthy situation as well as in the faulty case.
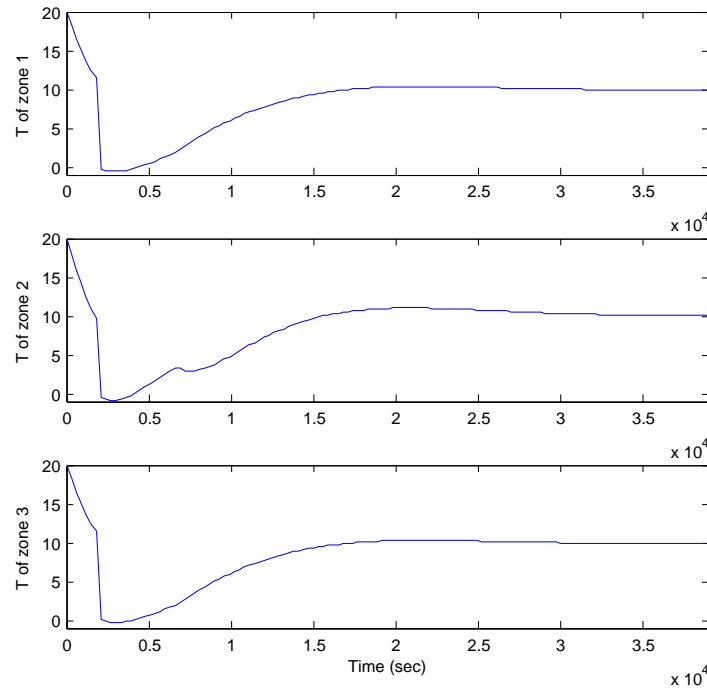
Figure 4.2: Simulation results with a controller designed to tolerate 95% actuator failure for the fault-free system
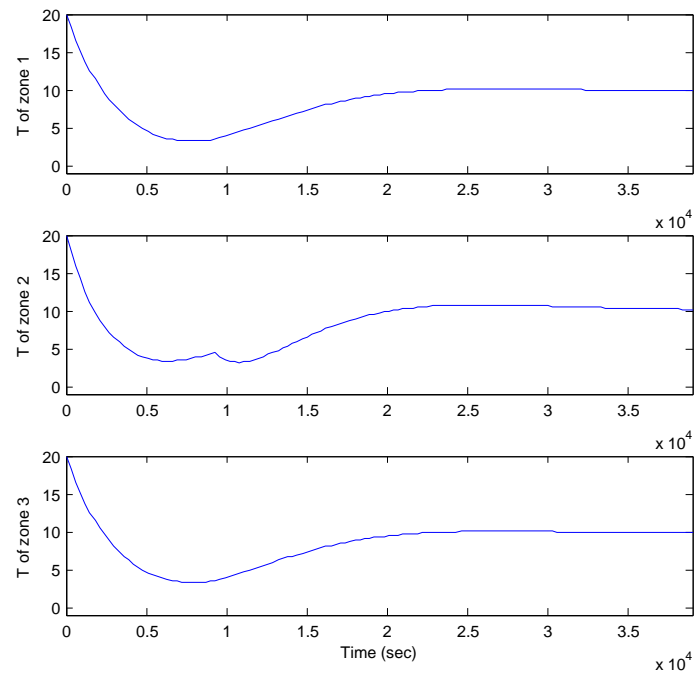
Figure 4.3: Simulation results with a controller designed to tolerate 95% actuator failure for the faulty system
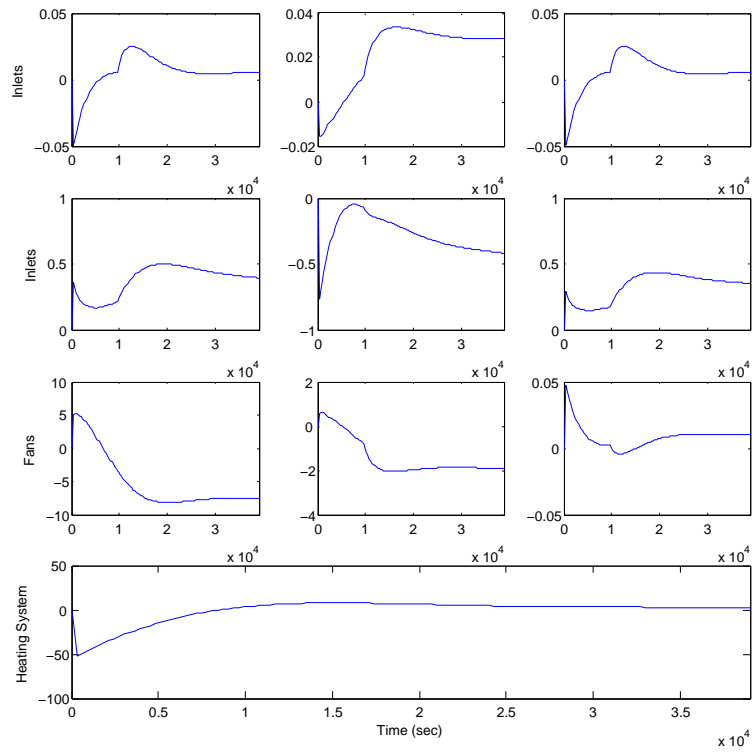
Figure 4.4: Angle of the inlets, voltages of the fans and temperature of the heating system. The inlet 1 to 3 and fan 3 lose 95% of their efficiency

5 | Conclusion

Nowadays, the live-stock buildings modernized with an intensive number of components such as different kinds of ventilation systems to increase farming production. Obviously, one of the most important issue for the live-stock buildings is safety and reliability of such systems. In this thesis, it was tried to investigate fault detection, identification (FDI) and fault tolerant control (FTC) of the climate control systems of live-stock buildings. First step was conducting a conceptual multi-zone model for indoor climate comfort of a pig stable. In order to derive a representation of the system, the internal stationary flow between neighboring zone was considered. The direction of the flow changes due to the environmental elements, which results in a piecewise modeling. Estimation of the coefficient of the nonlinear piecewise model is a challenge and was conducted by a extended Kalman filter (EKF). The EKF depends on the initial values and tuning factors, hereby a prior knowledge of the system is required. This knowledge was obtained by simplifying the modeling part into a single-zone model, and obtaining a rough estimation of the coefficient by a standard least mean square methods (LMS). comparison of simulated results with measurements confirmed the performance of the EKF and generally the multi-zone model, and showed that the model output tracks the trace of real data; however, some discrepancy between model and measurement values were observed. The model uncertainty is an unavoidable aspect of model identification and here related to environment disturbances, e.g., fluctuation of the wind speed and direction, ambient temperature and humidity. Note that, only temperature was considered for measuring the indoor climate comfort, and humidity has been disregarded as the sprinkler equipment was not installed at the time of measurement data acquisition. However, the dynamical model of humidity is similar to the temperature model, and it is straightforward to apply the fault diagnosis and fault tolerant algorithm for the humidity model.

The second step of this research was proposing a method for active fault detection and isolation in hybrid systems, which is based on off-line design of the excitation signal using sensitivity analysis. Designing the signals off-line reduces the computational efforts in the active fault diagnosis (AFD) algorithm. The problem of designing the inputs is formulated as a non-convex optimization problem for obtaining the maximum sensitivity for each individual system parameter, and it was solved by a genetic algorithm (GA). The faults are identified by comparing the nominal parameters of the system by those estimated by an EKF and a new adaptive filter. Simulation outcomes shows that the adaptive filter is able to detect actuator faults of the system faster than the EKF. It also illustrates that the adaptive filter is sensitive to the measurement and it is not able converge correctly to the parameters when the inputs are not provided by the sensitivity analysis.

Note that, the stable ventilation system is stable in open-loop and implementing the AFD algorithm over a short period does not destabilize it. However, for systems which are unstable in open-loop, stabilization criteria should be investigated in the AFD algorithm.

The required assumption for the AFD method is that the value of the system parameters are known and the system is only subject to actuator fault. This method is more beneficial in comparison with a bank of EKF where prior knowledge about the system faults and a model for each individual fault are required. Dedicating a model for each fault is computationally expensive for a system with a large number of sensors and actuators which can also be subject to different kinds of faults.

The last step was designing an active fault tolerant control (AFTC) based on a supervision scheme and a set of passive fault tolerant controllers (PFTC), which are designed off-line, and robust to a set of known faults. When a fault occurs in the system, the FDI scheme send the required information about the location and magnitude of the fault to the supervisor, the supervision scheme, which consists of a set of logic rules, e.g. if-then-else rules, switches from normal controller to a passive fault tolerant controller such that the system remains stable and a degraded performance is held. Design of the supervision scheme is simple and it has been disregarded here. Also in design of the passive fault tolerant controller, only actuator faults were considered.

The passive fault tolerant controller is designed for a discrete-time piecewise affine (PWA) model of the piecewise nonlinear model, the multi-zone model of the stable. The PWA model switches not only based on the state but also based on the control input. Design of the fault tolerant controller is based on H_∞ analysis. The stability guarantee of the closed loop system is investigated by a piecewise-quadratic (PWQ) Lyapunov function. The control problem is reformulated as a set of LMIs. The simulation illustrates that the controller is able to tolerate 90% actuator fault with an acceptable performance degradation. In this method, the input constraints are disregarded; while in many industrial systems, the control inputs can not take any value, and they should be less than a threshold. Hence, the input limitations are also integrated in the passive fault tolerant control design. By a common Lyapunov function for stability analysis and a state feedback controller, the control designed problem is cast as feasibility of a set of LMIs. The results show that the closed-loop system with a PFTC scheme tracks the reference signal precisely while the actuators are subject to 95% efficiency loss.

The contributions of the thesis are:

- A conceptual multi-zone model for indoor climate comfort of livestock stables.

- A method for active fault detection and isolation in hybrid systems based on sensitivity analysis and EKF.

- A method for active fault detection and isolation in hybrid systems based on sensitivity analysis and a new adaptive filter.

- A passive fault tolerant controller against actuator faults for discrete-time piecewise affine (PWA) systems based on H_∞ analysis. Here, the PWA system switches not only due to the state but also due to the control input.

- A passive fault tolerant controller (PFTC) based on state feedback for discrete-time piecewise affine (PWA) systems. The controller is tolerant against actuator faults and is able to track the reference signal while the control inputs are bounded.

- An approach for reconfigurability of discrete time PWA systems. Reconfigurability is defined as both stability and admissibility of the upper bound on the quadratic cost. Sufficient conditions for reconfigurability of a system subject to a fault with respect to a given threshold on the quadratic performance cost are given in terms of LMI. The upper bound is minimized by solving a convex optimization problem with LMIs constraints. Different cases where the system is reconfigurable with maximum number of actuator outages are defined. The simulation results illustrates that the performance of the system is acceptable

5.1 Future Work

There are different phenomena which effect on the climate control systems of the stables which generate large uncertainties in modeling of such systems. For example, ambient air flow reach the live-stock with different pattern with respect to different seasons, or amount of incoming air flow depends on the direction and speed of the ambient air, the type of the inlet and hanged flap of the inlet and etc. Therefore, deriving a physical formulation for each phenomenon in the stable is not neither simple nor real representative of the physics of the system. A useful modeling could be analytical input-output modeling instead of gray box, such as neural network. One of the important property of the indoor climate in stables is humidity, hence it is addressed to derive a model for humidity.

Since the majority of the systems are not open-loop stable, or AFD controller may destabilize the system, it is suggested to apply the AFD approach for closed loop systems, with considering model uncertainties, external disturbance, and stability analysis.

Since a system is not always full-state observable, it is recommended to use output-feedback controller. The model uncertainties should also be investigated. In the current literature, the output feedback problem is cast as a set of BMIs problem, and solved by a iteration algorithm. It is desirable to investigate the future research on formulating the BMIs problem into LMIs problem which are solvable by the free softwares.

It is addressed to design the supervision scheme. Sensor fault is on of the common fault in every system, and it is important to investigate the fault tolerant controllers which are robust against sensor faults and components faults. Since the closed loop active fault tolerant system switches between a set of predefined controllers, the stability of the overall system should also be considered .

References

[AC01]   A. Alessandri and P. Coletta. Design of Luenberger observers for a class of hybrid linear systems. *Hybrid systems: computation and control*, pages 7–18, 2001.

[ANC09]   Esna Ashari Alireza, Ramine Nikoukhah, and Stephen L. Campbell. Active Robust Fault Detection of Closed-Loop Systems: General Cost Case. In *The 7th IFAC Symposium on Fault Detection, Supervision and Safety of Technical Processes*, pages 585–590, June 2009.

[And08]   I.V. Andjelkovic. *Auxiliary Signal Design for Fault Detection for Nonlinear Systems: Direct Approach*. PhD thesis, North Carolina State University, 2008.

[ASC08]   I. Andjelkovic, K. Sweetingham, and S.L. Campbell. Active fault detection in nonlinear systems using auxiliary signals. In *American Control Conference*, pages 2142–2147, Seattle, WA, 2008.

[BBBSV02]   A. Balluchi, L. Benvenuti, M. D. D Benedetto, and A.L. Sangiovanni-Vincentelli. Design of observers for hybrid systems. In *5th International Workshop on Hybrid Systems: Computation and Control*, pages 76–89, London, UK, 2002. Springer-Verlag.

[BKLS06]   M. Blanke, M. Kinnaert, J. Lunze, and M. Staroswiecki. *Diagnosis and Fault-Tolerant Control*. Springer-Verlag, 2006.

[BL10]   M. Benosman and K.Y. Lum. Passive actuators' fault-tolerant control for affine nonlinear systems. *Control Systems Technology, IEEE Transactions on*, 18(1):152–163, 2010.

[BN93]   M. Basseville and I.V. Nikiforov. *Detection of abrupt changes: theory and application*, volume 10. Citeseer, 1993.

[BTMO09]   M. Bayoudh, L. Travé-Massuyes, and X. Olive. Active diagnosis of hybrid systems guided by diagnosability properties. In *7th IFAC Symposium on Fault Detection, Supervision and Safety of Technical Processes*, 2009.

[CCN09]   D. Choe, S. L. Campbell, and R. Nikoukhah. Optimal piecewise-constant signal design for active fault detection. *International Journal of Control*, 82(1):130–146, 2009.

REFERENCES

[CCR97]   J. Boaventura Cunha, C. Couto, and A. E. Ruano. Real-time parameter estimation of dynamic temperature models for greenhouse environmental control. *Control Engineering Practice*, 5(10):1473 – 1481, 1997.

[CDA+06]   S. L. Campbell, K. J. Drake, I. Andjelkovic, K. Sweetingham, and D. Choe. Model based failure detection using test signals from linearizations: A case study. In *IEEE International Conference on Control Applications*, pages 2659–2664, 2006.

[CEMS04]   V. Cocquempot, T. El Mezyani, and M. Staroswiecki. Fault detection and isolation for hybrid systems using structured parity residuals. In *5th Asian Control Conference,*, volume 2, 2004.

[CFN+00]   R. Caponetto, L. Fortuna, G. Nunnari, L. Occhipinti, and M.G. Xibilia. Soft computing for greenhouse climate control. *Fuzzy Systems, IEEE Transactions on*, 8(6):753 –760, dec 2000.

[CFPF94]   A. Chipperfield, P. Fleming, H. Pohlheim, and C. Fonseca. Genetic Algorithm Toolbox for use with MATLAB. 1994.

[CH98]   Chuei-Tin Chang and Jung-Ing Hwang. Simplification techniques for ekf computations in fault diagnosis–suboptimal gains. *Chemical Engineering Science*, 53(22):3853 – 3862, 1998.

[CHN02]   S. L. Campbell, K. G. Horton, and R. Nikoukhah. Auxiliary signal design for rapid multi-model identification using optimization. *Automatica*, 38(8):1313–1325, 2002.

[Cla79]   R. N. Clark. The dedicated observer approach to instrument failure detection. In *Proc. of The 18th IEEE Conf. on Decision & Control*, pages 237–241, Fort Lauderdale, Fla., December 1979.

[CM01]   F.A. Cuzzola and M. Morari. A generalized approach for analysis and control of discrete-time piecewise affine and hybrid systems. *Hybrid Systems: Computation and Control*, 2034:189–203, 2001.

[CP99]   J. Chen and R.J. Patton. *Robust model-based fault diagnosis for dynamic systems*. Kluwer Academic Publishers Norwell, MA, USA, 1999.

[DGM+02]   O. Durou, V. Godet, L. Mangane, D. Prarnaud, and R. Roques. Hierarchical fault detection, isolation and recovery applied to cof and atv avionics. *Acta Astronautica*, 50(9):547 – 556, 2002.

[DKB09]   M. J. Daigle, X. D. Koutsoukos, and G. Biswas. An event-based approach to integrated parametric and discrete fault diagnosis in hybrid systems. *Transactions of the Institute of Measurement and Control*, pages 1–24, 2009.

[ERH05]   N.M. El-Rabaie and IA Hameed. Fuzzy neural fault detection and isolation. *Proc. of the 7th Intl. Livestock*, pages 89–96, 2005.

[FC09]   Martene Fair and Stephen L. Campbell. Active incipient fault detection with two simultaneous faults. In *The 7th IFAC Symposium on Fault Detection, Supervision and Safety of Technical Processes*, pages 585–590, June 2009.

[FD97]   P. M. Frank and X. Ding. Survey of robust residual generation and evaluation methods in observer-based fault detection systems. *Journal of process control*, 7(6):403–424, 1997.

[Fen02]   G. Feng. Controller design and analysis of uncertain piecewise-linear systems. *IEEE Transactions on Circuits and Systems I: Fundamental Theory and Applications*, 49(2):224 –232, 2002.

[Fra90]   Paul M. Frank. Fault diagnosis in dynamic systems using analytical and knowledge-based redundancy: A survey and some new results. *Automatica*, 26(3):459 – 474, 1990.

[GB09]   Esteban R. Gelso and Mogens Blanke. Structural analysis extended with active fault isolation - methods and algorithms. In *The 7th IFAC Symposium on Fault Detection, Supervision and Safety of Technical Processes*, June 2009.

[GCF⁺95]   J. Gertler, M. Costin, Xiaowen Fang, Z. Kowalczuk, M. Kunwer, and R. Monajemy. Model based diagnosis for automotive engines-algorithm development and testing on a production vehicle. *Control Systems Technology, IEEE Transactions on*, 3(1):61 –69, mar 1995.

[GCSB11a]   M. Gholami, V. Cocquempot, H. Schiler, and T. Bak. Passive fault tolerant control of piecewise affine systems based on h infinity synthesis. In *Submitted to IFAC 18th World Congress*, 2011.

[GCSB11b]   M. Gholami, V. Cocquempot, H. Schiler, and T. Bak. Passive fault tolerant control of piecewise affine systems with reference tracking and input constraints. In *Accepted in IEEE Multi-Conference on Systems and Control * September 28-30, 2011 * Denver, CO 80202, USA*, 2011.

[Ger91]   J. Gertler. Analytical redundancy methods in fault detection and isolation. In *IFAC Symposium Safeprocess*, volume 1, pages 9–21, 1991.

[GLC09]   Y. Gao, Z. Liu, and H. Chen. Robust h infinity control for constrained discrete-time piecewise affine systems with time-varying parametric uncertainties. *Control Theory Applications, IET*, 3(8):1132 –1144, august 2009.

[GSB11a]   M. Gholami, H. Schiler, and T. Bak. Active fault diagnosis for hybrid systems based on sensitivity analysis and adaptive filter. In *Accepted in IEEE Multi-Conference on Systems and Control * September 28-30, 2011 * Denver, CO 80202, USA*, 2011.

REFERENCES

[GSB11b] M. Gholami, H. Schiler, and T. Bak. Active fault diagnosis for hybrid systems based on sensitivity analysis and ekf. In *American Control Conference (ACC 2011), accepted*, 2011.

[GSS10] M. Gholami, H. Shioler, and T. Soltani, M. Bak. Multi-Zone Hybrid Model for Failure Detection of the Stable Ventialation System. In *Proceedings of Industrial Electronic Society*, 2010.

[Hei04] P. Heiselberg. Natural and hybrid ventilation. Technical report, Aalborg University of Denmark, 2004.

[Jan09] Lunze Jan. Diagnosability of Deterministic I/O Automata. In *7th IFAC Symposium on Fault Detection, Supervision and Safety of Technical Processes*, pages 1378–1383, June 2009.

[Jes07] Jan Jacob Jessen. *Embedded Controller Design for Pig Stable Ventilation Systems*. Department of Control Engineering, Aalborg University, 2007.

[JSB06] J.J. Jessen, H. Schioler, and F. Bajersvej. Parameter estimation for zone based climate dynamics. In *IASTED International Conference on Computational Intelligence*, volume 523, page 6, 2006.

[JVBZD+04] K. Janssens, A. Van Brecht, T. Zerihun Desta, C. Boonen, and D. Berckmans. Modeling the internal dynamics of energy and mass transfer in an imperfectly mixed ventilated airspace. *Indoor Air*, 14(3):146–153, 2004.

[KAR07] Greisen S. K., Pedersen N. A., and Hansen J. R. Efficient and reliable indoor climate control for livestock stables. Master's thesis, Dept. Elect. Eng , AALBORG UNIVERSITY, 2007.

[Knu03] M. Knudsen. Experimental modelling of dynamic systems. Technical report, Department of Control Engineering, Aalborg University, 2003.

[KRD+03] N. Kabbaj, M. Ramzi, B. Dahhou, H. Youlal, and G. Enea. Fault detection and isolation in a greenhouse using parity relations. In *Emerging Technologies and Factory Automation, 2003. Proceedings. ETFA '03. IEEE Conference*, volume 2, pages 747 – 752 vol.2, sept. 2003.

[KV02] S. Kanev and M. Verhaegen. Reconfigurable robust fault-tolerant control and state estimation. In *Proceedings of the 15th IFAC World Congress on Automatic Control*, 2002.

[LGS02] R. Linker, P. O. Gutman, and I. Seginer. Observer-based robust failure detection and isolation in greenhouses. *Control Engineering Practice*, 10(5):519 – 531, 2002.

[LHD97] P. Lindskorg, H. Hellendoorn, and D. Driankov. Fuzzy Model Identification: Selected Approaches. *Fuzzy Model Identification: Selected Approaches*, 1997.

[LR08]   S. LeBel and L. Rodrigues. Piecewise-affine parameter-varying control of wheeled mobile robots. In *American Control Conference, 2008*, pages 195–200. IEEE, 2008.

[LRM08]   J. Lunze, JH Richter, and J. MACIEJOWSKI. Reconfigurable Fault-tolerant Control: A Tutorial Introduction. Discussion. Commentary. *European journal of control*, 14(5):359–390, 2008.

[Lun08]   J. Lunze. Fault diagnosis of discretely controlled continuous systems by means of discrete-event models. *Discrete Event Dynamic Systems*, 18(2):181–210, 2008.

[LXJ$^+$]   S. Lianqing, Z. Xiaodan, Q. Jiqing, Z. Changjie, Z. Yanchun, and G. Yuming. Robust passive fault-tolerant control for uncertain non-linear stochastic systems with distributed delays. In *Control Conference (CCC), 2010 29th Chinese*, pages 1949–1953. IEEE.

[MWL09]   S.K. Mishra, S.Y. Wang, and K.K. Lai. *Generalized convexity and vector optimization*. Springer Verlag, 2009.

[NB07]   S. Narasimhan and G. Biswas. Model-based diagnosis of hybrid systems. *IEEE transactions on man and cybernetics*, 37(3):347–361, 2007.

[NC06]   Ramine Nikoukhah and Stephen L. Campbell. Auxiliary signal design for active failure detection in uncertain linear systems with a priori information. *Automatica*, 42(2):219 – 228, 2006.

[NCD00]   R. Nikoukhah, S. L. Campbell, and F. Delebecque. Detection signal design for failure detection: a robust approach. *International Journal of Adaptive Control and Signal Processing*, 14(7):701–724, 2000.

[Nik98]   R. Nikoukhah. Guaranteed active failure detection and isolation for linear dynamical systems. *Automatica*, 34(11):1345–1358, 1998.

[NP09]   H. H. Niemann and N. K. Poulsen. Active Fault Diagnosis for Systems with Reduced Model Information. In *The 7th IFAC Symposium on Fault Detection, Supervision and Safety of Technical Processes*, June 2009.

[NRZ09]   N. Nayebpanah, L. Rodrigues, and Y. Zhang. Fault-tolerant controller synthesis for piecewise-affine systems. In *Proceedings of the IEEE American Control Conference*, pages 222–226, 2009.

[NS05]   H. H. Niemann and J. Stoustrup. Passive fault tolerant control of a double inverted penduluma case study. *Control engineering practice*, 13(8):1047–1059, 2005.

[OMP08]   C. Ocampo-Martinez and V. Puig. Fault-tolerant model predictive control within the hybrid systems framework: Application to sewer networks. *International Journal of Adaptive Control and Signal Processing*, 23(8):757–787, 2008.

REFERENCES

[Pat97]   R. J. Patton. Fault-tolerant control systems: The 1997 situation. In *3rd IFAC symposium on fault detection supervision and safety for technical processes*, volume 3, pages 1033–1054, 1997.

[PFC89]   R.J. Patton, P.M. Frank, and R.N. Clarke. *Fault diagnosis in dynamic systems: theory and application.* Prentice Hall, 1989.

[PN08]   N. K. Poulsen and H. H. Niemann. Active fault diagnosis based on stochastic tests. *International Journal of Applied Mathematics and Computer Science*, 18:487–496, 2008.

[PN09]   N. K. Poulsen and H. H. Niemann. Active fault diagnosis a stochastic approach. In *The 7th IFAC Symposium on Fault Detection, Supervision and Safety of Technical Processes*, 2009.

[QIJS03]   Zhihua Qu, Curtis M. Ihlefeld, Yufang Jin, and Apiwat Saengdeejing. Robust fault-tolerant self-recovering control of nonlinear uncertain systems. *Automatica*, 39(10):1763 – 1771, 2003.

[RB06]   L. Rodrigues and E.-K Boukas. Piecewise linear h_∞ controller synthesis with application to inventory control of switched production systems. *Automatica*, 42:1245–1254, 2006.

[RHvdWL10]   J. H. Richter, W. Heemels, N. van de Wouw, and J. Lunze. Reconfigurable control of piecewise affine systems with actuator and sensor faults: stability and tracking1. Technical report, Institute of Automation and Computer Control, Ruhr-Universität Bochum, 2010.

[RTAS07]   M. Rodrigues, D. Theilliol, S. Aberkane, and D. Sauter. Fault tolerant control design for polytopic LPV systems. *International Journal of Applied Mathematics and Computer Science*, 17(1):27–37, 2007.

[SPP00]   G. Schauberger, M. Piringer, and E. Petz. Steady-state balance model to calculate the indoor climate of livestock buildings, demonstrated for finishing pigs. *International Journal of Biometeorology*, 43:154–162, 2000.

[Sta02]   M. Staroswiecki. On reconfigurability with respect to actuator failures. In *Proceedings of the 15th Triennial World Congress of IFAC*, 2002.

[Sto09]   J. Stoustrup. An observer parameterization approach to active fault diagnosis with applications to a drag racing vehicle. In *Proceedings of the 7th IFAC Symposium on Fault Detection, Supervision and Safety of Technical Processes*, Barcelona, Spain, June 2009.

[SW]   C. Scherer and S. Weiland. Linear matrix inequalities in control. Lecture note, Dutch Institute for Systems and Control, Delft, The Netherlands; 2000.

[TIZBR10]   S. Tabatabaeipour, R. Izadi-Zamanabadi, T. Bak, and A. P. Ravn. Passive fault-tolerant control of piecewise linear systems against actuator faults. *submitted to International Journal of Systems Science*, 2010.

[TIZRB10]   S. Tabatabaeipour, R. Izadi-Zamanbadi, A. P. Ravn, and T. Bak. Stabilizable active diagnosis of hybrid systems. *submitted to International Journal of Control*, 2010.

[TRIZB10]   S. Tabatabaeipour, A. P. Ravn, R. Izadi-Zamnabadi, and T. Bak. Active diagnosis of MLD systems using distinguishable steady outputs. In *IEEE International Symposium on Industrial Electronics*, 2010.

[Vei95]   R.J. Veillette. Reliable linear-quadratic state-feedback control. *Automatica*, 31(1):137–144, 1995.

[VF05]   Villella and Fortunato. An hybrid approach to fault detection diannosis and reconfiguration in a pig stable with distribute measurements. Master's thesis, Aalborg University, 2005.

[VRK03]   V. Venkatasubramanian, R. Rengaswamy, and S.N. Kavuri. A review of process fault detection and diagnosis:: Part II: Qualitative models and search strategies. *Computers & Chemical Engineering*, 27(3):313–326, 2003.

[VRKY03]   V. Venkatasubramanian, R. Rengaswamy, S.N. Kavuri, and K. Yin. A review of process fault detection and diagnosis:: Part III: Process history based methods. *Computers & Chemical Engineering*, 27(3):327–346, 2003.

[VRYK03]   V. Venkatasubramanian, R. Rengaswamy, K. Yin, and S.N. Kavuri. A review of process fault detection and diagnosis:: Part I: Quantitative modelbased methods. *Computers & Chemical Engineering*, 27(3):293–311, 2003.

[WDC75]   A.S. Willsky, JJ Deyst, and BS Crawford. Two self-test methods applied to an inertial system problem. *Journal of Spacecraft and Rockets*, 12:434–437, 1975.

[Wil76]   Alan S. Willsky. A survey of design methods for failure detection in dynamic systems. *Automatica*, 12(6):601 – 611, 1976.

[Wil86]   Alan S. Willsky. Detection of abrupt changes in dynamic systems. In *Detection of Abrupt Changes in Signals and Dynamical Systems, number 77 in Lecture Notes in Control and Information Sciences*, pages 27–49. Springer-Verlag, 1986.

[WLZ07]   R. Wang, M. Liu, and J. Zhao. Reliable H_∞ control for a class of switched nonlinear systems with actuator failures. *Nonlinear Analysis: Hybrid Systems*, 1(3):317–325, 2007.

[WLZL07]   W. Wang, L. Li, D. Zhou, and K. Liu. Robust state estimation and fault diagnosis for uncertain hybrid nonlinear systems. *Nonlinear Analysis: Hybrid Systems*, 1(1):2–15, 2007.

REFERENCES

[WSH08]   Z. Wu, J. Stoustrup, and P. Heiselberg. Parameter estimation of dynamic multi-zone models for livestock indoor climate control. In *29th AIVC Conference on advanced building ventilation and environmental technology for addressing climate change issues*, 2008.

[YJC09a]   H. Yang, B. Jiang, and V. Cocquempot. A fault tolerant control framework for periodic switched non-linear systems. *International Journal of Control*, 82(1):117–129, 2009.

[YJC09b]   Hao Yang, Bin Jiang, and Vincent Cocquempot. Fault tolerant control in hybrid systems: A brief survey. In *Safeprocess09*, 2009.

[YWS01]   G.H. Yang, J.L. Wang, and Y.C. Soh. Reliable H_∞ controller design for linear systems. *Automatica*, 37(5):717–725, 2001.

[ZJ08]   Y. Zhang and J. Jiang. Bibliographical review on reconfigurable fault-tolerant control systems. *Annual Reviews in Control*, 32(2):229–252, 2008.

[ZT09]   J. Zhang and W. Tang. Output feedback optimal guaranteed cost control of uncertain piecewise linear systems. *International Journal of Robust and Nonlinear Control*, 19:596–590, 2009.

Contributions

Paper A: Multi-Zone hybrid model for failure detection of the stable ventilation systems

Paper B: Active Fault Diagnosis for Hybrid Systems Based on Sensitivity Analysis and EKF

Paper C: Active Fault Diagnosis for Hybrid Systems Based on Sensitivity Analysis and Adaptive Filter

Paper D: Reconfigurability of Piecewise Affine Systems Against Actuator Faults

Paper E: Passive Fault Tolerant Control of Piecewise Affine Systems Based on H Infinity Synthesis

Paper F: Passive Fault Tolerant Control of Piecewise Affine Systems with Reference Tracking and Input Constraints

Paper A

**Multi-Zone hybrid model for failure detection of the stable
ventilation systems**

Mehdi Gholami , Henrik Schioler, Mohsen Soltani and Thomas Bak

Abstract

In this paper, a conceptual multi-zone model for climate control of a live stock building is elaborated. The main challenge of this research is to estimate the parameters of a nonlinear hybrid model. A recursive estimation algorithm, the Extended Kalman Filter (EKF) is implemented for estimation. Since the EKF is sensitive to the initial guess, in the following the estimation process is split up into simple parts and approximate parameters are found with a non recursive least squares method in order to provide good initial values. Results based on experiments from a real life stable facility are presented at the end.

1 Introduction

In order to improve live-stock production performance, modern stables are equipped with advanced controllers and equipments for providing a convenient indoor climate. Consequently, the failure detection of components and controllers are of crucial importance, as component failures may lead to unacceptable loss of animal productions. Besides, replacing the failed components is time consuming and costly for the farmer. The majority of failure detection methods are model-based, because detection of a fault or failure is easy and reliant on fault free in comparison with faulty model. Overall, there are two methods for modeling, the first one relies on analyzing input and output data and the second one is mathematical modeling which uses physical laws for the system. In [1] it is discussed how to perform a dynamic temperature modeling based on input and output data. In [2], a steady state indoor climate model for pig stable is presented. However; it must be noted that [3],[4] shows a third method which is a combination of the two main ideas such that at first physical laws is utilized to derive a model and thereafter its parameters are estimated by analyzing the input and output data. This is known as grey box modeling in the literature [5].

In reality the airspace inside a large livestock building is incompletely mixed, and this concept has fostered the idea of multi zone climate modeling. Where models separate into non-interacting [6] or interacting zone models [7].

The aim of the work presented here is to derive a model for active fault detection and isolation of the pig stable ventilation system which is validated by a laboratory as a typical equipped stable. The model is an extension of previous research in this laboratory [3],[4] aiming at a more representative model of the real systems. In fact, both previous works were conducted with control objective in mind, where robust control designs allow for less accurate modeling. In addition, standard control design tools restricts the model domain, while performance of fault detection mechanism depends on model accuracy and small improvement on an absolute linear scale may reduce the detection error rate by orders of magnitude. In both [3],[4], the experiment data for estimation of inlets and outlets is provided from manufacturer data sheets, therefore the simulated model do not fit well with the stable measurements. During the research presented here, it is tried to define the model parameters according to the laboratory experiments and rely on a nonlinear estimation method. In [4], the pressure for the entire stable is assumed constant and consequently the stationary flow between zones is considered insignificant in comparison with the incoming and outcoming flows and thus neglected. Whereas, the

pressures of zones of the stable are allowed to differ in [3], approximations are introduced by linearization, which reducing model accuracy.

In the present work, the pressure is defined by more precise equations and consequently the stationary flows between zonal borders are included. Due to the indoor and outdoor conditions, the airflow direction varies between any adjacent zones. Therefore, the system behavior is represented with different discrete dynamic equations (piecewise equation). In the literature, these kinds of systems with behavior expressed by piecewise equations are classified as hybrid systems [8].

Multi-zone hybrid models are generally not linear in their parameters and their estimation is one of the challenges for this research. The parameters are estimated by a recursive estimation algorithm, the extended kalman filter (EKF), as it is able to converge precisely to the parameters of the nonlinear hybrid models. Furthermore, the EKF is sensitive to the parameter changes which are useful for online or active fault detection. A data set is acquired from a real scale pig stable. The verification of the prediction and measurement output validates the performance of the simulated model.

The paper is organized as follows: in Section 2 descriptions of the mathematical modeling are given. Thereafter the suggested estimation algorithm is presented in Section 3. Section 4 represents the experiments setup, and the accomplishments of EKF and modeling by presenting experimental results are described in Section 5. Finally the conclusion and remarks are presented in Section 6.

2   Model Description

The airspace inside the stable is incompletely mixed, so it is divided into three conceptually homogeneous parts which is called multi-zone climate modeling. Due to the indoor and outdoor conditions, the airflow direction varies between adjacent zones. Therefore, the system behavior is represented with different discrete dynamic equations. In more details, each flow direction depends on its relevant condition (invariant condition) and as long as the condition is met by the states, the system behavior is expressed according to the appropriate dynamic equations. Once the states violates the invariant condition and satisfies a new one, the system behavior is defined with a new equation. A schematic diagram of the stable system is illustrated in Fig. 6.1, and general information of the facility of laboratory is given in [4]. More details about the relevant condition for the airflow direction are illustrated in Fig. 6.2 and their relevant equations are given:

$$q_{i-1,i}^{st} = m_1(P_{i-1} - P_i) \tag{6.1}$$

$$q_{i,i+1}^{st} = m_2(P_i - P_{i+1}) \tag{6.2}$$

$$q_{i-1,i}^{st} = \left\{q_{i-1,i}^{st}\right\}^{+} - \left\{q_{i-1,i}^{st}\right\}^{-} \tag{6.3}$$

where P_i is pressure inside zone i, which is calculated by the mass balance equation for each zone i. m_1 and m_2 are constants coefficients, and $q_{i-1,i}^{st}$ and $q_{i,i+1}^{st}$ are stationary flows. The use of curly brackets is defined as:

$$\left\{q_{i-1,i}^{st}\right\}^{+} = max(0, q_{i-1,i}^{st}), \;\; \left\{q_{i-1,i}^{st}\right\}^{-} = min(0, q_{i-1,i}^{st}) \tag{6.4}$$
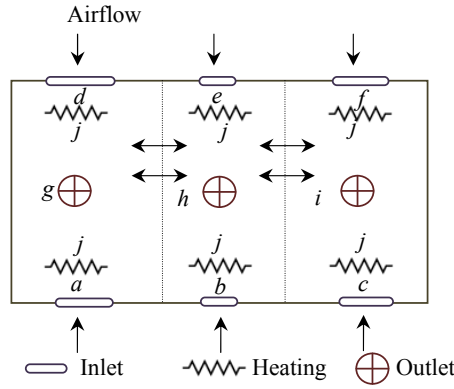
Figure 6.1: The top view of the test stable
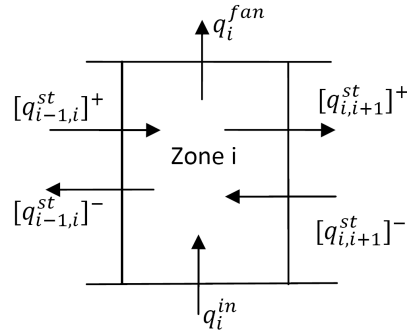
Figure 6.2: Illustration flow for zone i.

2.1 MATHMATICAL MODELING

The model is intended to be a realistic representation of internal temperatures for all multizone types of livestock buildings. It is divided into subsystems as follows: Inlet model for both windward and leeward, outlet model, and stable heating system, and finally the dynamic model of temperature based on the heat balance equation.

2.1.1 Inlet Model

An inlet is basically built into an opening in the wall and it consists of a hinged flap for adjusting amount and direction of the incoming air. Compared to the results in [3, 4], the following approximated model for airflow q_i^{in} $[m^3/s]$ into the zone i is suggested.

$$q_i^{in} = k_i(a_i + leak)\Delta P_{inlet}^i \tag{6.5}$$

$$\Delta P_{inlet}^i = 0.5C_P V_{ref}^2 - P_i + \rho g(1 - \frac{T_o}{T_i})(H_{NLP} - H_{inlet}) \tag{6.6}$$

where k_i and $leak$ are constants, a_i is the opening angle of the inlets, ΔP_{inlet}^i is the pressure difference across the opening area and wind effect, ρ is the outside air density,

V_{ref} is the wind speed, C_p stands for the wind pressure coefficient. H stands for height and H_{NLP} is the neutral pressure level which is calculated from mass balance equation [9]. T_i and T_o are temperature inside and outside the stable and g is gravity constant.

2.1.2 Outlet Model

The outlet is a chimney with an electrically controlled fan and plate inside. The following simple linear model for the airflow out of zone i is given by [3],[4]:

$$q_i^{fan} = u_{fan}^i c_i - d_i \Delta P_{outlet}^i \tag{6.7}$$

with defining ΔP_{outlet} as [10]:

$$\Delta P_{outlet}^i = 0.5 C_{Poutlet} V_{ref}^2 - P_i + \rho g (1 - \frac{T_i}{T_o})(H_{NLP} \tag{6.8}$$

$$-H_{outlet})$$

$$\sum_{i=1}^{3} q_i^{in} \rho \frac{\Delta P_{inlet}^i}{|\Delta P_{inlet}^i|} + \sum_{i=1}^{3} q_i^{out} \rho = 0 \tag{6.9}$$

where c_i and d_i are constants, u_{fan}^i is fan voltage and the number of zones is 3.

2.1.3 Stable Heating Model

The overall stable heating model is taken from [11] and represented by the equations:

$$\dot{Q}_{heater} = C_1(T_{in} - T_{win})C_2 \tag{6.10}$$

$$C_1 = \dot{m}_{heater} c_{pwater} \tag{6.11}$$

$$C_2 = exp\left[\frac{-U_{heater} A_{pipe}}{\dot{m}_{heater} c_{pwater}}\right] - 1 \tag{6.12}$$

where $\dot{m}_{heater}$ is the mass flow rate of heating system, the heat capacity is presented by c_{pwater}, T_{in} and T_{win} are temperature inside and outside the stable and incoming flow of the heating system, U_{heater} is the overall average heat transfer coefficient and A_{pipe} is the cross area of the pipe. In order to derive a more precise stable heating model, C_2 is estimated from the laboratory experiments.

2.1.4 Modeling Climate Dynamics

The following formulation for the dynamical model of the temperature for each zone inside the stable is driven by thermodynamic laws. The dynamical model includes four piecewise nonlinear models which describe the heat exchange between adjacent zones:

$$M_i c_{p,i} \frac{\partial T_i}{\partial t} = Q_{i-1,i} + Q_{i,i-1} + Q_{i,i+1} + Q_{i+1,i} + Q_{in,i} \tag{6.13}$$

$$+ Q_{out,i} + Q_{conv,i} + Q_{source,i}$$

$$Q = \dot{m} c_p T_i, \quad Q_{i-1,i} = \left\{q_{i-1,i}^{st}\right\}^+ \rho c_p T_{i-1}, \tag{6.14}$$

$$Q_{i,i-1} = \left\{q_{i-1,i}^{st}\right\}^- \rho c_p T_i$$

where $Q_{in,i}$, and $Q_{out,i}$ represent the heat transfer by mass flow through inlet and outlet, $Q_{i-1,i}$ denotes heat exchange from zone $i-1$ to zone i which cause by stationary flow between zones. Q_{conv} is the convective heat loss through the building envelope and described as $UA_{wall}(T_i - T_o)$, $Q_{source,i}$ is the heat source, $\dot{m}$ is the mass flow rate, c_i is the heat capacity and M is the mass of the air inside zone i.

As seen in Fig. 6.3, there are four different directions for the stationary flow in the stable based on defined invariant conditions by pressure as (1-4), which yields four piecewise smooth equations for the indoor temperature of each zone. In the following the model is presented as hybrid state space equations:

$$\frac{dT}{dt} = f(T, u, q), \tag{6.15}$$

$$q = h_3(T, P, U) = \left[q_i^{in}, q_{1,2}^{st}, q_{2,3}^{st}, q_i^{out}\right]^T, i = 1, \ldots, 3 \tag{6.16}$$

$$U = \left[a_j, V_{fan}^i, Q_{heater}\right]^T, j = 1, \ldots, 6 \tag{6.17}$$

$$z = h_1(T, U) \tag{6.18}$$

$$h_2(P, T, U) = 0, \tag{6.19}$$

where f represents the hybrid state space equation for dynamics of the temperature, and flow equations are comprised in h_3. U is input, P denote the vector of pressures insides each zone and output of the system is given by z, and the h_2 function comprises the mass balance equation of (8.36).
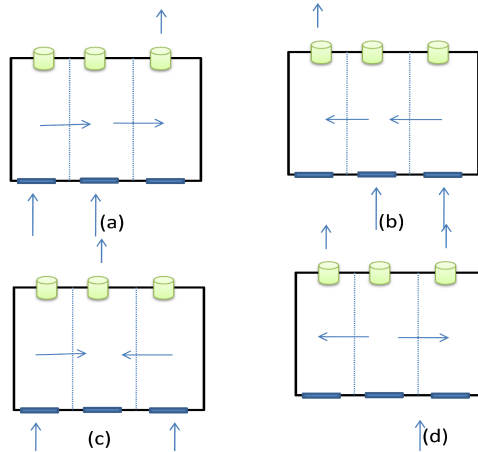
Figure 6.3: Four piecewise nonlinear models defined by different direction of the flow based on indoor pressure.

3 Parameter Estimation

In order to identify the model parameters by EKF, the state space model must be augmented by parameter variation dynamics:

$$\dot{X} = \begin{bmatrix} \dot{T} \\ \dot{C} \end{bmatrix} = \begin{bmatrix} f(T, U, q, \theta) + v \\ 0_{l \times 1} \end{bmatrix} \tag{6.20}$$

$$q = h_3(X, P, U) \tag{6.21}$$

$$h_2(P, X, U) = 0, \tag{6.22}$$

$$z = h_1 X + w, \tag{6.23}$$

where C is the coefficient matrix with zero dynamics, w is the measurement noise and consequently will be defined from sensor errors and is assumed to be zero mean. v is the process noise and can be estimated from variance error of the actuators and other equipments of the ventilation system. A discrete model is given as:

$$X(K) = f(T_{k-1}, u_{k-1}, q_{k-1}) + \begin{bmatrix} v_{k-1} \\ 0_{l \times 1} \end{bmatrix} \tag{6.24}$$

$$z_{k-1} = h_1(X_{k-1}) + w_{k-1} \tag{6.25}$$

$$\tag{6.26}$$

$$q_{k-1} = h_3(X_{k-1}, P_{k-1}, U_{k-1}) \tag{6.27}$$

$$h_2(P_{k-1}, X_{k-1}, U_{k-1}) = 0, \tag{6.28}$$

$$C = \begin{bmatrix} m_1 & m_2 & UA_{wall_{i=1,\ldots,3}} & K_{1\ i=1,\ldots,3} & C_{1\ i=1,\ldots,3} \\ & C_d & leak & c & d \end{bmatrix}^T \tag{6.29}$$

After extension of the space model with parameters, the next step in the EKF for achieving the estimation step is to linearizing the non-linear discrete equation 6.24 using a first order Taylor series expansion around the estimate

$$X_{k-1}(-),\ X_k \cong f(X_{k-1}(-)) + \phi_{X-1}(X_{k-1} - X_{k-1}(-)) + \tag{6.30}$$
$$\begin{bmatrix} v_{k-1} \\ 0_{l \times 1} \end{bmatrix},$$

where ϕ_X is the Jacobian matrix of f with respect to X. Since f is a function of X, U, q and their relations are implicit, the chain rule for several variable hypotheses is used to find the Jacobian matrix:

$$\phi_X = \frac{\partial f(X, U, q)}{\partial X} = f_X(X, U, q)\frac{\partial X}{\partial X} + f_q(X, U, q) \tag{6.31}$$
$$\frac{\partial q(X, U, P)}{\partial X},$$

$$\frac{\partial q(X, U, P)}{\partial X} = h_{3X}(X, U, P)\frac{\partial X}{\partial X} + h_{3P}(X, U, P)\frac{\partial P}{\partial X}, \tag{6.32}$$

according to Eq. 6.24:

$$\frac{\partial h_2(X, U, P)}{\partial X} = 0 = h_{2P}(X, U, P)\frac{\partial P}{\partial X} + h_{2X}(X, U, P)\frac{\partial X}{\partial X}, \quad (6.33)$$

$$\Rightarrow h_{2P}(X, U, P)\frac{\partial P}{\partial X} = -h_{2X}(X, U, P)$$

with respect that $h_{2p}(X, U, P)$ is a square matrix, and multiplying the both side of equation with $(h_{2p}(X, U, P))^{-1}$ it can be written as:

$$\frac{\partial P}{\partial X} = (h_{2P}(X, U, P))^{-1}h_{2X}(X, U, P)) \quad (6.34)$$

and finally with substituting the equation of (6.32) and (6.34)in (6.31) and implementing the appropriate invariant condition due to the equations of (8.2-8.9), the Jacobian matrix for the hybrid model will be defined. The discrete extended kalman algorithm which consists of two steps is presented as follows:

1. Prediction stage:

$$\hat{X}_k(-) = f_{k-1}(\hat{X}_{k-1}(+)) \quad (6.35)$$

$$P_k(-) = \phi_{k-1}P_{k-1}(+)\phi_{k-1}^T + Q_{k-1} \quad (6.36)$$

2. Update stage

$$\bar{K}_k = P_k(-)H_k^T[H_kP_k(-)H_k^T + R_k]^{-1} \quad (6.37)$$

$$\hat{X}_k(+) = \hat{X}_k(-) + \bar{K}_k(z_k - \hat{z}_k) \quad (6.38)$$

$$P_k(+) = 1 - \bar{K}_kH_kP_k(-), \quad (6.39)$$

where $Q = E(\begin{bmatrix}(v_{k-1})\\0_{l\times 1}\end{bmatrix}\begin{bmatrix}(v_{k-1})\\0_{l\times 1}\end{bmatrix}$ is the covariance matrix of the process noise, and $R = E[w_{k-1}\ w_{k-1}^T]$ is the covariance matrix of the measurement noise. $\bar{K}_k$ is the Kalman gain at time t_k, $\hat{X}_k(+)$ the expected value of X_k given the k measurements, $\hat{X}_k(-)$ is the predicted estate estimation and $H_k \approx \frac{\partial h_k}{\partial X}\big|_{X=\hat{X}_k(-)}$.

$$X_k(+) = E(X_k/Z_i, \ i = 1, \ldots, k), \quad (6.40)$$

$$(6.41)$$

P_K- is the covariance matrix of the prediction error

$$P_k(-) = E[(X_k - X_k(-))(X_k - X_k(-))^T/Z_i, \ i = 1, \ldots, k], \quad (6.42)$$

$$(6.43)$$

P_K+ is the covariance matrix of the estimation error

$$P_k(+) = E[(X_k - X_k(+))(X_k - X_k(+))^T/Z_i, \ i = 1, \ldots, k], \quad (6.44)$$

4   Experiment Outline

The experimental data were collected form a real large scale live-stock building with slow dynamic behavior with time constants around 10 minutes. The actuator settings (control signals) for ventilation systems are a Pseudo-Random Digital Signal (PRDS) with time granularity of 10 minutes and an amplitude variation. In fact, in order to excite the dynamic of the system, the amplitude of the control signals vary with multi-rate, for example voltage of the fan (substitute inside the chimney) changes between $0 - 2$ volt and after 2 hours it turns to $5 - 8$ volt and so on. There is also a similar scenario for the inlets. Temperature of the stable heating systems is held at 40 degrees with small oscillation; while, the flow of the heating system is fixed. For further information about the experiment design; see [4]. The system was running totally around 7 hours with a two minutes sampling period. The two-third of experiments is implemented for parameter estimation or in other word for constructing the appropriate model and the remaining is utilized for model validation. The experiment was conducted during spring when the deviation of wind is large and this additional disturbance cause more model uncertainty. In the following, the signals for different inputs are illustrated, as it is shown in Fig. 6.4.a and b, the ventilation systems changed considerably in order to obtain more temperature deviation for precise validation. The stable heating systems are constant; Fig. 6.4.c and d

5   Results and Discusion

The results are divided in two parts, the EKF result and model validation.

5.1   EKF estimation

In according to the literature [9], the EKF algorithm is highly depended on prior knowledge of the system and tuning factors, such as initial value of the parameters, process and measurements noise and covariance matrix. In order to find rough estimates of the parameters, the modeling task is divided into several parts. At first a model with single input and output (SISO) is defined, then the results are implemented for a modified model as a multi input-output (MIMO) system and finally the multi-zone system is obtained relying on previous results. The preliminary estimation and parameters of inlet and outlets for the simplified SISO model are conducted by standard least square. The EKF algorithm is used to estimate 14 parameters. The state and measurement for the EKF are:

$x = [T_1, T_2, T_3, m_1, m_2, UA_{wall1}, UA_{wall2}, UA_{wall3}, k_{11}, k_{12}, k_{13}, C_{11}, C_{12}$
$, C_{13}, V_1, V_2, V_3]$ and $z = [T_1, T_2, T_3, Q_{out1}, Q_{out2}, Q_{out3}, \Delta P_{in1}, \Delta P_{in2} \Delta P_{in3}]$

The initial and final values of the parameters are given in Table 6.1 and the result of EKF are illustrated in Fig. 5. The figure illustrates the results of prediction error by the constant predictor and the EKF according to the following equations:

$$\epsilon_{cp} = \sqrt{\sum (y_{k-1} - y_k)^2} \tag{6.45}$$

$$\epsilon_{EKF} = \sqrt{\sum (\hat{y}_k - y_k)^2} \tag{6.46}$$

Table 6.1: Amplitude and frequency of the input signals

Coefficients	Initial values	The EKF Values
m_1	1	2.5
m_2	1	2.5
UA_{wall1}	1000	893.194
UA_{wall2}	100000	136969.76
UA_{wall3}	10000	12580.385
k_{11}	500	8.99877620×10^2
k_{12}	500	9.01644600×10^2
k_{13}	500	8.99897274×10^2
C_{11}	1	-0.02560
C_{12}	1	-3.96949
C_{13}	1	-0.17612
C_d	0.01	0.03705
$leak$	0.01	0.0254097
c	0.1	0.6479337
d	0.01	0.0499638
V_1	10000	10687.91
V_2	100000	377403.62
V_3	10000	65461.13

where $\hat{y}_k$ is estimated state and y_k is the measurement. As it is clearly seen from Fig. 6.5, the EKF estimation error is less than the constant prediction error. So, it illustrates the benefits of the recursive estimations algorithm for the case of nonlinear parameter estimation

5.2 Model Validation

As it was mentioned in the previous part, the dynamic model for the indoor temperature of the stable is derived in multi-steps. At first the approximated parameters of the inlet and outlet are derived from SISO modeling, and thereafter the relevant equations for the stationary flows are analyzed and rough approximation of the parameters of the dynamic temperature equation are defined according to MIMO modeling. Finally the entire relevant parameters are estimated by the EKF. The result not only yields consistent positive estimation of the parameters value, but also confirms the performance of simulated model in comparison with the measurement. However, the model of the inlet is a simple linear model, the Fig. 6.6 for the prediction and measurement flow, illustrates that the model quite fits the measurements except for the peak of the graph, where there is a small discrepancy. In Fig. 6.7, the surface demonstrates the characteristic of the fan with pressure-voltage-flow data for the prediction and measurement data. As it is clearly seen, the linear model almost fits the real data except for the 0 and 10 voltages. This discrepancy yields that the linear model cannot represent well the nonlinear characteristic of the fan for those of points. The validation is carried out for open loop and with the inputs

signals which were not used in the estimation process. Then the simulation output was compared with the measurements. Fig. 6.8 presents the measurement and predicted data of the indoor temperature of the stable for every zone. It illustrates, that there is non neglectable discrepancy attributed to modeling error. The modeling error can be contributed to several factors such as sharp deviation of wind which mentioned before, heat capacity of the construction material, the latent heat loose through evaporation, the degree of air mixing, building leakage and large scale livestock building which cause high uncertainty.

6 Conclusion

A conceptual multi zone model for the indoor climate of a live-stock building was derived. The model was nonlinear in its parameters. An Extended Kalman Filter (EKF) was used because it is able to converge to the parameters of the nonlinear hybrid models; besides, the next aim of this research is active fault detection, and recursive estimation methods are well suited for such problems. It must be noted that, the EKF depends on the initial values and tuning factors, hereby a prior knowledge of the system is required. An experiment confirmed the performance of the EKF and generally the multi-zone model, which tracks the trace of real data; however, some discrepancy between predicted and measurement values were observed. The model uncertainty is an unavoidable aspect of model identification and here related to undesirable environment disturbances. Future work will address open questions for using analytical input-output modeling instead of grey box.

7 Acknowledgments

References

[1] J. B. Cunha, C. Couto, and A. E. Ruano, "Real-time parameter estimation of dynamic temperature models for greenhouse environmental control," *Control Engineering Practice*, vol. 5, no. 10, pp. 1473 – 1481, 1997.

[2] G. Schauberger, M. Piringer, and E. Petz, "Steady-state balance model to calculate the indoor climate of livestock buildings, demonstrated for finishing pigs," *International Journal of Biometeorology*, vol. 43, pp. 154–162, 2000.

[3] J. Jessen, H. Schioler, and F. Bajersvej, "Parameter estimation for zone based climate dynamics," in *IASTED International Conference on Computational Intelligence*, vol. 523, no. 2, 2006, p. 6.

[4] Z. Wu, J. Stoustrup, and P. Heiselberg, "Parameter estimation of dynamic multi-zone models for livestock indoor climate control," in *29th AIVC Conference on advanced building ventilation and environmental technology for addressing climate change issues*, 2008.

[5] P. Lindskorg, H. Hellendoorn, and D. Driankov, "Fuzzy Model Identification: Selected Approaches," *Fuzzy Model Identification: Selected Approaches*, 1997.

[6] K. Janssens, A. Van Brecht, T. Zerihun Desta, C. Boonen, and D. Berckmans, "Modeling the internal dynamics of energy and mass transfer in an imperfectly mixed ventilated airspace," *Indoor Air*, vol. 14, no. 3, pp. 146–153, 2004.

[7] R. Caponetto, L. Fortuna, G. Nunnari, L. Occhipinti, and M. Xibilia, "Soft computing for greenhouse climate control," *Fuzzy Systems, IEEE Transactions on*, vol. 8, no. 6, pp. 753 –760, dec 2000.

[8] A. Bemporad and M. Morari, "Control of systems integrating logic, dynamics, and constraints," *Automatica*, vol. 35, pp. 407–428, 1999.

[9] M. Gautier and P. Poignet, "Extended kalman filtering and weighted least squares dynamic identification of robot," *Control Engineering Practice*, vol. 9, no. 12, pp. 1361 – 1372, 2001.

[10] P. Heiselberg, "Natural and hybrid ventilation," Aalborg University of Denmark, Tech. Rep., 2004.

[11] G. S. K., P. N. A., and H. J. R., "Efficient and reliable indoor climate control for livestock stables," Master's thesis, Dept. Elect. Eng , AALBORG UNIVERSITY, 2007.
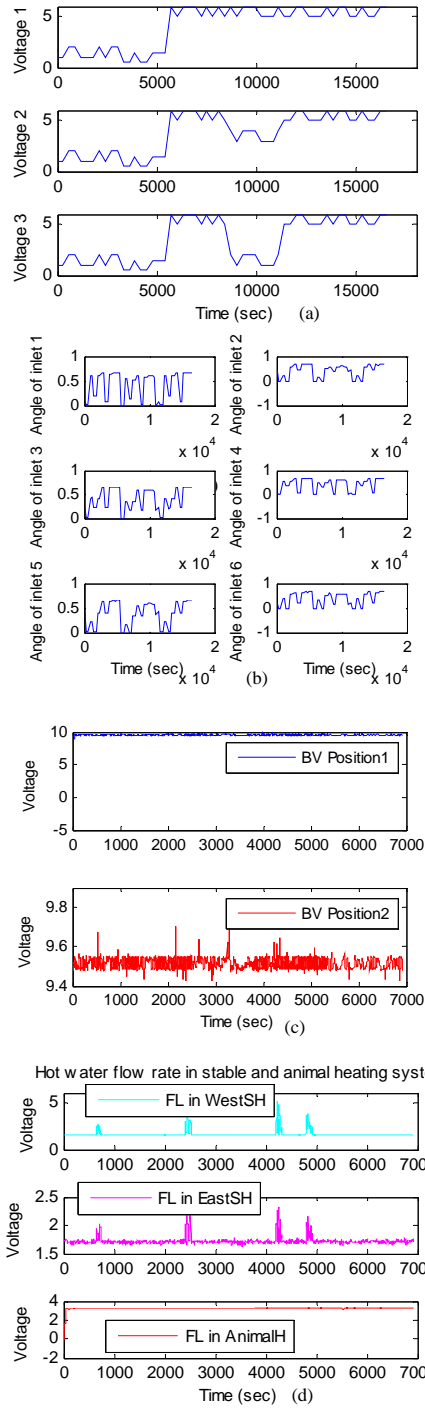
Figure 6.4: (a) voltage of fan, (b) the angle of inlets, (c) Ball-valve position for animal and stable heating systems, (d) Hot water flow rate in stable and.
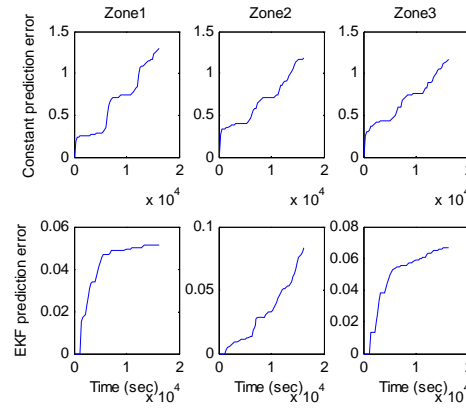
Figure 6.5: The prediction error by constant and EKF predictor.
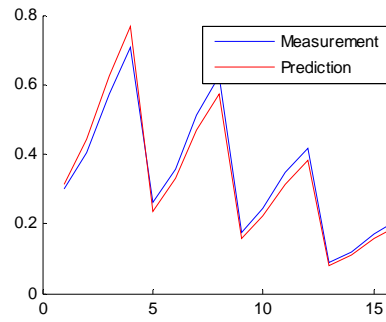
Figure 6.6: Graph for measurement and predicted flow for inlet.
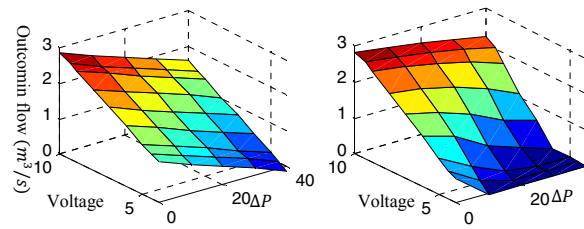
Figure 6.7: (a) Graph for predicted data. (b) Graph for measurement data.
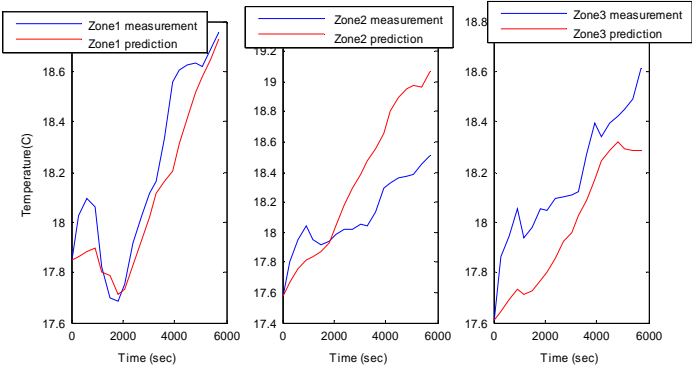
Figure 6.8: Indoor temperature for every zone.

Paper B

Active Fault Diagnosis for Hybrid Systems Based on Sensitivity Analysis and EKF

Mehdi Gholami, Henrik Schioler and Thomas Bak

Abstract

An active fault diagnosis (AFD) approach for different kinds of faults is proposed. The AFD approach excites the system by injecting a so-called excitation input. The input is designed off-line based on a sensitivity analysis in order that the maximum sensitivity for each individual system parameter is obtained. Using the maximum sensitivity results in better precision in the estimation of the corresponding parameter. The fault detection and isolation is done by comparing the nominal parameters with those estimated by an extended Kalman filter. In this study, Gaussian noise is used as the input disturbance as well as the measurement noise for simulation. This method is implemented on a large scale livestock hybrid ventilation model which was obtained during previous research.

1 Introduction

THE performance of modern control systems typically depends on a number of strongly interconnected components. Component faults may degrade the performance of the system or even result in a loss of functionality. In applications such as climate control systems for livestock buildings, this is unacceptable as it may lead to a loss of animal life. The methods for detection and isolation of component faults are either passive or active. Passive fault diagnosis (PFD), without acting upon the system decides if a fault has occurred based on observations of the system input and output. In active fault diagnosis (AFD), a diagnoser generates a so-called excitation input, which shapes the input to the system, in order to decide whether the output represents normal or faulty behaviour and if it is possible to decide which kind of fault has occurred. There are two perspectives for the benefit of AFD. The first one is to identify the faults that may be hidden due to the regulatory actions of controllers during the normal operation of the system. The second is to isolate the faults in systems with slow responses. Fault diagnosis of hybrid systems attracts the attentions of researchers because complex industrial systems involve both discrete and continuous components. Examples of AFD for linear system are in [1], [2], [3], [4] and [5]. AFD of hybrid systems has been addressed in [6], [7], [8], [9], [10] and [11]. In [11] and [8] the AFD approach is based on generating the excitation inputs online, and using model predictive control (MPC). The idea of AFD in [7] is quite different and uses selectively blocking or executing controllable events such that the fault detection is faster and more precise. In [6] the problem is addressed as a discrete event system and a finite state machine is used to guide the identification. In this paper, as in [4] and [12], we design the excitation inputs for AFD in an off-line mode. A benefit of off-line input design is that the online computational efforts of the fault diagnoser can focus only on the detection/isolation problem. This benefit is considerable when the system comprises a large number of inputs. Our approach embarks from a sensitivity analysis in order to generate the inputs. Here, the amplitude and frequency of the inputs are defined such that the maximum sensitivity value for each parameter of the system is obtained. Note that it is also possible to limit the value of the input signal by defining a boundary on the signal in the sensitivity analysis problem. Shaping the input according to the sensitivity analysis allows faults in the parameters to be easily identified. Finding the highest sensitivity for each parameter is a non-convex optimization problem. In order to solve a non-convex optimization problem with classical approaches, it must be reformulated as

Nomenclature	
$k, leak, c, d$	constants
a	opening angle of the inlets
ΔP_{inlet}	the pressure difference across the opening area of the inlet
i	the zone number
ρ	the outside air density
V_{ref}	the ambient wind speed
C_P	the wind pressure coefficient
H	Height
H_{NLP}	NLP stands for the neutral pressure level
P_i	pressure inside zone i
g	gravity constant
V_{fan}	fan voltage of the chimney in the stable
$C_{P_{outlet}}$	the wind pressure coefficient
T_i and T_o	temperature inside and outside the stable
m_1, m_2	constants,
$q^{st}_{i-1,i}, q^{st}_{i,i+1}$	stationary flows between two adjacent zones
$Q_{in,i}, Q_{out,i}$	heat transfer by mass flow
$Q_{i-1,i}$	heat exchange from zone $i-1$ to zone i
$Q_{i,i-1}$	heat exchange from zone i to $i-1$
Q_{conv}	convective heat loss through the building envelope and described as $UA_{wall}(T_i - T_o)$
Q_{source}	the heat source
$\dot{m}$	mass flow rate
c_P	heat capacity
F_A	actuator faults
N_i	regions neighbouring region i
$\hat{\theta}, \theta^*, \theta_N$ and $\theta \in \mathcal{R}^l$	the estimated, true, nominal and running parameter vectors of the system
$v(k)$ and $w(k)$	disturbance and measurement noises
y_m and y	output prediction and the measurement
ζ, ξ	a white Gaussian sequence
σ, λ	singular and eigenvalue
f_i	vector fields of the state space description.
$\mathfrak{g}_i$	a known function.

a convex problem. This reformulation is possible as long as some necessary conditions are satisfied, which is not always feasible. Hence we have used a genetic algorithm (GA) to solve the problem. The excitation inputs are applied in open loop and the required parameters of the system are estimated by the extended Kalman filter (EKF). By comparing the normal with the estimated parameters of the system, different incipient and severe faults can be identified. Note that it is not desirable to disturb a system continuously, therefore at first, the abnormal behaviour of the system is observed by a common PFD method, and then the AFD approach is applied over a shorter period. The climate control problem, used in the current research, is stable in open loop mode and application of the AFD over a short period does not destabilize it. However, for systems which are unstable in open loop, stabilization guarantees should be considered in the AFD algorithm. These guarantees are provided by the satisfaction of stability constraints.

This paper is organized as follows. Section II presents the preliminaries and problem formulation. The design of the input using sensitivity analysis is discussed in Section III. Section IV is dedicated to the EKF setup. An example is presented in Section V, and the experimental setup is discussed in VI. The results are given in Section VII, while the conclusion is presented in the last section.

2 Preliminaries and Problem Formulation

2.1 State-Input Dependent Nonlinear Switching Systems

The class of systems considered here are hybrid nonlinear systems with uncontrollable state-input dependent switching:

$$x(k+1) = f_i(x(k), u(k), k, \theta, F_A, v(k)), \ for \ \begin{bmatrix} x(k) \\ u(k) \end{bmatrix} \in \mathcal{X}_i \qquad (7.1)$$

$$y_m(k) = Cx(k) + F_s + w(k), \qquad (7.2)$$

where F_A and F_s are the actuator and sensor faults, $u(k) \in \mathbb{R}^m$ is the control input and $x(k) \in \mathbb{R}^n$ is the state, and $y_m(k) \in \mathbb{R}^p$ is the output. All variables are at time k, the sets

$$\mathcal{X}_i \underline{\triangleq} \{ \begin{bmatrix} x(k)^T u(k)^T \end{bmatrix}^T \ | \mathfrak{g}_i(x, u) \leq K_i, i = 1, \ldots, s \} \qquad (7.3)$$

are manifolds (possibly un-bounded) in the state-input space, $\theta \in \mathcal{R}^l$ is the parameter vector, $v(k)$ and $w(k)$ are the disturbance and measurement noise respectively, f_i are vector fields of the state space description, and $\mathfrak{g}_i$ is a known function. Here, it is assumed that the hybrid system is continuous:

$$f_i(x_*(k), u_*(k)) = f_j(x_*(k), u_*(k)) \quad j \in N_i \qquad (7.4)$$

where $(x_*(k), u_*(k))$ are the sampling points corresponding to the boundary between two neighbouring regions and N_i is the region neighbouring region i. Here, only the actuator fault is considered; however, we believe that it is also possible to detect the sensor fault by this parameter estimation technique and this will be considered in future work.

2.2 General Problem of AFD and Main Work

In the current research, the system parameters are related to the actuators. Assume that a faulty actuator is used rarely during the normal operation of the system, and hence has little effect on the system response. Consequently, its parameter is not identified correctly and a fault is not detected. In order to detect correctly the faulty behaviour of the system, a sequential input signal over a finite time interval is applied to the system. At the end of the interval, a fault isolation algorithm is executed to isolate the fault. Excitation of the system by the input leads the actuator to affect the system response; therefore the parameter may be estimated more precisely and the fault becomes observable. The main work is separated into two parts:

1. Design of the excitation input, off-line and relying on so-called sensitivity analysis in order that the maximum sensitivity for each individual system parameter is obtained.

2. Deriving the fault isolation algorithm, based on estimation of the system parameters with EKF and comparing those parameters with the normal values. The values are considered as a prior knowledge of the system.

3 Design of Excitation Input Using GA and Sensitivity Analysis

The goal is to design the excitation input using sensitivity analysis for more precise parameter estimation and consequently better fault isolation. To achieve this goal, first we analyse a parameter estimation algorithm based on a least mean square (LMS) method where the measurement signal includes noise, and a criterion for better estimation by the LMS algorithm in the presence of noisy signal is shown. Then the correspondence between the parameter estimation LMS algorithm and sensitivity analysis is described. Finally the excitation input signal is designed using GA and sensitivity analysis.

Let us assume that the problem is to estimate the system parameters through the following LMS approach.

$$\hat{\theta} = \underset{\theta}{\operatorname{argmin}} P(u, y, \theta, \xi) \tag{7.5}$$

where the performance function P is given by

$$P(u, y, \theta, \xi) = \frac{1}{2N} \sum_{k=1}^{N} \epsilon^2(k, u, y, \theta, \xi) \tag{7.6}$$

$$\epsilon(k, \theta, \xi) = y_m(k, \theta) - y(k, \xi), \tag{7.7}$$

where ξ is the noise signal, $y(k, \xi)$ is the measurement signal approximated as $y(k, \xi) = y_m(k, \theta^*, \xi)$, $y_m(k, \theta^*, \xi)$ is the output of the model when it depends on the noise signal ξ, and $y_m(k, \theta)$ is the output of the model when it does not depend on the noise signal ξ, we assume ξ is zero. Estimated, running and true parameter vectors are represented by $\hat{\theta}$, θ, θ^*. In the following we omit u and y from the notation. Consider the following

definitions:

$$\theta^* = \underset{\theta}{\operatorname{argmin}} P(\theta^*, 0) \Rightarrow [D_\theta P](\theta^*, 0) = 0 \tag{7.8}$$

$$\hat{\theta} = \underset{\theta}{\operatorname{argmin}} P(\hat{\theta}, \xi) \Rightarrow [D_\theta P](\hat{\theta}, \xi) = 0. \tag{7.9}$$

Let the performance function be approximated using the first and second order terms of a Taylor series expansion with respect to θ and ξ at θ^* and 0:

$$P(\theta, \xi) \approx P(\theta^*, 0) + [D_\theta P](\theta^*, 0)(\theta - \theta^*) + [D_\xi P](\theta^*, 0)\xi \tag{7.10}$$
$$+ (\theta - \theta^*)^T [D_{\theta,\theta} P](\theta^*, 0)(\theta - \theta^*) + \xi^T [D_{\xi,\xi} P](\theta^*, 0)\xi$$
$$+ \xi^T [D_{\theta,\xi} P](\theta^*, 0)(\theta - \theta^*) + (\theta - \theta^*)[D_{\xi,\theta} P](\theta^*, 0)\xi$$

where $D_\theta P = \frac{\partial P}{\partial \theta}$ and $D_{\theta,\xi} P = \frac{\partial^2 P}{\partial \theta \partial \xi}$. In order to derive the parameter θ from the smooth performance function $P(\theta, \xi)$, we apply the partial derivative of (8.9) on the performance function, the result is:

$$2[D_{\theta,\theta} P](\theta^*, 0)(\hat{\theta} - \theta^*) + \xi^T [D_{\theta,\xi} P](\theta^*, 0) \tag{7.11}$$
$$+ [D_{\xi,\theta} P](\theta^*, 0)\xi = 0 \Rightarrow$$
$$H(\hat{\theta} - \theta^*) = \zeta,$$

where $H = [D_{\theta,\theta} P](\theta^*, 0)$, and $\zeta = \xi^T [D_{\theta\xi} P](\theta^*, 0) + [D_{\xi\theta} P](\theta^*, 0)\xi$. ζ is the noisy signal, thus its large error should cause a small error in $\hat{\theta} - \theta^*$. This means that the condition number of matrix H should be small [14]. The condition number of the matrix H is:

$$\kappa(H) = \frac{\sigma_{max}(H)}{\sigma_{min}(H)}, \tag{7.12}$$

where σ_{max} and σ_{min} are the maximum and minimum of the singular values of the Hessian matrix H. In fact, assuming a small value of the condition number $\kappa(H)$, the LMS algorithm is able to estimate the parameter of the system more precisely in the presence of the noise.

Here, we specify the importance of (7.12) from the sensitivity analysis point of view. According to [13], a larger value of sensitivity for parameter θ leads to a smaller deviation of θ from the true value θ^* generates significant deviation in the value of ϵ. This fact results in more precise parameters estimation, as it is obvious from (7.5) to (7.7), and as discussed in detail in [13]. For obtaining high sensitivity for the entire system parameters, the ratio of maximum to minimum sensitivity should be small, i.e,

$$R = \frac{S_{max}}{S_{min}} = \frac{\sqrt{\lambda_{max}}}{\sqrt{\lambda_{min}}} = \frac{\sigma_{max}(H)}{\sigma_{min}(H)} \tag{7.13}$$

where the sensitivity is $S = \frac{\partial \epsilon}{\partial \theta}$ and λ is the eigenvalue of the Hessian matrix of H. As is obvious, the ratio in (7.13) is equal to the condition number (7.12), which shows the correspondence between the sensitivity analysis and parameter estimation algorithm based on the LMS approach.

In the following, we assume the input is a sinusoidal signal and its amplitude α and frequency $\mathfrak{f}$ are designed so that the minimum R is obtained:

$$U = \alpha sin(2\pi \mathfrak{f} t) \tag{7.14}$$

$$(\alpha, \mathfrak{f}) = \underset{\alpha, \mathfrak{f}}{\operatorname{argmin}} R \tag{7.15}$$

$$s.t. \begin{cases} (1) \\ \alpha_{min} \leqslant \alpha \leqslant \alpha_{max} \\ \mathfrak{f}_{min} \leqslant \mathfrak{f} \leqslant \mathfrak{f}_{max} \end{cases}$$

where α_{min} and α_{max} are minimum and maximum values of α, and $\mathfrak{f}_{min}$ and $\mathfrak{f}_{max}$ are the minimum and maximum values of $\mathfrak{f}$. In some cases, it may be necessary to consider more than one periodic signal in U for estimation of different parameters.

Equation (7.15) is non-convex and non-differentiable. To solve the problem with classical approaches, the problem must be changed to a convex problem by defining some constraints. Obtaining these constraints is not always feasible and is considered an open issue in the literature: see [14]. Using evolutionary search algorithms such as GA avoids having to change the problem to a convex one. As the optimization problem is calculated off-line, the computational effort is not important. The reader is referred to [15] for more details of the GA.

4   The EKF Setup

The aim of using the EKF is to estimate the parameters after exciting the system by the designed inputs. The abnormal behaviour of the system is detected from the estimated parameters.

According to a current literature survey about Kalman filtering (KF), [16] and [17], the EKF is similar to the parameter estimation procedure using the LMS approach as in (7.5). Hence, the result of the sensitivity analysis for parameter estimation problems based on the LMS approach is also relevant for the EKF.

The performance of the EKF depends on the matrix P. This matrix is independent of the system inputs, when the system operating point is constant, as in the stationary Kalman filter. The EKF algorithm approximates the nonlinear system by a Taylor series expansion around an operating point for every sample instant. If the operating point changes in each sample due to the input, the covariance matrix will depend on the input. The excitation input changes the operating point such that the covariance matrix rapidly decreases to zero. However, large variations are in most cases not desirable over long periods. Hence, at first an abnormal behaviour of the system is observed by a common PFD method. Then the AFD algorithm is applied for a short interval to identify different faults and those hidden during normal operation of the system.

Fault isolation relies on a simple algorithm. The algorithm isolates the fault F_i according to the residual generator $r_i = \hat{\theta}_i - \theta_{Ni}$, where θ_{Ni} is the nominal value of the ith parameter of the system, which is assumed as prior knowledge of the system, and $\hat{\theta}_i$ is the parameter estimated by the EKF. The fault isolation algorithm is given in Table 7.1. If r_i is greater than a predefined threshold δ, the system is subject to the fault F_i.

Table 7.1: Fault Isolation Algorithm

Algorithm 1

For $i = 0 \; to \; l$

    IF $r_i = \left| \hat{\theta}_i - \theta_{Ni} \right| > \delta$

        $F = F_i$

    End IF

End For

5 Example

The AFD algorithm is applied to the climate control system of a live-stock building, which was obtained during previous research, [18]. The general schematic of the large scale live-stock building equipped with its climate control system is illustrated in Fig. 7.1. In a large stable, the indoor airspace is incompletely mixed; therefore it is divided into conceptually homogeneous parts called zones. Due to the indoor and outdoor conditions, the airflow direction varies between adjacent zones. Therefore, the system behaviour is represented by a finite number of different dynamic equations. The model is intended to be a realistic representation of internal temperatures for all multi-zone types of livestock buildings. The model is divided into subsystems as follows:

5.1 Inlet Model

An inlet is built into an opening in the wall. The following approximated model for airflow, q_i^{in} into the zone i is used.

$$q_i^{in} = k_i(a_i + leak)\Delta P_{inlet}^i \tag{7.16}$$

$$\Delta P_{inlet}^i = 0.5 C_P V_{ref}^2 - P_i + \rho g(1 - \frac{T_o}{T_i})(H_{NLP} - H_{inlet}) \tag{7.17}$$

where P_i is the pressure inside zone i, k_i and $leak$ are constants, a_i is the opening angle of the inlets, ΔP_{inlet}^i is the pressure difference across the opening area and wind effect, ρ is
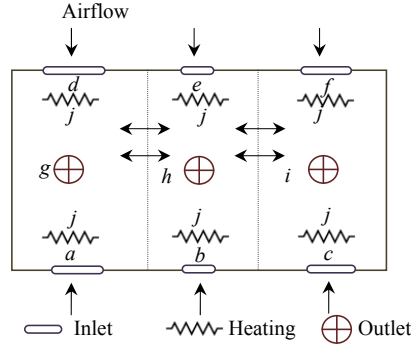
Figure 7.1: The top view of the test stable

the outside air density, V_{ref} is the wind speed, C_p stands for the wind pressure coefficient. H stands for the height and H_{NLP} is the neutral pressure level which is calculated from the mass balance equation. T_i and T_o are the temperature inside and outside the stable and g is the gravity constant.

5.2 Outlet Model

The outlet is a chimney with an electrically controlled fan and plate inside. A simple linear model for the airflow out of zone i is given by:

$$q_i^{out} = V_{fan}^i c_i - d_i \Delta P_{outlet}^i \tag{7.18}$$

$$\Delta P_{outlet}^i = 0.5 C_P V_{ref}^2 - P_i + \rho g(1 - \frac{T_i}{T_o})(H_{NLP} \tag{7.19}$$

$$-H_{outlet})$$

$$\sum_{i=1}^{3} q_i^{in} \rho \frac{\Delta P_{inlet}^i}{|\Delta P_{inlet}^i|} + \sum_{i=1}^{3} q_i^{out} \rho = 0 \tag{7.20}$$

where c_i and d_i are constants, V_{fan}^i is the fan voltage, and the number of zones is three. The stationary flows, $q_{i-1,i}^{st}$ and $q_{i,i+1}^{st}$, through the zonal border of two adjacent zones is given by:

$$q_{i-1,i}^{st} = m_1(P_{i-1} - P_i) \tag{7.21}$$

$$q_{i,i+1}^{st} = m_2(P_i - P_{i+1}) \tag{7.22}$$

$$q_{i-1,i}^{st} = \left\{q_{i-1,i}^{st}\right\}^+ - \left\{q_{i-1,i}^{st}\right\}^- \tag{7.23}$$

where m_1 and m_2 are constant coefficients. The use of curly brackets is defined by:

$$\left\{q_{i-1,i}^{st}\right\}^+ = max(0, q_{i-1,i}^{st}), \quad \left\{q_{i-1,i}^{st}\right\}^- = min(0, q_{i-1,i}^{st}) \tag{7.24}$$

5.3 Modeling Climate Dynamics

The following formulation for the dynamical model of the temperature for each zone inside the stable is driven by thermodynamic laws. The dynamical model includes four piecewise nonlinear models which describe the heat exchange between adjacent zones:

$$M_i c_i \frac{\partial T_i}{\partial t} = Q_{i-1,i} + Q_{i,i-1} + Q_{i,i+1} + Q_{i+1,i} + Q_{in,i} \tag{7.25}$$

$$+Q_{out,i} + Q_{conv,i} + Q_{source,i}$$

$$Q = \dot{m} c_p T_i, \quad Q_{i-1,i} = \left\{q_{i-1,i}^{st}\right\}^+ \rho c_p T_{i-1}, \tag{7.26}$$

$$Q_{i,i-1} = \left\{q_{i-1,i}^{st}\right\}^- \rho c_p T_i$$

where $Q_{in,i}$ and $Q_{out,i}$ represent the heat transfer by mass flow through the inlet and outlet, and $Q_{i-1,i}$ denotes the heat exchange from zone $i-1$ to zone i caused by stationary flow between zones. Q_{conv} is the convective heat loss through the building envelope, $Q_{source,i}$ is the heat source, $\dot{m}$ is the mass flow rate, c_i is the heat capacity, and M is the mass of the air inside zone i.

For the EKF, the state space model must be augmented by the parameter dynamics, i.e.:

$$\dot{X} = \begin{bmatrix} \dot{T} \\ \dot{\theta} \end{bmatrix} = \begin{bmatrix} f_j(T, U, q, \theta) + v \\ 0_{l \times 1} \end{bmatrix} \quad for \quad \begin{bmatrix} T \\ U \end{bmatrix} \in \mathcal{X}_j \tag{7.27}$$

$$q = h_3(X, P, U, \theta) = \begin{bmatrix} q_i^{in}, q_{1,2}^{st}, q_{2,3}^{st}, q_i^{out} \end{bmatrix}^T, i = 1, \dots, 3 \tag{7.28}$$

$$h_2(P, T, U, \theta) = 0, \quad \theta = \begin{bmatrix} c_1, c_2, c_3 \end{bmatrix}^T, \tag{7.29}$$

$$U = \begin{bmatrix} a_i, V_{fan}^i, Q_{heater} \end{bmatrix}^T$$

$$y = CT + w \quad j = 1, \dots, 4 \tag{7.30}$$

where f_j is dedicated to each piecewise state space model, h_2 denotes the mass balance equation (7.20) for obtaining the indoor pressure in each zone, and U is the system input.

6   Simulation Setup

Here, only the temperature is measured. The initial conditions are taken as follows: $T_1 = T_2 = T_3 = 17.5, T_o = 2\,^oC, V_{ref} = 14, P_1 = 5.6, P_2 = 6$ and $P_3 = 7$.

Two kinds of inputs are implemented in the simulation, one designed based on sensitivity analysis and one chosen arbitrarily. Their amplitude α and frequency $\mathfrak{f}$ are given in Table 7.2. As is seen from the table, there are ten inputs in the system. Inputs 1 to 6 belong to the angle of the inlets. The value of 0 represents a closed inlet and 1 represents a fully open inlet. Inputs 7 to 9 belong to the voltage of the fans and they change from 0 to 7. The last input belongs to the temperature of the heating system and it changes from 0 to 40. The proposed AFD approach is implemented on a simulated full scale live-stock building with a slow dynamic behaviour and a sample time of 5 minutes. In such systems, the fault is sometimes hidden during normal operation of the system due to the control actions, or the fault may influence the response of the system only very slowly. Here, the AFD approach is used for a sanity check of the actuators, such as the inlets, fans, and heating system. In the winter due to the cold weather there is no need for full time ventilation mechanism, therefore the controller closes the inlets and turns off the fans or excites them very slowly, and without AFD, it may take a long time to detect the abnormal behaviour of the actuators. In the following, the algorithm is applied to detection/isolation of fault in the fans. The procedure consists of two parts. First, the input designed off-line using sensitivity analysis is applied to the system over a time horizon h as; $U = \{U(0), \dots, U(h)\}$, and the parameters of the system are estimated by the EKF. Then, the residual which is the discrepancy between the normal and estimated parameters is examined at the end of the time horizon h. In order to simulate realistic conditions, two Gaussian noises with standard deviation 0.5 and 0.4 are considered as an input disturbance and measurement noise

7   Results

The results of the AFD algorithm are illustrated in Figs. 7.2 and 7.3. In Fig. 7.2, the temperature of each zone and the real and estimated parameters of the fans are shown. As can be seen, the EKF tracks the fan parameters correctly before the occurrence of any

Table 7.2: Amplitude and frequency of the input signals

inputs	α with sensitivity	$\mathfrak{f}$ with sensitivity	α without sensitivity	$\mathfrak{f}$ without sensitivity
1,3 4,6	0.7	10^{-3}	0.7	10^{-7}
2,5	0.7	2×10^{-3}	0.7	2×10^{-7}
7,9	7	2×10^{-3}	2	0.2×10^{-7}
8	7	0.08×10^{-3}	2	0.08×10^{-7}
10	20	0.01×10^{-3}	20	0.2×10^{-7}

fault. After 3.5 hours, it is assumed that fan 1 and fan 3 are stuck, and they are turned off. At first there is a considerable discrepancy between the estimate and the real values, then this discrepancy decreases quickly, indicating that the algorithm is able to detect that fan 2 is in a healthy condition and the other fans are faulty. It is seen in Fig. 7.2 that there is a small discrepancy between the estimated and real values, which can be considered as an admissible boundary, where it is possible to distinguish between a faulty and a healthy condition. One of the necessary conditions for stabilizing the EKF is that the extended system must be uniformly completely observable [19] which is tested by looking at the observability matrix. The EKF algorithm approximates the nonlinear model by a first order Taylor series expansion at every sample instant. Therefore, the observability matrix for the linear model is calculated in each sample. The observations confirm that the matrix is always full rank.

Next, the simulation is executed with different inputs without applying the sensitivity analysis. Fig. 7.3 shows that there is a large discrepancy between the estimated and real parameters, in which it is not possible to infer whether a fan is in a faulty or healthy condition. Here, the condition number of the observability matrix according to (7.12) is calculated, which has the value of 3.0269×10^6 for the input from the sensitivity analysis and the value of 7.3806×10^6 without sensitivity. It is obvious that the condition number obtained by the input from the sensitivity analysis has a smaller value, which shows that the input defined by the sensitivity analysis leads to better estimation of the parameters.

8   Conclusions and Future Work

This paper proposed a method for active fault detection and isolation in hybrid systems, which is based on off-line design of the excitation signal using sensitivity analysis. Deriving the signals off-line reduces the computational burden on the AFD algorithm. The problem of designing the inputs is formulated as a non-convex optimization problem for obtaining the maximum sensitivity for each individual system parameter and it was solved by a genetic algorithm (GA). The simulation results illustrate that the EKF converges quickly to the real parameters with the input from the sensitivity analysis; while it is unable to converge correctly to the parameters when the inputs are not provided by the sensitivity analysis.
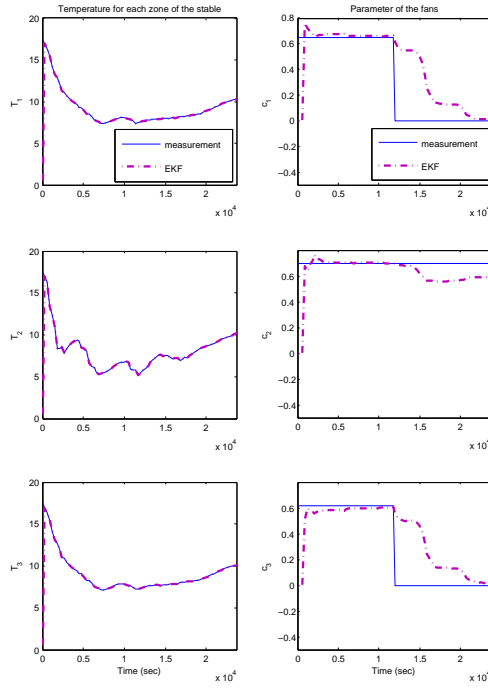
Figure 7.2: The real and estimated values by EKF for indoor temperature and parameter of the fan for each zone of the stable. The excitation input is designed by sensitivity analysis.

The required assumption for the AFD method is that the value of the system parameter is known and the system is only subject to actuator fault. This method is more beneficial in comparison with a bank of EKF where prior knowledge about the system faults and a model for each individual fault are required. Dedicating a model for each fault is computationally expensive for a system with a large number of sensors and actuators which can also be subject to different kinds of faults. In the future, the AFD approach will be applied to closed loop systems, where the faulty model is assumed as a stochastic process and a necessary and sufficient condition for exponential stability of the system is derived.

References

[1] S. L. Campbell, K. G. Horton, and R. Nikoukhah, "Auxiliary signal design for rapid multi-model identification using optimization," *Automatica*, vol. 38, no. 8, pp. 1313–1325, 2002.

[2] H. H. Niemann, "A setup for active fault diagnosis," *IEEE Transactions on Automatic Control*, vol. 51, no. 9, pp. 1572–1578, 2006.
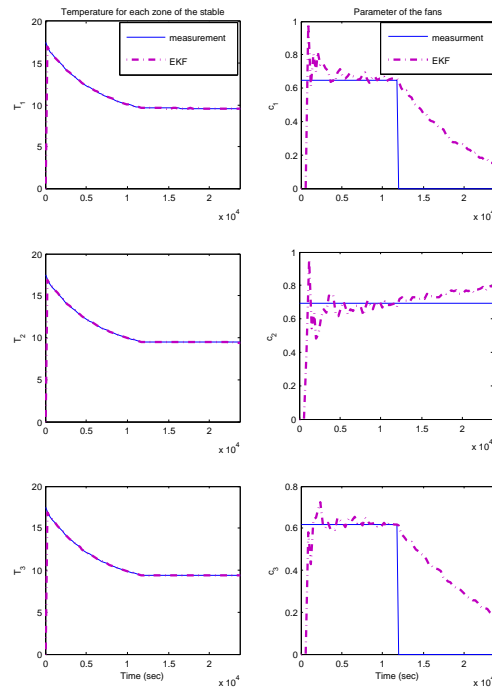
Figure 7.3: The real and estimated values by EKF for indoor temperature and parameter of the fan for each zone of the stable. The excitation input is chosen arbitrary without sensitivity analysis.

[3] R. Nikoukhah and S. L. Campbell, "Auxiliary signal design for active failure detection in uncertain linear systems with a priori information," *Automatica*, vol. 42, no. 2, pp. 219–228, 2006.

[4] R. Nikoukhah, S. L. Campbell, and F. Delebecque, "Detection signal design for failure detection: a robust approach," *International Journal of Adaptive Control and Signal Processing*, vol. 14, no. 7, pp. 701–724, 2000.

[5] J. Stoustrup, "An observer parameterization approach to active fault diagnosis with applications to a drag racing vehicle," in *Safeprocess09*, 2009, pp. 591–596.

[6] M. Bayoudh, L. Travé-Massuyes, and X. Olive, "Active diagnosis of hybrid systems guided by diagnosability properties," in *7th IFAC Symposium on Fault Detection, Supervision and Safety of Technical Processes*, 2009.

[7] M. J. Daigle and G. Biswas, "Improving diagnosability of hybrid systems through active diagnosis," in *Safeprocess09*, 2009, pp. 217–222.

[8] M. Gholami, H. Schiler, T. Bak, and S. M. Tabatabaeipour, "Active fault detection and isolation for hybrid systems," in *ICSE 2009 Twentieth International Conference on Systems Engineering, accepted.*

[9] M. Gholami, H. Schiler, and T. Bak, "Active fault diagnosis for hybrid systems based on sensitivity analysis and ekf," in *American Control Conference (ACC 2011), accepted*, 2011.

[10] S. M. Puncochar, Ivo, "A feasible design of active detector and input signal generator," in *Fault Detection, Supervision and Safety of Technical Processes(Safeprocess09)*, 2009.

[11] S. Tabatabaeipour, A. P. Ravn, R. Izadi-Zamanabadi, and T. Bak, "Active fault diagnosis-a model predictive approach," in *IEEE ICCA'09*, 2009.

[12] R. Nikoukhah and S. L. Campbell, "Auxiliary signal design for active failure detection in uncertain linear systems with a priori information," *Automatica*, vol. 42, no. 2, pp. 219 – 228, 2006.

[13] M. Knudsen, "Experimental modelling of dynamic systems," Department of Control Engineering, Aalborg University, Tech. Rep., 2003.

[14] S. Mishra, S. Wang, and K. Lai, *Generalized convexity and vector optimization*. Springer Verlag, 2009.

[15] A. Chipperfield, P. Fleming, H. Pohlheim, and C. Fonseca, "Genetic Algorithm Toolbox for use with MATLAB," 1994.

[16] M. Basseville and I. Nikiforov, *Detection of abrupt changes: theory and application*. Citeseer, 1993, vol. 10.

[17] V. Venkatasubramanian, R. Rengaswamy, K. Yin, and S. Kavuri, "A review of process fault detection and diagnosis:: Part I: Quantitative model-based methods," *Computers & Chemical Engineering*, vol. 27, no. 3, pp. 293–311, 2003.

[18] M. Gholami, H. Shioler, and T. Soltani, M. Bak, "Multi-Zone Hybrid Model for Failure Detection of the Stable Ventialation System," in *Proceedings of Industrial Electronic Society*, 2010.

[19] Q. Zhang, "Adaptive bserver for mimo linear time varying systems," INRIA, Research Report RR-4111, 2001.

Paper C

Active Fault Diagnosis for Hybrid Systems Based on Sensitivity Analysis and Adaptive Filter

Mehdi Gholami, Henrik Schioler and Thomas Bak

Abstract

An active fault diagnostic (AFD) approach for diagnosis of actuator faults is proposed. The AFD approach excites the system by injecting a so-called excitation input. Here, the input is designed off-line based on sensitivity analysis such that the maximum sensitivity for each individual system parameter is obtained. Using maximum sensitivity, results in a better precision in the estimation of the corresponding parameter. The fault detection and isolation is done by comparing the nominal parameters with those estimated by an adaptive filter. Gaussian noise is used as the input disturbance as well as the measurement noise for simulation. The method is implemented and demonstrated on the large scale livestock hybrid ventilation model which was obtained during previous research.

1 Iintroduction

The modern control systems such as stables are equipped with different controllers and components. This modernization sometimes causes contradictory results. For example, malfunction behavior of a component may result in degradation or loss of overall performance of the system. These results may be sometimes catastrophic; such as death of animal in the climate control systems of the stable. Therefore, it is desirable to diagnose the malfunction behaviour of the system. Methods for detection and isolation of component faults are either passive or active. Passive fault diagnosis (PFD), decides without acting upon the system if a fault has occurred based on observations of the input and output of system. In active fault diagnosis (AFD), a diagnoser generates a so-called excitation input, which shapes the input to the system, in order to decide whether the output represents a normal or a faulty behavior and possibly decide which kind of fault has occurred. There are two possible benefit of AFD. The first one is to identify faults that may be hidden due to the regulatory actions of controllers during normal operation of the system. The second is to isolate the faults in systems with slow response. Recently, the research on AFD has focused on hybrid systems, as this class of systems allows us to capture complex industrial systems that involve both discrete and continuous components. For AFD of the linear systems, the readers are referred to [1], [2], [3], [4] and [5]. There is little research on AFD of hybrid systems, such as, [6], [7], [8], [9], [10] and [11]. In [11], the AFD approach is based on generating the excitation inputs, online and using a model predictive control (MPC). [7] uses a qualitative event-based AFD approach for better fault detection and isolation. In the method, the controller tries to execute or block the controllable event such that the fault is detectable faster. In [6], the problem is addressed as a discrete event system. A finite state machine is used to guide the system from its operating point where the fault is not distinguishable to an operating point when the fault is distinguishable.

In this paper, we design the excitation inputs for hybrid systems in offline mode as in [4]. A benefit of offline input design is that the online computational efforts of the fault diagnoser can focus only on the detection/isolation problem. This benefit is considerable when the system has a large number of inputs. Our approach as in [9] embarks from a sensitivity analysis in order to generate the inputs. In fact, the inputs are designed such that the maximum sensitivity value for each parameter of the system is obtained. The designed input based on sensitivity analysis let the faults in the parameters to be easily

Nomenclature	
$k, leak, c, d$	constants
a	opening angle of the inlets
ΔP_{inlet}	the pressure difference across the opening area of the inlet
i	the zone number
ρ	the outside air density
V_{ref}	the ambient wind speed
C_P	the wind pressure coefficient
H	Height
H_{NLP}	NLP stands for the neutral pressure level
P_i	pressure inside zone i
g	gravity constant
V_{fan}	fan voltage of the chimney in the stable
$C_{P_{outlet}}$	the wind pressure coefficient
T_i and T_o	temperature inside and outside the stable
m_1, m_2	constants,
$q_{i-1,i}^{st}, q_{i,i+1}^{st}$	stationary flows between two adjacent zones
$Q_{in,i}, Q_{out,i}$	heat transfer by mass flow
$Q_{i-1,i}$	heat exchange from zone $i-1$ to zone i
$Q_{i,i-1}$	heat exchange from zone i to $i-1$
Q_{conv}	convective heat loss through the building envelope and described as $UA_{wall}(T_i - T_o)$
Q_{source}	the heat source
$\dot{m}$	mass flow rate
c_P	heat capacity
F_A	actuator faults
N_i	regions neighboring region i
$\hat{\theta}, \theta^*, \theta_N$ and $\theta \in \mathcal{R}^l$	the estimated, true, nominal and running parameter vectors of the system
$v(k)$ and $w(k)$	disturbance and measurement noises
y_m and y	output prediction and the measurement
ζ, ξ	a white Gaussian sequence
σ, λ	singular and eigenvalue
f_i	vector fields of the state space description.
$\mathfrak{g}_i$	a known function.

identified. Finding the highest sensitivity for each parameter is a non-convex optimization problem. Since it is not possible to cast our problem directly as a solvable convex problem, we have used a genetic algorithm (GA) to solve the problem. The excitation inputs are applied in open loop and the required parameters of the system are estimated by an adaptive filter. By comparing the nominal parameters of the system and those estimated, different incipient and severe faults can be identified. In [9], the parameters of the system are estimated by extended Kalman filter (EKF). In this paper, we use an adaptive filter, proposed in [12], for joint state-parameter estimation. The pros and cons of the EKF in contrast to the new adaptive filter are presented as follows; joint state and parameter estimation by EKF requires that the EKF state is extended with the unknown parameters. Since dynamics of the system are time varying due to occurrence of the fault, it is not easy to guarantee the convergence of the EKF. The new adaptive filter estimates the state and the parameters separately and does not need state space extension. Convergence of the new filter is always guaranteed for the time varying systems as long as a persistent excitation condition is satisfied. Application of EKF requires uniform complete observability, [13]. In practice, it is difficult to check uniform complete observability of the extended system. Here, the new filter needs only observability of the normal system.

Note that it is not desirable to disturb a system continuously, therefore at first, the abnormal behaviour of the system is observed by a common PFD method, and then the AFD approach for fault diagnosis is applied over a short period. The stable ventilation system, investigated in this paper, is stable in open loop mode and application of the AFD over a short period does not destabilize it. However, for systems which are unstable in open loop, stabilization guarantees should be considered in the AFD algorithm.

The paper is organized as follows. Section II presents the preliminaries and problem formulation. Design of the excitation input is discussed in section III. Section IV is dedicated to the adaptive filter setup. Example is presented in section V, and the simulation setup is given in VI. The results are discussed in section VII, while the conclusion is presented in the last section.

2 Preliminaries and Problem Formulation

2.1 State-Input Dependent Nonlinear Switching Systems

The class of systems considered here are hybrid nonlinear systems with uncontrollable state-input dependent switching:

$$x(k+1) = f_i(x(k), u(k), k, \theta, F_A, v(k)), \; for \; \begin{bmatrix} x(k) \\ u(k) \end{bmatrix} \in \mathcal{X}_i \qquad (8.1)$$

$$y_m(k) = Cx(k) + w(k) \qquad (8.2)$$

where F_A is actuator fault, $u(k) \in \mathbb{R}^m$ is the control input and $x(k) \in \mathbb{R}^n$ is the state, and $y_m(k) \in \mathbb{R}^p$ is the output. All variables are at time k, the set

$$\mathcal{X}_i \underline{\underline{\Delta}} \{ \begin{bmatrix} x(k)^T u(k)^T \end{bmatrix}^T | \mathfrak{g}_i(x,u) \le K_i, i = 1, \dots, s \} \qquad (8.3)$$

are manifolds (possibly un-bounded) in the state-input space $\theta \in \mathcal{R}^l$ is the parameter vector, $v(k)$ and $w(k)$ are disturbance and measurement noise respectively, f_i is vector

fields of the state space description, $\mathfrak{g}_i$ is a known function. Here, it is assumed that the hybrid system is continuous:

$$f_i(x_*(k), u_*(k)) = f_j(x_*(k), u_*(k)) \quad j \in N_i \tag{8.4}$$

where $(x_*(k), u_*(k))$ are the sampling points corresponding to the boundary between two neighboring regions and N_i is the regions neighboring region i. Here, the sensor fault is not considered and only actuator fault is assumed. Because, applying the new adaptive filter requires that the model of the system be reformulated with output injection as in [14], where we have to assume that the measurement signal is not destroyed by the sensor fault.

2.2 General Problem of AFD and Main Work

In the current research, the system parameters are related to the actuators. Assume that a faulty actuator is used rarely during the normal operation of the system, and hence it has small effect on the system response. Consequently, its parameter is not identified correctly and a fault is not detected. In order to detect correctly the faulty behaviour of the system, a sequential input signal over a finite time interval is applied to the system. At the end of the interval, a fault isolation algorithm is executed to isolate the fault. Excitation of the system by the input leads the actuator to affect the system response; therefore the parameter may be estimated more precisely and the fault observable. The main work is separated into two parts:

1. Design of the excitation input, off-line and relying on the so-called sensitivity analysis such that the maximum sensitivity for each individual system parameter is obtained.

2. Deriving the fault isolation algorithm, based on estimation of the system parameters with an adaptive filter and comparing those parameters with the normal values that are considered known.

3 Design of Excitation Input Using GA and Sensitivity Analysis

The goal is to design the excitation input using sensitivity analysis for more precise parameter estimation and consequently a better fault isolation. To achieve this goal, first we analysis a parameter estimation algorithm based on a least mean square (LMS) method where the measurement signal includes noise, and a criterion for better estimation by the LMS algorithm at the presence of noisy signal is shown. Then the correspondence between the parameter estimation LMS algorithm and sensitivity analysis is described. Finally the excitation input signal is designed using GA and sensitivity analysis.

Let us assume that the problem is to estimate the system parameters through the following LMS approach

$$\hat{\theta} = \underset{\theta}{\operatorname{argmin}} P(u, y, \theta, \xi) \tag{8.5}$$

where the performance function P is given by:

$$P(u, y, \theta, \xi) = \frac{1}{2N} \sum_{k=1}^{N} \epsilon^2(k, u, y, \theta, \xi) \tag{8.6}$$

$$\epsilon(k, \theta, \xi) = y_m(k, \theta) - y(k, \xi), \tag{8.7}$$

where ξ is the noise signal, $y(k, \xi)$ is the measurement signal approximated as $y(k, \xi) = y_m(k, \theta^*, \xi)$, $y_m(k, \theta^*, \xi)$ is the output of the model when it depends on the noise signal ξ, and $y_m(k, \theta)$ is the output of the model when it does not depend on the noise signal ξ, we assume ξ is zero. Estimated, running and true parameter vectors are presented by $\hat{\theta}$, θ, θ^*. In the following we omit u and y from the notation. Consider the following definitions:

$$\theta^* = \operatorname*{argmin}_{\theta} P(\theta^*, 0) \Rightarrow [D_\theta P](\theta^*, 0) = 0 \tag{8.8}$$

$$\hat{\theta} = \operatorname*{argmin}_{\theta} P(\hat{\theta}, \xi) \Rightarrow [D_\theta P](\hat{\theta}, \xi) = 0. \tag{8.9}$$

Let the performance function be approximated using the first and second order terms of a Taylor series expansion with respect to θ and ξ at θ^* and 0:

$$P(\theta, \xi) \approx P(\theta^*, 0) + [D_\theta P](\theta^*, 0)(\theta - \theta^*) + [D_\xi P](\theta^*, 0)\xi \tag{8.10}$$
$$+ (\theta - \theta^*)^T [D_{\theta, \theta} P](\theta^*, 0)(\theta - \theta^*) + \xi^T [D_{\xi, \xi} P](\theta^*, 0)\xi$$
$$+ \xi^T [D_{\theta, \xi} P](\theta^*, 0)(\theta - \theta^*) + (\theta - \theta^*)[D_{\xi, \theta} P](\theta^*, 0)\xi$$

where $D_\theta P = \frac{\partial P}{\partial \theta}$ and $D_{\theta, \xi} P = \frac{\partial^2 P}{\partial \theta \partial \xi}$. In order to derive the parameter θ from the smooth performance function $P(\theta, \xi)$, we apply the partial derivative of (8.9) on the performance function, the result is:

$$2[D_{\theta, \theta} P](\theta^*, 0)(\hat{\theta} - \theta^*) + \xi^T [D_{\theta, \xi} P](\theta^*, 0) \tag{8.11}$$
$$+ [D_{\xi, \theta} P](\theta^*, 0)\xi = 0 \Rightarrow$$
$$H(\hat{\theta} - \theta^*) = \zeta,$$

where $H = [D_{\theta, \theta} P](\theta^*, 0)$, and $\zeta = \xi^T [D_{\theta \xi} P](\theta^*, 0) + [D_{\xi \theta} P](\theta^*, 0)\xi$. ζ is the noisy signal, thus its large error should cause a small error in $\hat{\theta} - \theta^*$. It means that the condition number of matrix H should be small [14]. The condition number of the matrix H is :

$$\kappa(H) = \frac{\sigma_{max}(H)}{\sigma_{min}(H)}, \tag{8.12}$$

where, σ_{max} and σ_{min} are maximum and minimum of singular value of the hessian matrix H. In fact, assuming a small value of the condition number $\kappa(H)$, the LMS algorithm is able to estimate the parameter of the system more precisely at the presence of the noise.

Here, we specify the importance of equation (8.12) from the sensitivity analysis point of view. According to [15], a larger value of sensitivity for parameter θ leads to a smaller deviation of θ from the true value θ^* generates significant deviation in the value of ϵ. This

fact results in more precise parameters estimation, as it is obvious from (8.5) to (8.7), and it is discussed in details in [15]. For obtaining high sensitivity for the entire system parameters, the ratio of maximum to minimum sensitivity should be small

$$R = \frac{S_{max}}{S_{min}} = \frac{\sqrt{\lambda_{max}}}{\sqrt{\lambda_{min}}} = \frac{\sigma_{max}(H)}{\sigma_{min}(H)} \tag{8.13}$$

where the sensitivity is $S = \frac{\partial \epsilon}{\partial \theta}$ and λ is eigenvalue of the Hessian matrix of H. As it is obvious, the ratio equation (8.13) is equal to the condition number (8.12), which shows the correspondence between the sensitivity analysis and parameter estimation algorithms based on the LMS approach.

In the following, we assume the input as a sinusoidal signal and its amplitude α and frequency $\mathfrak{f}$ is designed such that the minimum R is obtained:

$$U = \alpha sin(2\pi \mathfrak{f} t) \tag{8.14}$$

$$(\alpha, \mathfrak{f}) = \underset{\alpha, \mathfrak{f}}{\operatorname{argmin}} R \tag{8.15}$$

$$s.t. \begin{cases} (1) \\ \alpha_{min} \leqslant \alpha \leqslant \alpha_{max} \\ \mathfrak{f}_{min} \leqslant \mathfrak{f} \leqslant \mathfrak{f}_{max} \end{cases}$$

where α_{min} and α_{max} are minimum and maximum values of α, and $\mathfrak{f}_{min}$ and $\mathfrak{f}_{max}$ are minimum and maximum values of $\mathfrak{f}$. In some cases, it may be necessary to consider more than one periodic signal in U for estimation of different parameters.

Equation (8.15) is non-convex and non-differentiable. To solve the problem with classical approaches, the problem must be changed to a convex problem by defining some constraints. Obtaining these constraints is not always feasible and is considered an open issue in the literature; see [16]. Using evolutional search algorithms such as GA, avoids having to change the problem to a convex one. As the optimization problem is calculated offline, the computational effort is not important. The reader is referred to [17] for more details of the GA.

4   Setup for the Adaptive Filter

In this section, the aim is to use an adaptive filter mixed with a Kalman filter (KF) for joint state-parameter estimation after exciting the system by exerting the inputs. The abnormal behaviour of the system is detected from the estimated parameters.

We claim that the sensitivity analysis fulfils the persistence excitation criteria of the filter, and also the sensitivity leads to better performance of the filter.

The class of systems considered for this filter is so-called state-affine nonlinear systems, which are in the form of

$$x(k + 1) = A(k, u, y)x(k) + B(k, u, y)u(k) + \Psi(k, u, y)\theta \tag{8.16}$$

$$y(k) = C(k, u, y)x(k) + D(k, u, y)u(k) \tag{8.17}$$

where the dependence of A, B, C, D, Ψ, on k, u, y can be nonlinear. In order to transfer the system (8.1) to the form (8.16), the system (8.1) is approximated according by a

first order Taylor series expansion with respect to x and θ at $x(k-1)$ and the nominal parameter of the system, θ_N. With output injection; see [14], we have the following equation,

$$x(k+1) = A_i(k, u, y)x(k) + B_i(k, u, y)u(k) + \Psi_i(k, u, y)\theta \tag{8.18}$$

$$for \begin{bmatrix} x(k) \\ u(k) \end{bmatrix} \in \mathcal{X}_i$$

$$y(k) = Cx(k) \tag{8.19}$$

wher $A_i = \frac{\partial f_i}{\partial x}$, $\Psi_i = \frac{\partial f_i}{\partial \theta}$ and $B_i = 0$.

Under three assumptions, the adaptive filter is introduced.

Assumption 1. The time varying matrices $A_i(k)$ and C are such that there exists a bounded time varying $K(k) \in \mathbb{R}^n \times \mathbb{R}^m$ so that the linear time varying system

$$\eta(k+1) = (A_i(k) - K(k)C)\eta(k) \tag{8.20}$$

is exponentially stable.

If the time varying matrix pair $(A_i(k), C)$ is completely uniformly observable, the Kalman gain will fulfil the above assumption, [13].

Assumption 2. The scaler gain sequence $\mu(k) > 0$ is small enough so that

$$\left\| \sqrt{\mu(k)} C \Upsilon(k) \right\| \leq 1 \tag{8.21}$$

for all $k \geq 0$, where $\| \cdot \|$ denotes the matrix spectral norm.

Assumption 3. The matrix of signal Ψ is persistently exciting so that the matrix sequence $\Upsilon(k)$ and the gain sequence $\mu(k)$ satisfy, for some constants $\mathfrak{a}_1 > 0$, integer $L \geq 0$, and for all $k \geq 0$, the following inequality

$$\frac{1}{L} \sum_{i=k}^{k+L-1} \mu(i) \Upsilon^T(i) C^T C \Upsilon(i) \geq \mathfrak{a}_1 I. \tag{8.22}$$

Theorem 2. *([18]) under assumption 1-3, the ODE system*

$$\Upsilon(k+1) = (A_i(k) - K(k)C)\Upsilon(k) + \Psi_i(k) \tag{8.23}$$

$$\hat{\theta}(k+1) = \hat{\theta}(k) + \mu(k)\Upsilon(k)^T C^T(y(k) - C\hat{x}(k)) \tag{8.24}$$

$$\hat{x}(k+1) = A_i(k)\hat{x}(k) + B_i(k)u(k) + \Psi_i(k)\hat{\theta} \tag{8.25}$$

$$+K(k)(y(k) - C\hat{x}(k)) + \Upsilon(k+1)(\hat{\theta}(k+1) - \hat{\theta}(k))$$

is a global exponential adaptive filter for system (8.18), i.e., the errors $\hat{x}(k) - x(k)$ and $\hat{\theta}(k) - \theta(k)$ tend to zero exponentially fast when $k \to \infty$.

We provide the relation between sensitivity analysis and adaptive observer of Theorem 1 with the following Lemma1.

Lemma 2. *I) Larger sensitivity; S, will satisfy the assumption 3. II) Larger sensitivity; S, result in improvement of the adaptive filter from two point of views. First better precision in parameter estimation, second the convergence speed of the filter.*

Proof. I) In the following we omit F_A, $v(k)$, $u(k)$ form the notation. Let us write the definition of the sensitivity as

$$S = \frac{\partial \epsilon(k,\theta)}{\partial \theta} = \frac{\partial y_m(k,\theta) - y(k)}{\partial \theta} = \frac{\partial y_m(k,\theta)}{\partial \theta} \qquad (8.26)$$

according to system (8.2)

$$S = \frac{\partial y_m(k,\theta)}{\partial \theta} = C \frac{\partial x(k,\theta)}{\partial \theta} = C\big[\frac{\partial f_i(k-1,\theta)}{\partial x(k-1,\theta)} \qquad (8.27)$$
$$\times \frac{\partial x(k-1,\theta)}{\partial \theta} + \frac{\partial f_i(k-1,\theta)}{\partial \theta}\big]$$

now, we write again the equation of Υ as $\Upsilon(k+1) = [A_i(k)\Upsilon(k)+\Psi_i(k)]-K(k)C\Upsilon(k)$, it is obvious that the term inside of the bracket in the equation of Υ has similar structure as the term inside of bracket in the right side of equation S, (8.27), which shows that S has direct relation with Υ. Note that the only variable in the left side of inequality (8.22) is Υ, as the result with increase the amount of sensitivity and consequently Υ, it is possible to satisfy the inequality (8.22) and Assumption 3.

II) According to the proof of Theorem 7 in [18], from (8.18) and (8.25), it is obtained that

$$\tilde{x}(k + 1) = (A_i - K(k)C)\tilde{x} + \Psi_i(k)\tilde{\theta}(k) \qquad (8.28)$$
$$+\Upsilon(k + 1)(\tilde{\theta}(k + 1) - \tilde{\theta}(k))$$

where error sequences are $\tilde{x}(k) = \hat{x}(k) - x(k)$ and $\tilde{\theta}(k) = \hat{\theta}(k) - \theta(k)$. Since error sequence of the states $\tilde{x}(k)$ tends zero with $k \to \infty$, larger value of S and consequently Υ will penalize more the error sequences of parameters $(\tilde{\theta}(k+1)-\tilde{\theta}(k))$, which improves the precision of the filter. In the follow, we show the effect of S and Υ on the convergence speed of the adaptive filter. From Lemma 2 and proof of Theorem 1 in paper [18], it is obtained that the error sequence of the filter; $\tilde{x}(k)$ will tend zero fast if $z(k)$ tends zero fast. The system $z(k)$ is

$$z(k + 1) = (I - \phi^T(k)\phi(k))z(k) \qquad (8.29)$$

where $\phi(k) = \sqrt{\mu(k)}C\Upsilon(k)$. Now, we investigate the asymptotic stability of the system (8.29) with respect to the appendix A of the paper [18]. The Lyapunov function candidate is defined as $V(k) = z^T(k)z(k)$, then this inequality is hold according to [18]:

$$V(k + L) \leq (1 - \varsigma)V(k), \ \ 0 < \varsigma = \frac{\beta_1^2 L}{(1 + \phi_{max}^2 L)^2} < 1, \qquad (8.30)$$

where β_1 is the minimum value of the equation (8.22) as $\mathfrak{a}_1$, L is a finite horizon and $\phi_{max} = sup\,\|\phi(k)\|$. From equation (8.30), it is obtained that with smaller horizon L and larger value of β_1, the value of ς increases, as the result the Lyapunov function $V(k)$

Table 8.1: Fault Isolation Algorithm

Algorithm 1
For $i = 0 \: to \: l$
IF $r_i = \left| \hat{\theta}_i - \theta_{Ni} \right| > \delta$
$F = F_i$
End IF
End For

will tend zero faster. It means that the system (8.29) moves to its origin faster, on the other hand the adaptive filter converges faster. From equation (8.22), it is clear that β_1 has direct relation with Υ, which means that larger value of S, Υ and consequently β_1 result in convergence speed of the filter. $\qquad\square$

We can also define the large value of β_1 and small value of L with the following optimization problem:

$$\max_{L,\beta_1}(\frac{\beta_1}{L}) \qquad\qquad (8.31)$$

$$s.t. \: (8.22), \: (8.23)$$

and consider this problem directly as an extra constraint in the problem of (8.15).

Fault isolation relies on a simple algorithm. The algorithm isolate the fault F_i according to the residual generator $r_i = \hat{\theta}_i - \theta_{Ni}$, where θ_{Ni} is the nominal value of ith parameter of the system which is assumed as the prior knowledge of the system and $\hat{\theta}_i$ is the estimated parameter by the adaptive filter. The fault isolation algorithm is given as Table 8.1. If r_i is greater than a predefined threshold δ, the system is subject to the fault F_i.

5   Example

The AFD algorithm is applied to a climate control systems of a live-stock building, which was obtained during previous research, [19]. The general schematic of the large scale live-stock building equipped with climate control system is illustrated in Fig. 8.1. In a large scale stable, the indoor airspace is incompletely mixed; therefore it is divided into conceptually homogeneous parts called zones. Due to the indoor and outdoor conditions, the airflow direction varies between adjacent zones. Therefore, the system behavior is represented by a finite number of different dynamic equations. The model is intended to be a realistic representation of internal temperatures for all multi-zone types of livestock buildings. The model is divided into subsystems as follows:

5.1 Inlet Model

An inlet is built into an opening in the wall. The following approximated model for airflow, q_i^{in} into the zone i is used.

$$q_i^{in} = k_i(a_i + leak)\Delta P_{inlet}^i \tag{8.32}$$

$$\Delta P_{inlet}^i = 0.5 C_P V_{ref}^2 - P_i + \rho g (1 - \frac{T_o}{T_i})(H_{NLP} - H_{inlet}) \tag{8.33}$$

where P_i is the pressure inside zone i, k_i and $leak$ are constants, a_i is the opening angle of the inlets, ΔP_{inlet}^i is the pressure difference across the opening area and wind effect, ρ is the outside air density, V_{ref} is the wind speed, C_p stands for the wind pressure coefficient. H stands for height and H_{NLP} is the neutral pressure level which is calculated from mass balance equation. T_i and T_o are temperature inside and outside the stable and g is gravity constant.

5.2 Outlet Model

The outlet is a chimney with an electrically controlled fan and plate inside. A simple linear model for the airflow out of zone i is given by:

$$q_i^{out} = V_{fan}^i c_i - d_i \Delta P_{outlet}^i \tag{8.34}$$

$$\Delta P_{outlet}^i = 0.5 C_P V_{ref}^2 - P_i + \rho g (1 - \frac{T_i}{T_o})(H_{NLP} - H_{outlet}) \tag{8.35}$$

$$\sum_{i=1}^{3} q_i^{in} \rho \frac{\Delta P_{inlet}^i}{|\Delta P_{inlet}^i|} + \sum_{i=1}^{3} q_i^{out} \rho = 0 \tag{8.36}$$

where c_i and d_i are constants, V_{fan}^i is fan voltage and the number of zones is 3. The stationary flows, $q_{i-1,i}^{st}$ and $q_{i,i+1}^{st}$, which moves through the zonal border of two adjacent zones is given by:

$$q_{i-1,i}^{st} = m_1(P_{i-1} - P_i) \tag{8.37}$$

$$q_{i,i+1}^{st} = m_2(P_i - P_{i+1}) \tag{8.38}$$

$$q_{i-1,i}^{st} = \left\{q_{i-1,i}^{st}\right\}^+ - \left\{q_{i-1,i}^{st}\right\}^- \tag{8.39}$$

where m_1 and m_2 are constants coefficients. The use of curly brackets is defined as:

$$\left\{q_{i-1,i}^{st}\right\}^+ = max(0, q_{i-1,i}^{st}), \quad \left\{q_{i-1,i}^{st}\right\}^- = min(0, q_{i-1,i}^{st}) \tag{8.40}$$

5.3 Modeling Climate Dynamics

The following formulation for the dynamical model of the temperature for each zone inside the stable is driven by thermodynamic laws. The dynamical model includes four

piecewise nonlinear models which describe the heat exchange between adjacent zones:

$$M_i c_i \frac{\partial T_i}{\partial t} = Q_{i-1,i} + Q_{i,i-1} + Q_{i,i+1} + Q_{i+1,i} + Q_{in,i} \qquad (8.41)$$

$$+ Q_{out,i} + Q_{conv,i} + Q_{source,i}$$

$$Q = \dot{m} c_p T_i, \;\; Q_{i-1,i} = \left\{ q_{i-1,i}^{st} \right\}^+ \rho c_p T_{i-1}, \qquad (8.42)$$

$$Q_{i,i-1} = \left\{ q_{i-1,i}^{st} \right\}^- \rho c_p T_i$$

where $Q_{in,i}$, and $Q_{out,i}$ represent the heat transfer by mass flow through inlet and outlet, $Q_{i-1,i}$ denotes heat exchange from zone $i-1$ to zone i which cause by stationary flow between zones. Q_{conv} is the convective heat loss through the building envelope, $Q_{source,i}$ is the heat source, $\dot{m}$ is the mass flow rate, c_i is the heat capacity and M is the mass of the air inside zone i.

The state space model is given by

$$\dot{T} = f_j(T, U, q) + v \;\; for \;\; \begin{bmatrix} T \\ U \end{bmatrix} \in \mathcal{X}_j, \; j = 1, \dots, 4 \qquad (8.43)$$

$$q = h_3(T, P, U, \theta) = \left[q_i^{in}, q_{1,2}^{st}, q_{2,3}^{st}, q_i^{out} \right]^T, i = 1, \dots, 3 \qquad (8.44)$$

$$h_2(P, T, U, \theta) = 0, \; \theta = \left[c_1, c_2, c_3 \right]^T, U = \left[a_i, V_{fan}^i, Q_{heater} \right]^T \qquad (8.45)$$

$$y = CT - w \qquad (8.46)$$

where f_j is dedicated to each piecewise state space model, h_2 denotes the mass balance equation (8.36) for obtaining the indoor pressure in each zone and U is the system inputs.

6 Simulation Setup

Here, only the temperature is measured. The initial conditions are considered as follows: $T_1 = T_2 = T_3 = 17.5, T_o = 2\ ^oC, V_{ref} = 14, P_1 = 5.6, P_2 = 6$ and $P_3 = 7$.

Two kinds of inputs are implemented in the simulation, the one designed based on sensitivity analysis and the one chosen arbitrary. Their amplitude α and frequency $\mathfrak{f}$ are given in Table 8.2. As it is seen from the table, there are 10 inputs in the system. Inputs 1 to 6 belong to the angle of the inlets. The value of 0 represents the closed inlet and 1 represents the full-open inlet. Inputs 7 to 9 belong to the voltage of the fans and they change from 0 to 7. The last input belongs to temperature of the heating system and it changes from 0 to 40. The proposed AFD approach is implemented on a simulated full scale live-stock building with a slow dynamic behaviour and a sample time, 5 minutes. In such systems, the fault is sometimes hidden during normal operation of the system due to the control actions, or the fault may influence the response of the system very slowly. Here, the AFD approach is used for sanity check of actuators, such as the inlets, fans and heating system. In the winter due to the cold weather there is no need for full time ventilation mechanism, therefore the controller closes the inlets and turns off the fans or excites them very slowly, and without AFD, it may take a long time to detect the abnormal behavior of the actuators. In the following, the algorithm is applied to detection/isolation of fault in the fans. The procedure consists of two parts. First, the input designed off-line using sensitivity analysis is applied to the system over a time horizon h as; $U =$

Table 8.2: Amplitude and frequency of the input signals

inputs	α with sensitivity	$\mathfrak{f}$ with sensitivity	α without sensitivity	$\mathfrak{f}$ without sensitivity
1,3 4,6	0.7	10^{-3}	0.7	10^{-7}
2,5	0.7	2×10^{-3}	0.7	2×10^{-7}
7,9	7	2×10^{-3}	2	0.2×10^{-7}
8	7	0.08×10^{-3}	2	0.08×10^{-7}
10	20	0.01×10^{-3}	20	0.2×10^{-7}

$\{U(0), \ldots, U(h)\}$, and the parameters of the system are estimated by the adaptive filter. Then, the residual which is the discrepancy between the normal and estimated parameters is examined at the end of the time horizon h. In order to simulate realistic conditions, Gaussian noise is considered as an input disturbance as well as measurement noise.

7   Results

The results of the AFD algorithm are illustrated in the following graphs. In Fig. 8.2, the temperature of each zone and the real and estimated parameters of the fans are illustrated. The estimation is done by both the adaptive filter and EKF. The illustration shows that both filter track the fans parameter correctly before occurrence of any fault. After 3.5 hours, it is assumed that the fan 1 and fan 3 are stuck, and they are turned off. As shown, the adaptive filter is able to detect that the fan 2 is in healthy condition and the other fans are faulty after few steps ; while the EKF has a delay to detect the faults. Note that since the adaptive filter is sensitive to the measurement, as a result it is also sensitive to the measurement noise. Large noise may degrades the filter performance. It is obvious from Fig. 8.2, that there is a small discrepancy between the estimated and real value of the paramater of the second fan. We assume this discrepancy as an admissible boundary. It means that if the difference of a estimated and real parameter is less than this boundary then the fan is in healthy condition otherwise the fan is faulty. In the following, the simulation is executed with an arbitrary input which was not designed by sensitivity analysis. Fig. 8.3, shows that there is a large discrepancy between the simulated and real parameters; in which it is not possible to infer if a fan is in a faulty or healthy condition. Here, the condition number of the observability matrix according to (8.12) is calculated, which has the value of 2.7317×10^3 for the input from the sensitivity analysis and the value of 3.1127×10^3 without sensitivity. Also their values are illustrated in Fig. 8.4. It is obvious that the condition number obtained by the input from the sensitivity analysis has smaller value, which shows that the input defined by the sensitivity analysis leads to better estimation of the parameters.
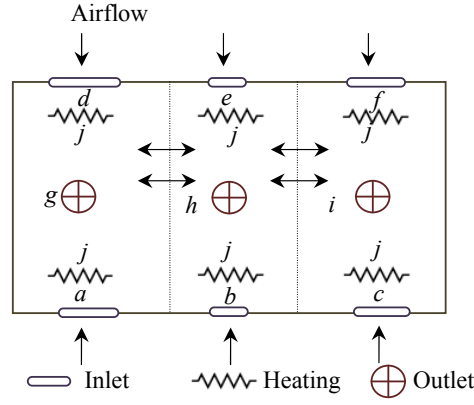
Figure 8.1: The top view of the test stable

8 Conclusion and Future Works

This paper proposed a method for active fault detection and isolation in hybrid systems, which is based on off-line design of the excitation signal using sensitivity analysis. Deriving the signals off-line reduces the computational efforts for the AFD algorithm. The problem of designing the inputs is formulated as a non-convex optimization problem for obtaining the maximum sensitivity for each individual system parameter and it was solved by Genetic Algorithm (GA). Simulation results illustrate that an adaptive filter is able to detect actuator faults of the system faster than the EKF. It also illustrates that the adaptive filter is sensitive to the measurement and it is not able converge correctly to the parameters when the inputs are not provided by the sensitivity.

The required assumption for the ADF method is that the value of the system parameter is known and the system is only subjected to actuator fault. This method is more beneficial in comparison with a bank of EKF where an prior knowledge about the system faults and a model for each individual fault are required. Dedicating model for each fault is computationally expensive for a system with large number of sensors and actuators which can also be subjected to different kinds of faults. For future work, the AFD approach will be applied to closed loop systems, where the faulty model is assumed as a stochastic process and a necessary and sufficient condition for exponential stability of the system is derived.

9 Acknowledgments

References

[1] S. L. Campbell, K. G. Horton, and R. Nikoukhah, "Auxiliary signal design for rapid multi-model identification using optimization," *Automatica*, vol. 38, no. 8, pp. 1313–1325, 2002.
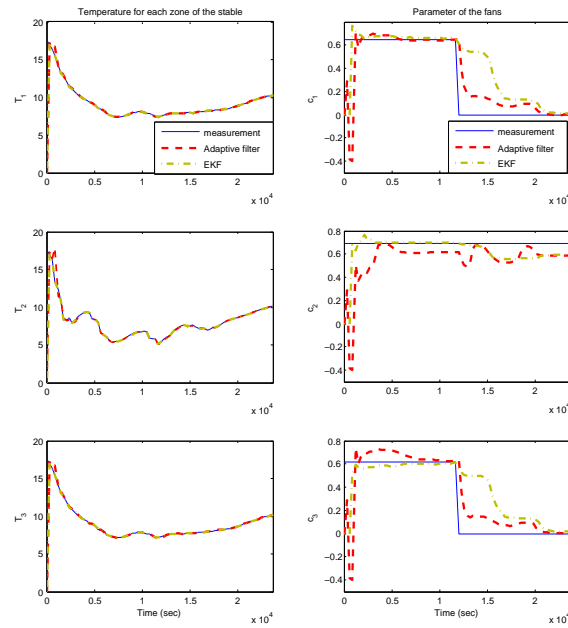
Figure 8.2: The real and estimated values by adaptive filter and EKF for indoor temperature and parameter of the fan for each zone of the stable. The excitation input is designed by sensitivity analysis.

[2] H. H. Niemann, "A setup for active fault diagnosis," *IEEE Transactions on Automatic Control*, vol. 51, no. 9, pp. 1572–1578, 2006.

[3] R. Nikoukhah and S. L. Campbell, "Auxiliary signal design for active failure detection in uncertain linear systems with a priori information," *Automatica*, vol. 42, no. 2, pp. 219–228, 2006.

[4] R. Nikoukhah, S. L. Campbell, and F. Delebecque, "Detection signal design for failure detection: a robust approach," *International Journal of Adaptive Control and Signal Processing*, vol. 14, no. 7, pp. 701–724, 2000.

[5] J. Stoustrup, "An observer parameterization approach to active fault diagnosis with applications to a drag racing vehicle," in *Safeprocess09*, 2009, pp. 591–596.

[6] M. Bayoudh, L. Travé-Massuyes, and X. Olive, "Active diagnosis of hybrid systems guided by diagnosability properties," in *7th IFAC Symposium on Fault Detection, Supervision and Safety of Technical Processes*, 2009.

[7] M. J. Daigle and G. Biswas, "Improving diagnosability of hybrid systems through active diagnosis," in *Safeprocess09*, 2009, pp. 217–222.

[8] M. Gholami, H. Schiler, T. Bak, and S. M. Tabatabaeipour, "Active fault detection and isolation for hybrid systems," in *ICSE 2009 Twentieth International Conference on Systems Engineering, accepted*.

Figure 8.3: The real and estimated values by adaptive filter and EKF for indoor temperature and parameter of the fan for each zone of the stable. The excitation input is chosen arbitrary without sensitivity analysis.
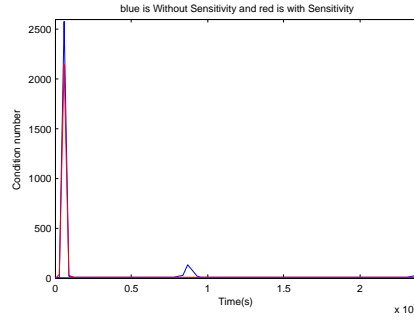
Figure 8.4: The condition number of the observability matrix obtained by the inputs from the sensitivity analysis and the inputs without sensitivity analysis.

[9] M. Gholami, H. Schiler, and T. Bak, "Active fault diagnosis for hybrid systems based on sensitivity analysis and ekf," in *American Control Conference (ACC 2011), accepted*, 2011.

[10] S. M. Puncochar, Ivo, "A feasible design of active detector and input signal generator," in *Fault Detection, Supervision and Safety of Technical Processes(Safeprocess09)*, 2009.

[11] S. Tabatabaeipour, A. P. Ravn, R. Izadi-Zamanabadi, and T. Bak, "Active fault diagnosis-a model predictive approach," in *IEEE ICCA'09*, 2009.

[12] Q. Zhang, "Adaptive bserver for mimo linear time varying systems," INRIA, Research Report RR-4111, 2001.

[13] A. Jazwinski, *Stochastic processes and filtering theory*. Academic Pr, 1970.

[14] H. Hammouri and M. Kinnaert, "A new procedure for time-varying linearization up to output injection," *Systems & Control Letters*, vol. 28, no. 3, pp. 151 – 157, 1996.

[15] M. Knudsen, "Experimental modelling of dynamic systems," Department of Control Engineering, Aalborg University, Tech. Rep., 2003.

[16] S. Mishra, S. Wang, and K. Lai, *Generalized convexity and vector optimization*. Springer Verlag, 2009.

[17] A. Chipperfield, P. Fleming, H. Pohlheim, and C. Fonseca, "Genetic Algorithm Toolbox for use with MATLAB," 1994.

[18] A. Guyader and Q. Zhang, "Adaptive observer for discrete time linear time varying systems," in *Proceedings of the 13th Symposium on System Identification*, pp. 1743–1748.

[19] M. Gholami, H. Shioler, and T. Soltani, M. Bak, "Multi-Zone Hybrid Model for Failure Detection of the Stable Ventialation System," in *Proceedings of Industrial Electronic Society*, 2010.

Paper D

Reconfigurability of Piecewise Affine Systems Against Actuator Faults

S. Tabatabaeipour, Mehdi Gholami,Thomas Bak and Henrik Schioler

Abstract

In this paper, we consider the problem of reconfigurability of peicewise affine (PWA) systems. Actuator faults are considered. A system subject to a fault is considered as reconfigurable if it can be stabilized by a state feedback controller and the optimal cost of the performance of the systems is admissible. Sufficient conditions for reconfigurability are derived in terms of feasibility of a set of Linear Matrix Inequalities (LMIs). The method is implemented on a large scale livestock hybrid ventilation model which was obtained during previous research.

1 Introduction

Performance of modern control systems typically relies on a number of strongly interconnected components. Component malfunctions may degrade performance of the system or even result in loss of functionality. In applications such as climate control systems for livestock buildings, this is unacceptable as it may lead to the loss of animal life. Therefore, it is desirable to develop control systems that are capable of tolerating component malfunctions whilst still maintaining desirable performance and stability properties. Such controllers are called fault tolerant. Fault tolerant control (FTC) is divided generally into two categories:passive (PFTC) and active (AFTC). In PFTC, the structure of the system is fixed and pre-designed such that it can tolerate a set of faults. In AFTC, first the fault is detected using a fault detection and diagnosis (FDD) scheme. Then, based on information from the FDD the controller is re-designed or reconfigured in the case of severe faults such that the overall system stability is preserved and an acceptable performance is provided. An important step in designing an AFTC is to analyze reconfigurability of the system subject to possible faults. Reconfigurability is the ability of the system to preserve some properties, e.g. stability or performance, of the system when a fault has occurred.

Reconfigurability of linear time invariant systems is measured by controllability and observability Grammians in [1]. A measure for control reconfigurability of linear systems is proposed in [2]. The smallest second-order mode is used as a measure for reconfigurability of the system to preserve an acceptable performance in the presence of a fault. In [3], the fault tolerant property of a configuration with respect to an actuator fault is investigated. Two cases are considered. In the first case, only achieving the control objective is considered, but in the second case the control objective must be achieved and the control energy must be admissible. The method uses a Grammian based approach. This result is extended to the admissibility of a linear quadratic cost function in [4]. [5] defines reconfigurability of the system not only based on the controllability Grammian, but also based on the system reliability. While in the aforementioned methods, the reconfigurability measures are computed off-line, an online method for calculation of the controllability Grammian using input/output data is proposed in [6].

The above methods are for linear systems. Most complex industrial systems either exhibit nonlinear behavior or involve both discrete and continuous components. An attractive modeling framework for such systems is the framework of piecewise affine systems (PWA). PWA systems have the capability to approximate nonlinear systems efficiently. Moreover, they arise in systems that contain PWA components such as deadzone, saturation, hysteresis, etc. This framework has been applied to several areas, such as, switched system, [7], and multi-zone climate control systems, [8].

Reconfigurability of a class of linear switched systems is considered in [9]. Reconfigurability is defined as the controllability of the system and an algebraic approach for reconfigurability is given. In our work, we consider reconfigurability of PWA systems against actuator faults, where only complete loss is considered. A system subject to a fault is called reconfigurable if it is not only stabilizable using a state feedback control law, but also the performance cost of the systems is admissible with any initial condition in a given bounded region. In other words, we have considered both stability and admissibility of the performance of the system as a criteria for reconfigurability. The problem is cast as the feasibility of a convex optimization problem with LMI constraints. Moreover, the optimal value of the cost function must be admissible. The optimization problem can be solved efficiently using available softwares such as YALMIP/SeDuMe or LMILAB.

The paper is organized as follows. In Section II, the PWA model and actuator faults are given. In Section III, reconfigurability is defined and sufficient conditions for reconfigurability are given. Section IV is dedicated to the simulation results for the climate control system. The conclusion is presented in the Section V.

2 Piecewise Affine Systems and Actuator Fault Models

2.1 Piecewise Affine Systems

We consider a PWA discrete time system of the following form:

$$x(k + 1) = A_i x(k) + B_i u(k) + b_i \quad for \ x \in \mathcal{X}_i, \tag{9.1}$$

where $x(k) \in \mathbb{R}^n$ is the state and $u(k) \in \mathbb{R}^m$ is the control input. $\{\mathcal{X}_i\}_{i=1}^s \subseteq \mathbb{R}^n$ denotes a partition of the state space into a number of polyhedral regions $\mathcal{X}_i, i \in \mathcal{I} = \{1, \cdots, s\}$. Each polyhedral region is represented by:

$$\mathcal{X}_i = \{x | H_i x \leq h_i\} \tag{9.2}$$

The set $\mathcal{I}$ is partitioned to $\mathcal{I}_0 \cup \mathcal{I}_1$, where $\mathcal{I}_0$ denotes the index set of subsystems that contain the origin and $\mathcal{I}_1$ is the index set of the subsystems that does not contain the origin. It is assumed that $b_i = 0$ for $i \in \mathcal{I}_0$.

Each polyhedral region $\mathcal{X}_i$ can be over-approximated with a union of l_i ellipsoids, i.e:

$$\mathcal{X}_i \subseteq \bigcup_{j=1}^{\ell_i} \mathcal{E}_{ij}, \tag{9.3}$$

where each ellipsoid is represented by the matrix E_{ij} and the scalar f_{ij} such that $\mathcal{E}_{ij} = \{x | \|E_{ij} x + f_{ij}\| \leq 1\}$, see [10]. This approximation is used in this paper to deal with the affine term for subsystems with $i \in \mathcal{I}_1$ which helps us to cast the control problem in terms of LMIs. This approximation is more efficient for PWA slab systems where the partitioning is defined as $\mathcal{X}_i = \{x | d_i^1 \leq c_i^T x \leq d_i^2\}$. For PWA slab systems each partition $\mathcal{X}_i$ is approximated exactly by one ellipsoid with:

$$E_{il} = \frac{2c_i^T}{d_i^2 - d_i^1}, \tag{9.4}$$

$$f_{il} = -\frac{d_i^1 + d_i^2}{d_i^2 - d_i^1}. \tag{9.5}$$

All possible switchings from region $\mathcal{X}_i$ to $\mathcal{X}_j$ are represented by the set $\mathcal{S}$:

$$\mathcal{S} := \{(i,j)|x(k) \in \mathcal{X}_i, x(k+1) \in \mathcal{X}_j\} \tag{9.6}$$

The set $\mathcal{S}$ can be computed using reachability analysis for MLD systems, see [11].

2.2 Fault Model

In this work, we consider actuator faults. Only complete loss of actuators is considered. Let u_i denote the $i'th$ actuator and u_i^F the failed $i'th$ actuator. We model a fault in an actuator as:

$$u_i^F = \delta_i u_i, \;\; \delta_i \in \{0, 1\}, \tag{9.7}$$

where $\delta_i = 1$ presents the case of no fault in the $i'th$ actuator, and $\delta_i = 0$ corresponds to complete loss of it. We define Δ as:

$$\Delta = diag\{\delta_1, \delta_2, \ldots, \delta_m\}. \tag{9.8}$$

Then

$$\mathbf{u}^F = \Delta\mathbf{u}. \tag{9.9}$$

The PWA model of the system with the fault f is given by:

$$x(k+1) = A_i x(k) + B_i \Delta^f u(k) + b_i \quad for \; x \in \mathcal{X}_i, \tag{9.10}$$

3 State Feedback Design for PWA systems

3.1 Piecewise Quadratic Stability

The problem of piecewise linear state feedback design is to design a state feedback of the form:

$$u(k) = K_i x(k) \;\; for \; x(k) \in \mathcal{X}_i \tag{9.11}$$

such that the closed loop PWA system

$$x(k+1) = \mathbf{A}_i x(k) + b_i, \tag{9.12}$$

where $\mathbf{A}_i = A_i + B_i K_i$, is exponentially stable. The following theorem gives the conditions for stability of a Piecewise affine system.

Theorem 3. *([11]) The system in (9.12) is exponentially stable if there exist matrices $P_i = P_i^T > 0$, $\forall i \in \mathcal{I}$, such that the positive definite function $V(x(k)) = x^T(k)P_i x(k), \forall x \in \mathcal{X}_i$, satisfies $V(x(k+1)) - V(x(k)) < 0$.*

3.2 PWL Quadratic Regulator (PWLQR)

The aim of the control design problem is to design a controller of the form (9.11) such that it stabilizes the system and provides an upper bound on the following quadratic cost function associated with the system:

$$J = \sum_{k=0}^{\infty} x^T(k)Q_i x(k) + u^T(k)R_i u(k), \tag{9.13}$$

where $Q_i \geq 0$ and $R_i \geq 0$ are given weighting matrices of appropriate dimensions.

Definition 4. The system (11.2) subject to fault f is called reconfigurable if there exist a state feedback control law of the form (9.11) which stabilizes the systems and the upper bound on the cost function (9.13) is admissible i.e. is less than a specified given threshold.

In the following, we derive sufficient conditions for a PWA systems to be stabilizable by a PWL state feedback controller.

Theorem 4. *If there exist symmetric matrices $X_i = X_i^T > 0$ and matrices Y_i such that:*

$$\begin{bmatrix} X_i & * & * \\ (A_i X_i + B_i \Delta^f Y_i) & X_j + \mu_{il} b_i b_i^T & * \\ E_{il} X_i & \mu_{il} f_{il} b_i^T & \mu_{il}(f_{il} f_{il}^T - 1) \end{bmatrix} > 0 \qquad (9.14)$$

$$\forall (i,j) \in \mathcal{S}, i \in \mathcal{I}_1, l = 1, \ldots, \ell_i,$$

$$\begin{bmatrix} -X_i & (A_i X_i + B_i \Delta^f Y_i) \\ (A_i X_i + B_i \Delta^f Y_i)^T & -X_j \end{bmatrix} < 0, \qquad (9.15)$$

$$\forall (i,j) \in \mathcal{S}, i \in \mathcal{I}_0,$$

then there exist a PWL state feedback control law of the form (9.11) for the PWA system (9.10) such that the closed loop system is exponentially stable. The piecewise linear feedback gains are given by:

$$K_i = Y_i X_i^{-1} \qquad (9.16)$$

Proof. We consider a piecewise Lyapunov candidate function of the form $V(x(k)) = x(k)^T P_i x(k), P_i > 0$ for $x(k) \in \mathcal{X}_i$. The condition to be satisfied is:

$$V(x(k+1)) - V(x(k)) < 0, \ \ \forall (i,j) \in \mathcal{S}. \qquad (9.17)$$

We consider the general case where $x(k) \in \mathcal{X}_i$ and $x(k+1) \in \mathcal{X}_j$. First, we consider those switchings with $i \in \mathcal{I}_1$. To deal with the affine term, we will use the ellipsoidal approximation of regions. The equivalent of (9.17) for the PWA system is:

$$[(A_i + B_i \Delta^f K_i) x(k) + b_i]^T P_j [(A_i + B_i \Delta^f K_i) x(k) + b_i]$$
$$-x(k)^T P_i x(k) < 0, l = 1, \qquad (9.18)$$

which is equal to:

$$\begin{bmatrix} x(k) \\ 1 \end{bmatrix}^T \begin{bmatrix} \mathcal{A}_i^T P_j \mathcal{A}_i - P_i & * \\ b_i^T P_j \mathcal{A}_i & b_i^T P_j b_i \end{bmatrix} \begin{bmatrix} x(k) \\ 1 \end{bmatrix} < 0, \qquad (9.19)$$

where $\mathcal{A}_i = A_i + B_i \Delta^f K_i$. The ellipsoidal approximation of $\mathcal{X}_i$ can be written as:

$$\begin{bmatrix} x(k) \\ 1 \end{bmatrix}^T \begin{bmatrix} E_{il}^T & * \\ f_{il}^T E_{il} & f_{il}^T f_{il} - 1 \end{bmatrix} \begin{bmatrix} x(k) \\ 1 \end{bmatrix} \leq 0, l = 1, \ldots, \ell_i, \qquad (9.20)$$

The condition $x(k) \in \mathcal{X}_i$ is relaxed to the above approximation. Using the S-procedure, see [12], the equation (9.19) is satisfied if there exist multipliers $\lambda_{il} > 0$ such that :

$$(9.19) - \lambda_{il} \begin{bmatrix} x(k) \\ 1 \end{bmatrix}^T \begin{bmatrix} E_{il}^T & * \\ f_{il}^T E_{il} & f_{il}^T f_{il} - 1 \end{bmatrix} \begin{bmatrix} x(k) \\ 1 \end{bmatrix} < 0 \qquad (9.21)$$

Therefore, the following matrix inequality must be satisfied:

$$\begin{bmatrix} \mathcal{A}_i^T P_j \mathcal{A}_i - P_i & \mathcal{A}_i^T P_j b_i \\ b_i^T P_j \mathcal{A}_i & b_i^T P_j b_i \end{bmatrix} - \lambda_{il} \begin{bmatrix} E_{il}^T & * \\ f_{il}^T E_{il} & f_{il}^T f_{il} - 1 \end{bmatrix} < 0, \tag{9.22}$$

This is equivalent to:

$$\begin{bmatrix} P_i + \lambda_{il} E_{il}^T E_{il} & * \\ \lambda_{il} f_{il}^T E_{il} & \lambda_{il}(f_{il}^T f_{il} - 1) \end{bmatrix} - \begin{bmatrix} \mathcal{A}_i^T \\ b_i^T \end{bmatrix} P_j \begin{bmatrix} A_i & b_i \end{bmatrix} > 0. \tag{9.23}$$

Applying Schur complement to the above equation we have:

$$\begin{bmatrix} P_i + \lambda_{il} E_{il}^T E_{il} & * & * \\ \lambda_{il} f_{il}^T E_{il} & \lambda_{il}(f_{il}^T f_{il} - 1) & * \\ \mathcal{A}_i & b_i & P_j^{-1} \end{bmatrix} > 0. \tag{9.24}$$

Pre- and Post-multiplying the above equation with $diag\{I, \begin{bmatrix} 0 & * \\ I & 0 \end{bmatrix}\}$, we have:

$$\begin{bmatrix} P_i + \lambda_{il} E_{il}^T E_{il} & * & * \\ \mathcal{A}_i & P_j^{-1} & * \\ \lambda_{il} f_{il}^T E_{il} & b_i^T & \lambda_{il}(f_{il}^T f_{il} - 1) \end{bmatrix} > 0. \tag{9.25}$$

Using Schur complement, it is equivalent to:

$$\begin{bmatrix} P_i + \lambda_{il} E_{il}^T E_{il} & * \\ \mathcal{A}_i & P_j^{-1} \end{bmatrix} - \tag{9.26}$$

$$\begin{bmatrix} \lambda_{il} E_{il}^T f_{il} \\ b_i \end{bmatrix} \lambda_{il}^{-1}(f_{il}^T f_{il} - 1)^{-1} \begin{bmatrix} \lambda_{il} f_{il}^T E_{il} & b_i^T \end{bmatrix} > 0, \tag{9.27}$$

which is equal to:

$$\begin{bmatrix} P_i + \lambda_{il} E_{il}^T E_{il} & * \\ \mathcal{A}_i & P_j^{-1} \end{bmatrix} -$$

$$\begin{bmatrix} \lambda_{il} E_{il}^T f_{il}(f_{il}^T f_{il} - 1)^{-1} f_{il}^T E_{il} & * \\ b_i(f_{il}^T f_{il} - 1)^{-1} f_{il}^T E_{il} & \lambda_{il}^{-1} b_i(f_{il}^T f_{il} - 1)^{-1} b_i^T \end{bmatrix} > 0. \tag{9.28}$$

Using the matrix inversion Lemma, we have:

$$(1 - f_{il}^T f_{il})^{-1} = 1 + f_{il}^T (1 - f_{il} f_{il}^T)^{-1} f_{il}. \tag{9.29}$$

The inequality (9.28) can be written as:

$$\begin{bmatrix} P_i + \lambda_{il} E_{il}^T E_{il} & * \\ \mathcal{A}_i & P_j^{-1} \end{bmatrix} - \begin{bmatrix} \lambda_{il} E_{il}^T E_{il} & * \\ 0 & -\lambda_{il}^{-1} b_i b_i^T \end{bmatrix} + \tag{9.30}$$

$$\begin{bmatrix} E_{il}^T \\ \lambda_{il}^{-1} b_i f_{il}^T \end{bmatrix} \lambda_{il}(f_{il} f_{il}^T - I)^{-1} \begin{bmatrix} E_{il} & \lambda_{il}^{-1} f_{il} b_i^T \end{bmatrix} > 0,$$

which, by using Schur complement, is equal to:

$$\begin{bmatrix} P_i & * & * \\ \mathcal{A}_i & P_j^{-1} + \mu_{il} b_i b_i^T & * \\ E_{il} & \mu_{il} f_{il} b_i^T & \mu_{il}(f_{il} f_{il}^T - I) \end{bmatrix} > 0, \tag{9.31}$$

where $\mu_{il} = \lambda_{il}^{-1}$. Replacing $\mathcal{A}_i$ by $A_i + B_i \Delta^f K_i$, it is equivalent to:

$$\begin{bmatrix} P_i & * & * \\ (A_i + B_i \Delta^f K_i) & P_j^{-1} + \mu_{il} b_i b_i^T & * \\ E_{il} & \mu_{il} f_{il} b_i^T & \mu_{il}(f_{il} f_{il}^T - 1) \end{bmatrix} > 0, \tag{9.32}$$

Pre- and post-multiply (9.32) by $diag\{P_i^{-1}, I, I\}$, and defining $X_i = P_i^{-1}, Y_i = K_i P_i^{-1}$, we get (9.14). For subsystems that contain the origin i.e. $i \in \mathcal{I}_0$, we have $f_{il} f_{il}^T - I < 0$ which means that the LMI (9.14) is not feasible. For these subsystems the LMI (9.15) is considered and there is no need to include the region information. Therefore, the following matrix inequality must be satisfied:

$$(A_i + B_i \Delta^f K_i)^T P_j (A_i + B_i \Delta^f K_i) - P_i < 0 \tag{9.33}$$

Using Schur complement, the above inequality is equivalent to:

$$\begin{bmatrix} -P_i & (A_i + B_i \Delta^f K_i)^T \\ (A_i + B_i \Delta^f K_i) & -P_j^{-1} \end{bmatrix} < 0 \tag{9.34}$$

By pre- and post-multiplying (9.34) by $diag\{P_i^{-1}, I\}$, then defining $X_i = P_i^{-1}, Y_i = K_i P_i^{-1}$, we get (9.15). $\qquad\square\qquad\qquad\square$

The above theorem only considers stability. In many situations, the system might be stabilizable but the cost of reaching to the origin from the initial state might not be admissible. To include admissibility of the upper bound on the cost function we introduce the following theorem.

Theorem 5. *If there exist symmetric matrices $X_i = X_i^T > 0$ and matrices Y_i and positive constants such that:*

$$\begin{bmatrix} X_i & * & * & * & * \\ (A_i X_i + B_i \Delta^f Y_i) & X_j + \mu_{il} b_i b_i^T & * & * & * \\ E_{il} X_i & \mu_{il} f_{il} b_i^T & \mu_{il}(f_{il} f_{il}^T - 1) & * & * \\ \Delta^f Y_i & 0 & 0 & R_i^{-1} & * \\ X_i & 0 & 0 & 0 & Q_i^{-1} \end{bmatrix} > 0 \tag{9.35}$$

$$\forall (i,j) \in \mathcal{S}, i \in \mathcal{I}_1, l = 1, \ldots, \ell_i,$$

$$\begin{bmatrix} -X_i & * & * & * \\ (A_i X_i + B_i \Delta^f Y_i) & -X_j & 0 & 0 \\ \Delta^f Y_i & 0 & R_i^{-1} & * \\ X_i & 0 & 0 & Q_i^{-1} \end{bmatrix} < 0, \tag{9.36}$$

$$\forall (i,j) \in \mathcal{S}, i \in \mathcal{I}_0$$

then there exist a PWL state feedback control law of the form (9.11) for the PWA system (9.1) subject to fault f such that the closed system is exponentially stable. The PWL feedback gains are given by:

$$K_i = Y_i X_i^{-1}, \tag{9.37}$$

and the upper bound on the cost function (9.13) satisfies:

$$J \leq x(0)^T X_{i_0}^{-1} x(0), \tag{9.38}$$

where i_0 is the region index for the initial condition, i.e. $x(0) \in \mathcal{X}_{i_0}$.

Proof. We consider a piecewise Lyapunov candidate function of the form $V(x(k)) = x(k)^T P_i x(k)$, $P_i > 0$ for $x(k) \in \mathcal{X}_i$. The condition to be satisfied is:

$$V(x(k+1)) - V(x(k)) + x(k)^T Q_i x(k) + \tag{9.39}$$
$$x(k)^T K_i^T R_i K_i x(k) < 0, \forall (i,j) \in \mathcal{S}.$$

The proof of stability is very similar to the previous theorem except that to deal with the term $x(k)^T Q_i x(k) + x(k)^T K_i^T R_i K_i x(k)$ we use the Schur complement two more times at the end of the proof. To prove that (9.38) is satisfied we sum up (9.39) from $k = 0$ to $k = \infty$, which results in:

$$V(x(\infty)) - V(x(0)) + \Sigma_0^\infty (x^T(k) Q_i x(k) + u^T(k) R_i u(k)) < 0 \tag{9.40}$$

Because Q_i and R_i are positive, hence $x(k)^T Q_i x(k) + x(k)^T K_i^T R K_i x(k) \geq 0$. Therefore, if (9.39) is satisfied the system is stable which means $V(x(\infty)) = 0$. As $V(x(0)) = x(0)^T P_{i_0} x(0)$. Therefore we have:

$$\sum_{k=0}^\infty (x^T(k) Q_i x(k) + u^T(k) R_i u(k)) < x^T(0) P_{i_0} x(0). \quad \square$$

$\square$

The upper bound found in the theorem (5) is not optimal. We are interested to minimize this cost to find a controller with the minimum cost. The upper bound of (9.13), could be minimized in the following way. The initial condition is considered as a random variable with uniform distribution in a bounded region $\overline{\mathcal{X}}$. Then, it is tried to minimize the expected value of the cost function. We have:

$$E(J) \leq E(tr(P_{i_0} x(0) x^T(0))) \leq \sum_{i \in \mathcal{I}} \sigma_i tr(P_i L_i), \tag{9.41}$$

where $L_i = E(x(0) x^T(0))$ is the expectation of $x(0) x^T(0)$ corresponding to $x(0) \in \mathcal{X}_i, i \in \mathcal{I}$, $tr(\cdot)$ is the trace operator and σ_i is the probability of $x(0) \in \mathcal{X}_i$. Then, the optimization problem is:

$$J^* = \min_{X_i, Y_i} \sum_{i \in \mathcal{I}} \sigma_i tr(X_i^{-1} L_i) \tag{9.42}$$

$$s.t. \begin{cases} (9.35) \\ (9.36) \\ X_i = X_i^T > 0, \end{cases}$$

The above optimization problem is non-convex. To convert it to a convex optimization problem , we introduce new variables $V_i, i \in \mathcal{I}$, which satisfies:

$$\begin{bmatrix} V_i & I \\ I & Z_i \end{bmatrix} \geq 0. \tag{9.43}$$

Using Schur complement, the above constraint is equivalent to $Z_i^{-1} \leq V_i$. Therefore, the objective function in (9.42), which is nonlinear in term of Z_i, can be converted to $\sum_{i \in \mathcal{I}} \sigma_i tr(V_i L_i)$. Consequently, the optimization problem (9.42) can be transformed to the following convex form:

$$J^* = \min_{X_i, Y_i, V_i, \epsilon_i} \sum_{i \in \mathcal{I}} \sigma_i tr(V_i L_i) \tag{9.44}$$

$$s.t. \begin{cases} (9.35), \\ (9.36), \\ (9.43), \\ X_i = X_i^T > 0, \end{cases}$$

In the following theorem we consider the properties for reconfigurability to be stability and admissibility of the optimal upper bound on the cost function.

Theorem 6. *The system (9.1) subject to fault f with respect to admissibility threshold $\overline{J}$ on the cost function (9.13) is reconfigurable if:*

- *(9.14) and (9.15) are satisfied,*

- *$J^* < \overline{J}$.*

Proof. Satisfaction of (9.14) and (9.15) guarantees that the system is stabilizable with a PWL state feedback controller and satisfying $J^* < \overline{J}$ is equal to admissibility of the cost. Therefore, based on definition 5 the system subject to fault f is reconfigurable. □ □

4 Example

The method is applied to a climate control systems of a live-stock building, which was obtained during previous research, [8]. The general schematic of the large scale live-stock building equipped with hybrid climate control system is illustrated in Figure. 9.1. In a large scale stable, the indoor airspace is incompletely mixed; therefore it is divided into conceptually homogeneous parts called zones. In our model, there are three zones which are not similar in size. Zone 1, the one on the left, is the biggest and Zone 2, the middle one, is the smallest. Due to the indoor and outdoor conditions, the airflow direction varies between adjacent zones. Therefore, the system behavior is represented by a finite number of different dynamic equations. The model is divided into subsystems as follows: Inlet model for both windward and leeward, outlet model, and stable heating system, and finally the dynamic model of temperature based on the heat balance equation. The nonlinear model of the system is approximated by a discrete-time PWA system with 4 regions based on the airflow direction. The model of the system are derived for the following polyhedral regions:

$$\mathcal{X}_1 = \{[x^T \ u^T]^T | F_1^x x + F_1^u \geq f_1, F_2^x x + F_2^u \geq f_2\}, \tag{9.45}$$

$$\mathcal{X}_2 = \{[x^T \ u^T]^T | F_1^x x + F_1^u < f_1, F_2^x x + F_2^u < f_2\}, \tag{9.46}$$

$$\mathcal{X}_3 = \{[x^T \ u^T]^T | F_1^x x + F_1^u < f_1, F_2^x x + F_2^u \geq f_2\}, \tag{9.47}$$

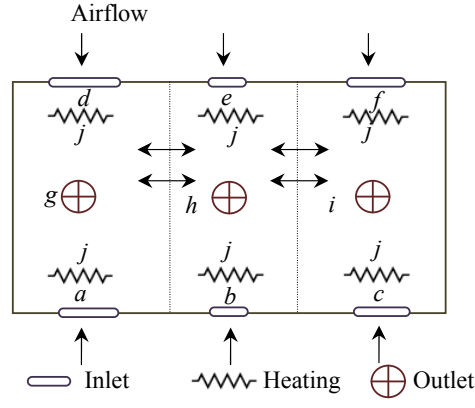$$\mathcal{X}_4 = \{[x^T \ u^T]^T | F_1^x x + F_1^u \geq f_1, F_2^x x + F_2^u < f_2\}, \tag{9.48}$$

Figure 9.1: The top view of the test stable

,where

$$F_1^x = \begin{bmatrix} 1.0817 & -0.0457 & -0.9938 \end{bmatrix}$$
$$F_2^x = \begin{bmatrix} -1.1144 & 0.0490 & 1.0187 \end{bmatrix}$$
$$F_1^u = \begin{bmatrix} 0.2323 & -0.0072 & 0.2323 & 0.2323 & -0.0072 \end{bmatrix}$$
$$0.2323 \quad -0.072 \quad 0.1349 \quad -0.0719 \quad -0.0064 \end{bmatrix},$$
$$F_2^u = \begin{bmatrix} -0.2558 & 0.0074 & -0.2558 & -0.2558 & 0.0074 \end{bmatrix}$$
$$-0.2558 \quad 0.0742 \quad -0.12 \quad 0.0742 \quad 0.0074 \end{bmatrix},$$
$$f_1 = 0.4058, f_2 = -0.4575 \tag{9.49}$$

As one can see from the description of regions, they are dependent on the input and the state at k. But $u(k)$ is unknown and is to be calculated based on the current region. Therefore, it is impossible to calculate the current mode. To remedy this problem, instead of a PWL controller, we consider a common controller for all regions, i.e.

$$u(k) = Kx(k) \tag{9.50}$$

The discrete-time PWA model is described by:

$$A_1 = \begin{bmatrix} 1.6361 & 0.0480 & -0.7716 \\ 1.5782 & 0.5522 & -0.9983 \\ 0.7747 & 0.0462 & 0.0990 \end{bmatrix}, \tag{9.51}$$

$$A_2 = \begin{bmatrix} 1.1145 & -0.0300 & -1.0590 \\ 1.6452 & 0.1010 & -1.4342 \\ 0.3008 & 0.0191 & -0.2324 \end{bmatrix}, \tag{9.52}$$

$$A_3 = \begin{bmatrix} 1.6340 & 0.0259 & -0.7150 \\ 1.5474 & 0.8335 & -1.4790 \\ 0.7674 & 0.0314 & 0.1456 \end{bmatrix}, \tag{9.53}$$

$$A_4 = \begin{bmatrix} 1.6274 & 0.0049 & -0.6987 \\ 1.6242 & 0.8163 & -1.4751 \\ 0.7623 & 0.0051 & 0.1640 \end{bmatrix}, \tag{9.54}$$

$$B_1 = \begin{bmatrix} -0.1163 & 0.0459 & -0.1163 & -0.1163 & 0.0459 \\ 0.5718 & -0.3768 & 0.5718 & 0.5718 & -0.3768 \\ -0.1147 & 0.0353 & -0.1147 & -0.1147 & 0.0353 \end{bmatrix}$$

$$\begin{matrix} -0.1163 & 0.0018 & -0.0567 & 0.0018 & 0.0070 \\ 0.5718 & -0.1518 & 0.2724 & -0.1518 & -0.0056 \\ -0.1147 & 0.0022 & -0.0553 & 0.0022 & 0.0071 \end{matrix}, \tag{9.55}$$

$$B_2 = \begin{bmatrix} 0.1137 & -0.0044 & 0.1137 & 0.1137 & -0.0044 \\ -0.0104 & 0.1057 & -0.0104 & -0.0104 & 0.1057 \\ 0.0581 & 0.0258 & 0.0581 & 0.0581 & 0.0258 \end{bmatrix}$$

$$\begin{matrix} 0.1137 & -0.0697 & 0.2883 & -0.0697 & 0.0023 \\ -0.0104 & 0.0183 & 0.8276 & 0.0183 & 0.1275 \\ 0.0581 & 0.0097 & 0.0939 & 0.0097 & 0.0273 \end{matrix}, \tag{9.56}$$

$$B_3 = \begin{bmatrix} -0.0677 & -0.0127 & -0.0677 & -0.0677 & -0.0127 \\ 0.2031 & 0.0778 & 0.2031 & 0.2031 & 0.0778 \\ -0.0697 & -0.0188 & -0.0697 & -0.0697 & -0.0188 \end{bmatrix}$$

$$\begin{matrix} -0.0677 & -0.0103 & -0.0080 & -0.0103 & 0.0078 \\ 0.2031 & -0.0594 & -0.0506 & -0.0594 & -0.0012 \\ -0.0697 & -0.0098 & -0.0087 & -0.0098 & 0.0075 \end{matrix}, \tag{9.57}$$

$$B_4 = \begin{bmatrix} -0.0393 & -0.0380 & -0.0393 & -0.0393 & -0.0380 \\ 0.0851 & 0.1683 & 0.0851 & 0.0851 & 0.1683 \\ -0.0414 & -0.0434 & -0.0414 & -0.0414 & -0.0434 \end{bmatrix}$$

$$\begin{matrix} -0.0393 & -0.0133 & -0.0234 & -0.0133 & 0.0086 \\ 0.0851 & -0.0568 & 0.0160 & -0.0568 & 0.0029 \\ -0.0414 & -0.0130 & -0.0241 & -0.0130 & 0.0085 \end{matrix}, \tag{9.58}$$

$$b_1 = \begin{bmatrix} 0.4749 \\ -0.9236 \\ 0.4214 \end{bmatrix}, \; b_2 = \begin{bmatrix} -0.0676 \\ 2.2442 \\ 0.3784 \end{bmatrix}, \tag{9.59}$$

$$b_3 = \begin{bmatrix} 0.2356 \\ 0.3694 \\ 0.2500 \end{bmatrix}, \; b_4 = \begin{bmatrix} 0.3510 \\ -0.5021 \\ 0.3682 \end{bmatrix}. \tag{9.60}$$

Here, the initial condition is $x(0) = \begin{bmatrix} 10 & 10 & 10 \end{bmatrix}^T$, and the set of the actuators of the system is $\{a, b, c, d, e, f, g, h, i, j\}$, where a, b, c, d, e, f are inlets, g, h, i are fans, and j is the heating systems. Actuator a, b, c, d, e, f respectively represent 12, 6, 12, 14, 6, 12 connected inlets. The control problem is to regulate the temperature of each zone around

19. To make notations simpler, we only write those actuator that are healthy. For example, $\{a, b, c, d\}$ means that only actuators a, b, c, and d are healthy and the rest are faulty. Results of the reconfigurability analysis shows that the system with more than 5 faulty actuators is not reconfigurable. It also shows that heating system, actuator j, should be healthy for reconfigurability of the system. In table 9.1, different faulty situations with 5 or 6 fault-free actuators are considered. Because of the lack of space we have just shown some cases to demonstrate the method. The first column shows the fault-free actuators and the second column shows the corresponding quadratic cost. We have only considered the cases that the system is stabilizable. The admissibility threshold of the cost is considered as 700. As it can be seen from the table, even though all the cases are stabilizable, some of them are not admissible; hence the system is not reconfigurable based on definition 5. The reconfigurable cases are boldfaced. Figure. 9.2 shows temperature of each zone for the fault-free system. As it is obvious the controller is able to regulate the temperature around the reference. Figure. 9.3 shows the output of the system for the case that the fault-free actuator set is $\{a, b, g, h, j\}$. As it can be seen, the controller is able to track the reference with some degradation in the performance which is admissible.

Table 9.1: Stabilizable actuator sets and associated quadratic cost

Fault-free actuators	quadratic cost
$\{a,b,h,i,j\}$	**668.8**
$\{a,b,g,h,j\}$	**668.1**
$\{e,f,h,i,j\}$	**670**
$\{e,f,g,h,j\}$	**669.4**
$\{d,e,f,g,h,j\}$	**675**
$\{a,b,c,g,h,j\}$	**665**
$\{a,b,c,h,i,j\}$	**667.2**
$\{d,e,f,h,i,j\}$	**668.2**
$\{a,f,g,h,j\}$	129220
$\{d,e,f,i,j\}$	271655
$\{a,b,c,g,i,j\}$	264750
$\{d,e,f,g,j\}$	261355
$\{a,f,h,i,j\}$	127770

5 Conclusion and Future works

We presented an approach for reconfigurability of discrete time PWA systems. Reconfigurability is defined as both stability and admissibility of the upper bound on the quadratic cost. Sufficient conditions for reconfigurability of a system subject to a fault with respect to a given threshold on the quadratic performance cost are given in terms of LMI. The upper bound is minimized by solving a convex optimization problem with LMI constraints. The approach is applied to the climate control system of a livestock building. Situations in which the system is reconfigurable with maximum number of actuator outages are found. The simulation results demonstrates that the performance of the system is still acceptable.
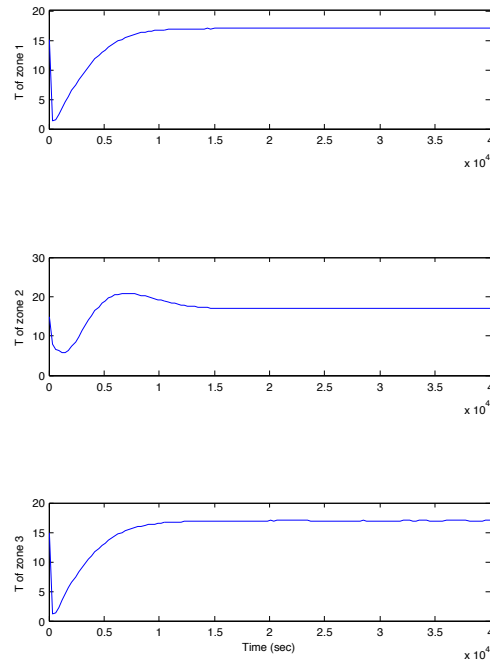
Figure 9.2: Simulation results with a controller designed for the fault-free system

Future works will consider application of the method in designing an AFTC with optimal number of control laws.

References

[1] C. Frei, F. Kraus, and M. Blanke, "Recoverability viewed as a system property," in *European Control Conference*, Karlsruhe, Germany, 1999.

[2] N. Wu, K. Zhou, and G. Salomon, "Control reconfigurability of linear time-invariant systems," *Automatica*, vol. 36, no. 11, pp. 1767–1771, 2000.

[3] M. Staroswiecki, "On reconfigurability with respect to actuator failures," in *Proceedings of the 15th Triennial World Congress of IFAC*, 2002.

[4] ——, "Actuator faults and the linear quadratic control problem," in *Proceedings of 42nd IEEE Conference on Decision and Control*, vol. 1, 2003, pp. 959 – 965.

[5] A. Khelassi, D. Theilliol, and P. Weber, "Reconfigurability analysis for reliable fault-tolerant control design," in *Proceedings of 7th Workshop on Advanced Control and Diagnosis*, 2009.

[6] B. M. Gonzalez-Contreras, D. Theilliol, and D. Sauter, "Online Reconfigurability Evaluation for Actuator Fault Using Input/Output Data," in *Proceedings of 7th IFAC*
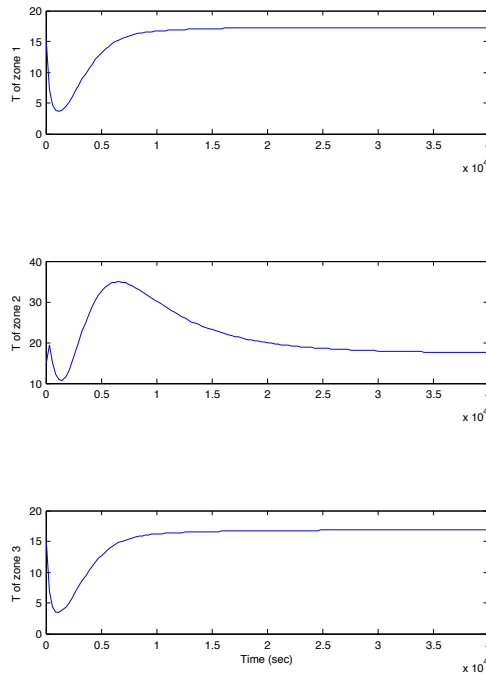
Figure 9.3: Simulation results with a controller designed for the system with the fault-free actuator set:$\{a, b, g, h, j\}$

Symposium on Fault Detection, Supervision and Safety of Technical Processes, Safeprocess09, 2009.

[7] L. Rodrigues and E.-K. Boukas, "Piecewise linear h_∞ controller synthesis with application to inventory control of switched production systems," *Automatica*, vol. 42, pp. 1245–1254, 2006.

[8] M. Gholami, H. Shioler, and T. Soltani, M. Bak, "Multi-Zone Hybrid Model for Failure Detection of the Stable Ventialation System," in *Proceedings of Industrial Electronic Society*, 2010.

[9] Z. Yang, "Reconfigurability analysis for a class of linear hybrid systems," in *Proceedings of 6th IFAC safeprocess*, 2006.

[10] L. Rodrigues and S. Boyd, "Piecewise-affine state feedback for piecewise-affine slab systems using convex optimization," *Systems & Control Letters*, vol. 54, no. 9, pp. 835–853, 2005.

[11] F. Cuzzola and M. Morari, "A generalized approach for analysis and control of discrete-time piecewise affine and hybrid systems," *Hybrid Systems: Computation and Control*, vol. 2034, pp. 189–203, 2001.

[12] S. Boyd, L. E. Ghaoui, E. Feron, and V. Balakrishnan, *Linear Matrix Inequalities in System and Control Theory*. Society for Industrial Mathematics, 1994.

Paper E

**Passive Fault Tolerant Control of Piecewise Affine Systems Based on
H Infinity Synthesis**

Mehdi Gholami, Vincent Cocquempot,Henrik Schioler and Thomas Bak

Abstract

In this paper we design a passive fault tolerant controller against actuator faults for discretetime piecewise affine (PWA) systems. By using dissipativity theory and H_∞ analysis, fault tolerant state feedback controller design is expressed as a set of linear matrix inequalities (LMIs). In the current paper, the PWA system switches not only due to the state but also due to the control input. The method is applied on a large scale livestock ventilation model.

1   Introduction

Performance of modern control systems typically relies on a number of strongly interconnected components. Component malfunctions may degrade performance of the system or even result in loss of functionality. In applications such as climate control systems for livestock buildings, this is unacceptable as it may lead to the loss of animal life. Therefore, it is desirable to develop control systems such that they are capable of tolerating component malfunctions while still maintaining desirable performance and stability properties.

Fault tolerant control (FTC) is divided generally into passive (PFTC) and active (AFTC) approaches. In AFTC, the control loop is adapted online according to information given by a fault detection and isolation (FDI) module. Generally speaking, AFTC systems are divided into three layers as proposed in [1]. The first layer is related to the control loop, the second layer corresponds to the FDI and accommodation modules and the last layer corresponds to the supervisor system. PFTC does not need any FDI or supervisor layer. In this technique the control laws are fixed and the fault is considered as a system disturbance or uncertainty. In fact, the control law is designed to preserve the system performance either in healthy or in faulty situation using robust control techniques, see [2], [3], and [4]. Most complex industrial systems either exhibit nonlinear behaviour or involve both discrete and continuous components. One of the modelling frameworks which is relevant for nonlinear and most classes of hybrid systems with both discrete and continuous behaviours, is piecewise affine systems (PWA). This framework has been applied in several areas, such as, switched system, [5], etc. For AFTC systems, the reader is referred to [6], where the authors developed an AFTC against actuator failures for discrete-time switched linear systems. In [7], an AFTC approach for continuous-time PWA system subject to actuator and sensor faults is proposed. In [8] a fault accommodation problem is discussed for a class of hybrid systems. A PFTC approach is presented in [9], where a state feedback controller is designed for continuous-time PWA systems subject to actuator faults.

In [10], a PFTC for discrete time PWA systems is presented. The approach is based on a state feedback control that is tolerant against actuator faults. The PWA systems switch only due to state variables. In this paper, we consider PFTC for the general class of discrete-time PWA models whose switching sequence depends on both state and input trajectories. We use a piecewise quadratic (PWQ) Lyapunov function and H_∞ analysis in order to design a state feedback controller such that the closed loop system is asymptotically stable in healthy and in actuators failure situations. The problem is cast as a set of linear matrix inequalities (LMI) and solved with YALMIP/ SeDumi, see [11]. The H_∞ analysis is based on the passivity theory for nonlinear systems as in [12].

The paper is organized as follows. Section II presents the piecewise affine model and actuator fault representation. Section III discusses H_∞ control design for PWA systems. The extension of H_∞ synthesis for fault tolerant control of piecewise affine systems is discussed in section IV. Section V is dedicated to the simulation results for the climate control system. The conclusion is presented in section VI.

2 Piecewise Affine Systems and Actuator Fault Representation

2.1 Piecewise Affine Systems

Consider a discrete-time piecewise affine system, $\sum_i$ as:

$$x(k+1) = A_i x(k) + B_i u(k) + a_i \quad for \begin{bmatrix} x(k) \\ u(k) \end{bmatrix} \in \mathcal{X}_i, \tag{10.1}$$

$$y(k) = Cx(k) \tag{10.2}$$

where $x(k) \in \mathbb{R}^n$ is the state, $u(k) \in \mathbb{R}^m$ is the control input, $y(k) \in \mathcal{R}^p$ is the output. The set $\mathbb{X} \subseteq \mathbb{R}^{n+m}$ represents every possible vector $\begin{bmatrix} x(k)^T u(k)^T \end{bmatrix}^T$, $\{\mathcal{X}_i\}_{i=1}^s$ denotes polyhedral regions of $\mathbb{X}$ and $a_i \in \mathbb{R}^n$ is a constant vector. Each polyhedral region is represented by:

$$\mathcal{X}_i = \{ \begin{bmatrix} x(k)^T u(k)^T \end{bmatrix}^T \mid F_i^x x \geq f_i^x \ and \ F_i^u u \geq f_i^u \} \tag{10.3}$$

It is assumed that the regions are defined with known matrices F_i^x, F_i^u, f_i^x and f_i^u. The following notations are defined as in [12]:

$$\bar{\mathcal{X}}_i = \{ x(k) \mid F_i^x x \geq f_i^x \} \tag{10.4}$$

and

$$S_j = \{ i \mid \exists x, u \ with \ x \in \bar{\mathcal{X}}_i, [x^T \ u^T]^T \in \mathcal{X}_i \} \tag{10.5}$$

S_j denotes the set of all indices i such that $\mathcal{X}_i$ is a region including a vector $[x^T \ u^T]^T$ when the condition $x \in \bar{\mathcal{X}}_i$ is satisfied. $\mathscr{I} = \{1, \cdots, s\}$ is the set of indices of regions $\mathcal{X}_i$ and $\mathcal{I} = \{1, \cdots, t\}$ is the set of indices of the regions $\bar{\mathcal{X}}_j$. All possible switchings from region $\mathcal{X}_i$ to $\mathcal{X}_j$ are defined by the set $\mathcal{S}$:

$$\mathcal{S} = \{ (i,j) : \ i,j \in \mathscr{I} \ and \ \exists \begin{bmatrix} x(k) \\ u(k) \end{bmatrix}, \begin{bmatrix} x(k+1) \\ u(k+1) \end{bmatrix} \in \mathbb{X} \tag{10.6}$$

$$\mid \begin{bmatrix} x(k) \\ u(k) \end{bmatrix} \in \mathcal{X}_i \ and \ \begin{bmatrix} x(k+1) \\ u(k+1) \end{bmatrix} \in \mathcal{X}_j \}$$

2.2 Fault Model

Actuator faults are considered. u_j is the actuator output. The partial loss of actuator can be formulated as

$$u_j^F = (1 - \alpha_j) u_j, \quad 0 \leq \alpha_j \leq \alpha_{Mj}, \tag{10.7}$$

where α_j is the percentage of efficiency loss of the actuator j and α_{Mj} is the maximum loss. $\alpha_j = 0$ corresponds to the nominal system, $\alpha_j = 1$ corresponds to 100% loss of the actuator and $0 \leq \alpha_j \leq 1$ corresponds to partial loss. Let us define α as

$$\alpha = diag\{\alpha_1, \alpha_2, \ldots, \alpha_m\}. \tag{10.8}$$

Then

$$u^F = \Gamma u, \tag{10.9}$$

where $\Gamma = (I_{m \times m} - \alpha)$, I is a identity matrix. Thus u^F represents the control signal that is applied in normal or faulty situation. The PWA model of the system with the fault F_i is

$$x(k+1) = A_i x(k) + B_i \Gamma_i u(k) + a_i \quad for \quad \begin{bmatrix} x(k) \\ u(k) \end{bmatrix} \in \mathcal{X}_i \tag{10.10}$$

3 H_∞ Control Design for Piecewise Affine Systems

3.1 H_∞ Performance

Consider the PWA system

$$x(k+1) = A_i x(k) + B_i u(k) + B_i^w w(k) + a_i \tag{10.11}$$
$$for \quad \begin{bmatrix} x(k) \\ u(k) \end{bmatrix} \in \mathcal{X}_i, \ x(k) \in \bar{\mathcal{X}}_j$$
$$z(k) = C_i x(k) + D_i u(k) + D_i^w w(k) \tag{10.12}$$

where $w(k) \in \mathbb{R}^r$ is a disturbance signal and $z(k) \in \mathbb{R}^s$ is a performance output. First, for the sake of simplicity, it is assumed that $a_i = 0$, and the control objective is to track the origin with the initial condition $x(0) = 0$. The H_∞ performance for each integer $N \geq 0$ is written as

$$\sum_{g=0}^{N} \|z(g)\|^2 \leq \gamma^2 \sum_{g=0}^{N} \|w(g)\|^2 \tag{10.13}$$

which expresses that the H_∞ norm from the edisturbance w to the performnace output z is less than γ.

3.2 Controller Structure

Consider a piecewise linear state feedback control with the following structure

$$u(k) = K_i x(k) \quad for \quad \begin{bmatrix} x(k) \\ u(k) \end{bmatrix} \in \mathcal{X}_i \tag{10.14}$$

where K_i is the controller gain which is designed to stabilize exponentially the closed loop PWA system. Since the index i is not a priori known, it is not possible to calculate $u(k)$. Hence, the problem is changed to the following structure

$$u(k) = K_j x(k) \ \ for \ x(k) \in \bar{\mathcal{X}}_j \tag{10.15}$$

It means that we do not consider a different controller in each region $\mathcal{X}_i$ with $i \in \mathscr{I}$ but a different one in each region $\bar{\mathcal{X}}_j$ with $j \in \mathcal{I}$.

Applying the control law (10.15) to the system (10.12) yields the following closed loop system:

$$x(k+1) = \mathcal{A}_{ij}x(k) + B_i^w w(k) \ for \ \begin{bmatrix} x(k) \\ u(k) \end{bmatrix} \in \mathcal{X}_i, \ x(k) \in \bar{\mathcal{X}}_j \tag{10.16}$$

$$z(k) = \mathcal{C}_{ij}x(k) + D_i^w w(k) \tag{10.17}$$

where $\mathcal{A}_{ij} = A_i + B_i K_j$, $\mathcal{C}_{ij} = C_i + D_i K_j$, and $u(k) = K_j x(k)$.

Lemma 3. *([13]) Let M, N, H be real matrices. If $H^T H \leq I$, then for every scalar $\epsilon > 0$ the following inequality hold:*

$$MHN + N^T H^T M^T \leq \epsilon MM^T + \epsilon^{-1} N^T N. \tag{10.18}$$

Lemma 4. *([12]) Consider the system (10.17) with zero initial condition $x(0) = 0$. If there exists a function $V(x,u) = x^T P_i x$ for $[x^T \ u^T]^T \in \mathcal{X}_i$ with $P_i = P_i^T > 0$ satisfying the dissipativity inequality*

$$\forall k, \ V(x(k+1), \ u(k+1)) - V(x(k), \ u(k)) \tag{10.19}$$
$$< \gamma^2 \|w(k)\|^2 - \|z(k)\|^2$$

then, the H_∞ performnace condition (10.13) is satisfied.

Furthermore, condition (10.19) is fulfilled if the following matrix inequalities are satisfied

$$\forall j \in \mathcal{I}, \ \forall i \in S_j, \ \forall l \ with \ (l,j) \in S, \ M_{l,ij} < 0. \tag{10.20}$$

where

$$M_{l,i,j} = \begin{bmatrix} \mathcal{A}_{ij}^T P_l \mathcal{A}_{ij} - P_i + \mathcal{C}_{ij}^T \mathcal{C}_{ij} & * \\ D_i^T \mathcal{C}_{ij} + B_i^T P_l \mathcal{A}_{ij} & B_i^T P_l B_i + D_i^T D_i - \gamma^2 I \end{bmatrix} \tag{10.21}$$

In the last case the system (10.17) is PWQ stable.

4 Extension of H_∞ Synthesis for Passive Fault Tolerant Control of Piecewise Affine Systems

It is assumed that the control objective is to track the reference x_r when the system is subject to fault F_i. With the change of coordinates $e = x - x_r$ the problem is transformed

into the origin tracking form. In these coordinates, the system dynamics (10.12) subject to the fault F_i are

$$e(k+1) = A_i e(k) + B_i \Gamma_i u(k) + \tilde{B}_i^w \tilde{w}(k) \quad \begin{bmatrix} e(k) \\ u(k) \end{bmatrix} \in \mathcal{X}_i, \qquad (10.22)$$

$$e(k) \in \bar{X}_i,$$

where $\tilde{w}(k) = \begin{bmatrix} w(k) \\ a_i + A_i x_r - x_r \end{bmatrix}$ and $\tilde{B}_i^w(k) = [B_i^w \ I]$.

The polyhedral regions are written as

$$\mathcal{X}_i = \{[e^T \ u^T]^T | \ F_i^x e \geq f_i^e \ and \ F_i^u \geq f_i^u\} \qquad (10.23)$$

$$\bar{X}_i = \{e| \ F_i^x e \geq f_i^e\} \qquad (10.24)$$

where $f_i^e = f_i^x - F_i^x x_r$.

Applying the control law (10.15) to the system (10.22) leads to the following closed loop system:

$$e(k+1) = \mathcal{A}_{ij} e(k) + \tilde{B}_i^w \tilde{w}(k) \quad \begin{bmatrix} e(k) \\ u(k) \end{bmatrix} \in \mathcal{X}_i, \ e(k) \in \bar{X}_i, \qquad (10.25)$$

where $\mathcal{A}_{ij} = A_i + B_i \Gamma_i K_j$, $u(k) = K_j e(k)$ and $z(k) = e(k)$.

4.1 Passive Fault Tolerant Control

Definition 5. A piecewise linear control law (10.15) is a passive fault-tolerant control if the closed loop system (10.25) is asymptotically stable and the H_∞ tracking performance is guaranteed for all $\tilde{w}(k)$. This definition is expressed in the following theorem.

Theorem 7. *The fault-tolerant piecewise linear controller (10.15) stabilizes the system (10.25) whilst fulfilling the dissipativity inequality (10.19), if there exist symmetric matrices $Q_i = Q_i^T > 0$, invertible matrices G_i, matrices Y_i and positive scalars $\epsilon_{ij} > 0$, $i \in \mathscr{I}$, $j \in \mathcal{I}$ such that*

$$\begin{bmatrix} Q_i - G_i^T - G_i & 0 & (A_i G_i + B_i Y_i)^T & G_j^T & Y_j^T \alpha_i \\ 0 & -\gamma^2 I & \tilde{B}_i^{w^T} & 0 & 0 \\ (A_i G_j + B_i Y_j) & \tilde{B}_i^w & -Q_l + \epsilon_{ij} B_i B_i^T & 0 & 0 \\ G_j & 0 & 0 & -I & 0 \\ \alpha_i Y_j & 0 & 0 & 0 & -\epsilon_{ij}^{-1} \end{bmatrix} < 0 \qquad (10.26)$$

$$\forall j \in \mathcal{I}, \ \forall i \in S_j, \ \forall l \ with \ (l, i) \in S_{all}$$

Then the piecewise affine feedback gains are obtained by:

$$K_j = Y_j G_j^{-1} \qquad (10.27)$$

Proof. Passivity inequality (10.19) is equivalent to:

$$(e(k)^T \mathcal{A}_{ij}^T + \tilde{w}^T(k)\tilde{B}_i^{w^T})P_l(e(k)^T \mathcal{A}_{ij}^T + \tilde{w}^T(k)\tilde{B}_i^{w^T})^T \tag{10.28}$$
$$-e(k)^T P_i e(k) + e(k)^T e(k) - \gamma^2 \tilde{w}_k^T \tilde{w}_k < 0$$

which is equivalent to

$$\begin{bmatrix} \mathcal{A}_{ij}^T P_l \mathcal{A}_{ij} - P_i + I & * \\ \tilde{B}_i^{w^T} P_l \mathcal{A}_{ij} & \tilde{B}_i^{w^T} P_l \tilde{B}_i^w - \gamma^2 I \end{bmatrix} < 0 \tag{10.29}$$

By substituting $Q = P^{-1}$, it is obtained:

$$\begin{bmatrix} -Q_i^{-1} + I & 0 \\ 0 & -\gamma^2 I \end{bmatrix} + \begin{bmatrix} \mathcal{A}_{ij}^T \\ \tilde{B}_i^{w^T} \end{bmatrix} Q_l^{-1} [\mathcal{A}_{ij} \ \tilde{B}_i^w] < 0 \tag{10.30}$$

Using Schur complement we get

$$\begin{bmatrix} -Q_i^{-1} & 0 & \mathcal{A}_{ij}^T & I \\ 0 & -\gamma^2 I & \tilde{B}_i^{w^T} & 0 \\ \mathcal{A}_{ij} & \tilde{B}_i^w & -Q_l & 0 \\ I & 0 & 0 & -I \end{bmatrix} < 0 \tag{10.31}$$

Pre- and post-multiplying the right side of (10.31) by diag $\{G_j^T, \ I, \ I, \ I\}$ and diag $\{G_j, \ I, \ I, \ I\}$, substituting the value of $\mathcal{A}_{ij}$, and using the fact that $G_j^T P_j G_j \geq G_j + G_j^T - P_j^{-1}$, as in [12], it is obtained that:

$$\begin{bmatrix} Q_i - G_j^T - G_j & 0 & (A_i G_j + B_i(I - \alpha_i)Y_j)^T & G_j^T \\ 0 & -\gamma^2 I & \tilde{B}_i^{w^T} & 0 \\ (A_i G_j + B_i(I - \alpha_i)Y_j) & \tilde{B}_i^w & -Q_l & 0 \\ G_j & 0 & 0 & -I \end{bmatrix} < 0 \tag{10.32}$$

which is equivalent to

$$\begin{bmatrix} Q_i - G_j^T - G_j & 0 & (A_i G_j + B_i Y_j)^T & G_j^T \\ 0 & -\gamma^2 I & \tilde{B}_i^{w^T} & 0 \\ (A_i G_j + B_i Y_j) & \tilde{B}_i^w & -Q_l & 0 \\ G_j & 0 & 0 & -I \end{bmatrix} - \tag{10.33}$$
$$\begin{bmatrix} 0 \\ 0 \\ B_i \\ 0 \end{bmatrix} [\alpha_i Y_j \ 0 \ 0 \ 0] - \begin{bmatrix} Y_j^T \alpha_i \\ 0 \\ 0 \\ 0 \end{bmatrix} [0 \ 0 \ B_i^T \ 0] < 0$$

Using Lemma 4 in [10] with $H = -I$, results in:

$$(10.33) \leq (*) + \epsilon_{ij} \begin{bmatrix} 0 \\ 0 \\ B_i \\ 0 \end{bmatrix} [0 \ 0 \ B_i^T \ 0] + \epsilon_{ij}^{-1} \begin{bmatrix} Y_j^T \alpha_i \\ 0 \\ 0 \\ 0 \end{bmatrix} [\alpha_i Y_j \ 0 \ 0 \ 0] \tag{10.34}$$
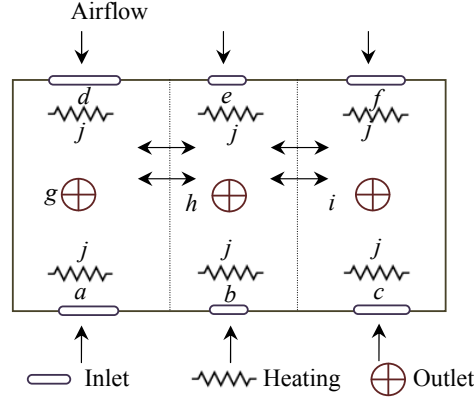
Figure 10.1: The top view of the test stable

where $(*)$ is the first matrix in (10.33). We have $\alpha_i \leq \alpha_{M_i}$, therefore it holds that:

$$(10.34) \leq \begin{bmatrix} \Lambda & 0 & (A_i G_j + B_i Y_j)^T & G_j^T \\ 0 & -\gamma^2 I & \tilde{B}_i^{w^T} & 0 \\ (A_i G_j + B_i Y_j) & \tilde{B}_i^w & -Q_l + \epsilon_{ij} B_i B_i^T & 0 \\ G_j & 0 & 0 & -I \end{bmatrix} < 0 \qquad (10.35)$$

where $\Lambda = Q_i - G_j^T - G_j + \epsilon_{ij}^{-1} Y_j^T \alpha_{M_i} \alpha_{M_i} Y_j$. With Schur complement we derive the LMI (10.26). $\qquad \square$

5 Simulation Results for a Climate Control System For a Live-Stock Building

The PFTC algorithm is applied to a hybrid climate control systems of a live-stock building, which was obtained in previous research, [14]. The general schematic of the large scale live-stock building equipped with a hybrid climate control system is illustrated in Figure. 10.1.

In a large scale stable, the indoor airspace is incompletely mixed; therefore it is divided into conceptually homogeneous parts called zones. Due to the indoor and outdoor conditions, the airflow direction varies between adjacent zones. Therefore, the system behavior is represented by a finite number of dynamic equations. The model is divided into subsystems as follows: Inlet model for both windward and leeward, outlet model, and stable heating system, and finally the dynamic model of temperature based on the heat balance equation. The dynamic model of the temperature turns out to be a piecewise nonlinear model. Since there is limited research on FTC of piecewise nonlinear models, the obtained model is approximated by a discrete-time PWA system of type (10.12) where each nonlinear model of every polyhedral region $\mathcal{X}_i$ is approximated by a liear model. The discrete-time PWA model has 4 regions $\mathcal{X}_1, \ldots, \mathcal{X}_4$.

The piecewise-affine model of the system is derived for the following polyhedral re-

gions of $\mathbb{X}$:

$$\mathcal{X}_1 = \{[x^T\ u^T]^T | F_1^x x + F_1^u \geq f_1, F_2^x x + F_2^u \geq f_2\}, \tag{10.36}$$

$$\mathcal{X}_2 = \{[x^T\ u^T]^T | F_1^x x + F_1^u < f_1, F_2^x x + F_2^u < f_2\}, \tag{10.37}$$

$$\mathcal{X}_3 = \{[x^T\ u^T]^T | F_1^x x + F_1^u < f_1, F_2^x x + F_2^u \geq f_2\}, \tag{10.38}$$

$$\mathcal{X}_4 = \{[x^T\ u^T]^T | F_1^x x + F_1^u \geq f_1, F_2^x x + F_2^u < f_2\}, \tag{10.39}$$

where

$$F_1^x = \begin{bmatrix} 1.0817 & -0.0457 & -0.9938 \end{bmatrix}$$
$$F_2^x = \begin{bmatrix} -1.1144 & 0.0490 & 1.0187 \end{bmatrix}$$
$$F_1^u = \begin{bmatrix} 0.2323 & -0.0072 & 0.2323 & 0.2323 & -0.0072 \end{bmatrix}$$
$$0.2323 \quad -0.072 \quad 0.1349 \quad -0.0719 \quad -0.0064 \end{bmatrix},$$
$$F_2^u = \begin{bmatrix} -0.2558 & 0.0074 & -0.2558 & -0.2558 & 0.0074 \end{bmatrix}$$
$$-0.2558 \quad 0.0742 \quad -0.12 \quad 0.0742 \quad 0.0074 \end{bmatrix},$$
$$f_1 = 0.4058, f_2 = -0.4575 \tag{10.40}$$

Here, the polyhedral region $\mathcal{X}_i$ is defined by two inequalities which depend on the state and input, while in (10.3), the $\mathcal{X}_i$ is defined by two inequalities independently based on the state or the input. It is not possible to define $\bar{\mathcal{X}}_i$ as in (10.4), therefore it is changed as $\bar{\mathcal{X}} = \{x\ such\ that\ x \in \mathbb{R}^n\}$. It denotes that the region $\bar{\mathcal{X}}$ for defining the controller is assumed to be common for $\mathbb{X}$.

The discrete-time PWA model is described by:

$$A_1 = \begin{bmatrix} 1.6361 & 0.0480 & -0.7716 \\ 1.5782 & 0.5522 & -0.9983 \\ 0.7747 & 0.0462 & 0.0990 \end{bmatrix}, \tag{10.41}$$

$$A_2 = \begin{bmatrix} 1.1145 & -0.0300 & -1.0590 \\ 1.6452 & 0.1010 & -1.4342 \\ 0.3008 & 0.0191 & -0.2324 \end{bmatrix}, \tag{10.42}$$

$$A_3 = \begin{bmatrix} 1.6340 & 0.0259 & -0.7150 \\ 1.5474 & 0.8335 & -1.4790 \\ 0.7674 & 0.0314 & 0.1456 \end{bmatrix}, \tag{10.43}$$

$$A_4 = \begin{bmatrix} 1.6274 & 0.0049 & -0.6987 \\ 1.6242 & 0.8163 & -1.4751 \\ 0.7623 & 0.0051 & 0.1640 \end{bmatrix}, \tag{10.44}$$

$$B_1 = \begin{bmatrix} -0.1163 & 0.0459 & -0.1163 & -0.1163 & 0.0459 \\ 0.5718 & -0.3768 & 0.5718 & 0.5718 & -0.3768 \\ -0.1147 & 0.0353 & -0.1147 & -0.1147 & 0.0353 \end{bmatrix}$$

$$\begin{bmatrix} -0.1163 & 0.0018 & -0.0567 & 0.0018 & 0.0070 \\ 0.5718 & -0.1518 & 0.2724 & -0.1518 & -0.0056 \\ -0.1147 & 0.0022 & -0.0553 & 0.0022 & 0.0071 \end{bmatrix}, \qquad (10.45)$$

$$B_2 = \begin{bmatrix} 0.1137 & -0.0044 & 0.1137 & 0.1137 & -0.0044 \\ -0.0104 & 0.1057 & -0.0104 & -0.0104 & 0.1057 \\ 0.0581 & 0.0258 & 0.0581 & 0.0581 & 0.0258 \end{bmatrix}$$

$$\begin{bmatrix} 0.1137 & -0.0697 & 0.2883 & -0.0697 & 0.0023 \\ -0.0104 & 0.0183 & 0.8276 & 0.0183 & 0.1275 \\ 0.0581 & 0.0097 & 0.0939 & 0.0097 & 0.0273 \end{bmatrix}, \qquad (10.46)$$

$$B_3 = \begin{bmatrix} -0.0677 & -0.0127 & -0.0677 & -0.0677 & -0.0127 \\ 0.2031 & 0.0778 & 0.2031 & 0.2031 & 0.0778 \\ -0.0697 & -0.0188 & -0.0697 & -0.0697 & -0.0188 \end{bmatrix}$$

$$\begin{bmatrix} -0.0677 & -0.0103 & -0.0080 & -0.0103 & 0.0078 \\ 0.2031 & -0.0594 & -0.0506 & -0.0594 & -0.0012 \\ -0.0697 & -0.0098 & -0.0087 & -0.0098 & 0.0075 \end{bmatrix}, \qquad (10.47)$$

$$B_4 = \begin{bmatrix} -0.0393 & -0.0380 & -0.0393 & -0.0393 & -0.0380 \\ 0.0851 & 0.1683 & 0.0851 & 0.0851 & 0.1683 \\ -0.0414 & -0.0434 & -0.0414 & -0.0414 & -0.0434 \end{bmatrix}$$

$$\begin{bmatrix} -0.0393 & -0.0133 & -0.0234 & -0.0133 & 0.0086 \\ 0.0851 & -0.0568 & 0.0160 & -0.0568 & 0.0029 \\ -0.0414 & -0.0130 & -0.0241 & -0.0130 & 0.0085 \end{bmatrix}, \qquad (10.48)$$

$$a_1 = \begin{bmatrix} 0.4749 \\ -0.9236 \\ 0.4214 \end{bmatrix}, \; a_2 = \begin{bmatrix} -0.0676 \\ 2.2442 \\ 0.3784 \end{bmatrix}, \qquad (10.49)$$

$$a_3 = \begin{bmatrix} 0.2356 \\ 0.3694 \\ 0.2500 \end{bmatrix}, \; a_4 = \begin{bmatrix} 0.3510 \\ -0.5021 \\ 0.3682 \end{bmatrix}. \qquad (10.50)$$

Here, there is not any disturbance input of type w and initial condition is considered as $x(0) = [10 \; 10 \; 10]^T$. We assume that 5 of the 6 inlets are faulty and lose 90% of their efficiency. The objective is to regulate the temperature of each zone, x around 20 ^oC. The passive fault-tolerant controller based on H_∞ synthesis obtained by Theorem 7 is designed for the system using YALMIP/ SeDuMi. The LMI (10.26) is not feasible for $\gamma < 8$, hence it is assumed that $\gamma = 8$.

We obtain

$$K = 10^3 \times \begin{bmatrix} -0.0000 & -0.0000 & -0.0000 \\ -0.0000 & -0.0001 & 0.0001 \\ -0.0000 & 0.0000 & 0.0000 \\ -0.0000 & -0.0000 & -0.0000 \\ -0.0000 & -0.0001 & 0.0001 \\ 0.0034 & -0.0006 & -0.0006 \\ 0.7971 & 0.7710 & -2.5273 \\ 0.0054 & 0.0013 & -0.0020 \\ -0.7614 & -0.7644 & 2.5521 \\ -0.0462 & -0.0083 & 0.0158 \end{bmatrix} \tag{10.51}$$

$$P_1 = \begin{bmatrix} 5.1016 & 0.0698 & -3.9781 \\ 0.0698 & 1.3854 & -0.5175 \\ -3.9781 & -0.5175 & 6.3529 \end{bmatrix} \tag{10.52}$$

$$P_2 = \begin{bmatrix} 4.8108 & 0.0594 & -3.7864 \\ 0.0594 & 1.3861 & -0.4458 \\ -3.7864 & -0.4458 & 6.3702 \end{bmatrix} \tag{10.53}$$

$$P_3 = \begin{bmatrix} 5.1644 & 0.0370 & -3.8885 \\ 0.0370 & 1.2987 & -0.4113 \\ -3.8885 & -0.4113 & 6.48669 \end{bmatrix} \tag{10.54}$$

$$P_4 = \begin{bmatrix} 5.1216 & 0.0509 & -4.0513 \\ 0.0509 & 1.4384 & -0.6108 \\ -4.0513 & -0.6108 & 6.1853 \end{bmatrix} \tag{10.55}$$

As it is obvious from Fig. 10.2, the fault-tolerant controller regulates the temperature of each zone around $T_1 = T_2 = T_3 = 19\ ^oC$ when there is no actuator efficiency loss. The difference between the regulated temperature $T = 19\ ^oC$ and the reference $T = 20\ ^oC$ is due to the large value of $\gamma = 8$, which leads to degradation of H_∞ performance, according to (10.13). In Fig. 10.3, it is assumed that 5 of the 10 actuators are faulty and loss 90% their efficiency at time 6000 second. As it is shown, the output of the closed loop system oscillates when the fault occurs. However the fault-tolerant controller stabilizes
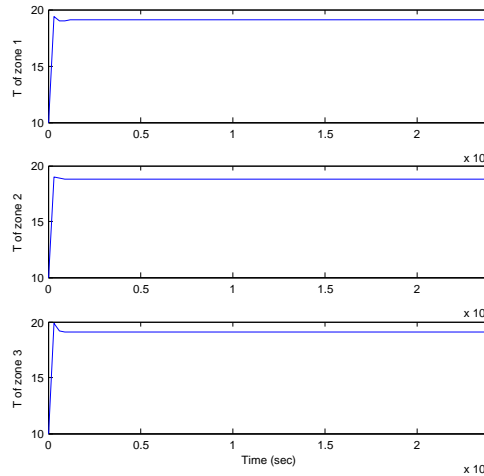

Figure 10.2: Simulation results with a controller designed to tolerate 90% actuator failure for the fault-free system with $\alpha = 0$.

the system with some performance degradation as $T_1 = 20.4$, $T_2 = 17$, $T_3 = 20.3\ ^oC$. The switching sequences of the fault-free closed loop system as well as faulty system are
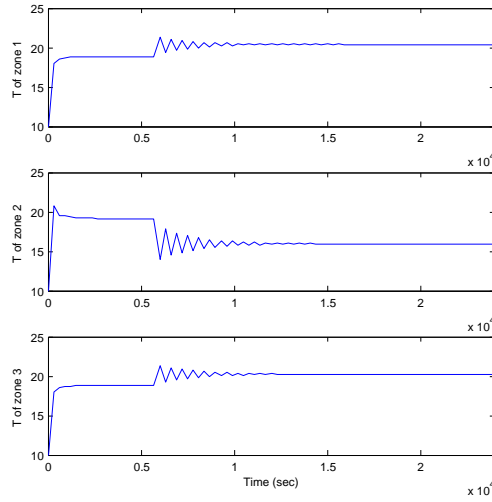

Figure 10.3: Simulation results with a controller designed to tolerate 90% actuator failure for the faulty system with $\alpha = 0.9$.
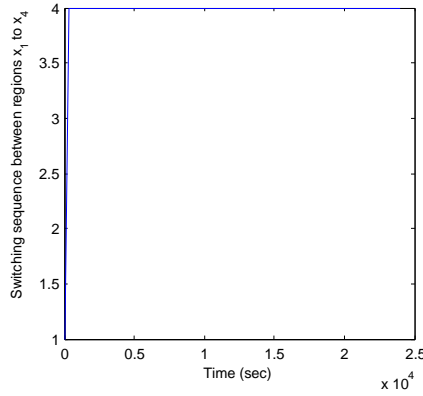
given in Fig. 10.4 and Fig. 10.5.

Figure 10.4: Switching sequence of the closed loop system between regions $\mathcal{X}_1, \ldots, \mathcal{X}_4$ when there is no fault.

As it was mentioned before, the fault-tolerant controller is not able to regulate the temperature exactly around the reference signal due to the large value of γ. The fault-tolerant controller is designed for the ventilation systems of the stable where the suitable temperature for animals should stay between $16\ ^oC$ and $21\ ^oC$. This performance degradation is therefore admissible.
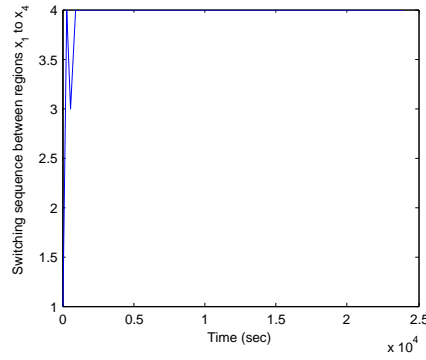
Figure 10.5: Switching sequence of the closed loop system between regions $\mathcal{X}_1, \ldots, \mathcal{X}_4$ when 90% actuator failure happen at the system.

6   Conclusion and Future works

In this paper, we derived a passive fault tolerant controller against actuator losses using a discrete-time PWA model of a piecewise nonlinear system. The PWA model switches not only based on the state but also based on the control input. The H_∞ analysis is used to design a fault tolerant controller. The stability guarantee of the closed loop system is investigated by a PWQ Lyapunov function. The controller design is reformulated as a set of LMIs. The simulation confirms that the controller is able to tolerate 90% actuator fault with acceptable performance degradation.

As future work, the model uncertainties and noise will be considered in the FTC problem.

References

[1]   M. Blanke, M. Kinnaert, J. Lunze, and M. Staroswiecki, *Diagnosis and Fault-Tolerant Control*.   Springer-Verlag, 2006.

[2]   J. Chen and R. Patton, *Robust model-based fault diagnosis for dynamic systems*. Kluwer Academic Publishers Norwell, MA, USA, 1999.

[3]   Z. Qu, C. Ihlefeld, J. Yufang, and A. Saengdeejing, "Robust control of a class of nonlinear uncertain systems. fault tolerance against sensor failures and subsequent self recovery," in *Decision and Control, 2001. Proceedings of Decision and Control, the 40th IEEE Conference*, vol. 2, 2001, pp. 1472 –1478.

[4]   Z. Qu, C. M. Ihlefeld, Y. Jin, and A. Saengdeejing, "Robust fault-tolerant self-recovering control of nonlinear uncertain systems," *Automatica*, vol. 39, no. 10, pp. 1763 – 1771, 2003.

[5]   L. Rodrigues and E.-K. Boukas, "Piecewise linear h_∞ controller synthesis with application to inventory control of switched production systems," *Automatica*, vol. 42, pp. 1245–1254, 2006.

[6]   M. Rodrigues, D. Theilliol, and D. Sauter, "Fault tolerant control design for switched systems," in *2nd IFAC Conference on Analysis and design of hybrid systems, Alghero Sardinia, Italy*, 2006, 10.3182/20060607-3-IT-3902.00041.

[7]   J. H. Richter, W. Heemels, N. van de Wouw, and J. Lunze, "Reconfigurable control of piecewise affine systems with actuator and sensor faults: stability and tracking1," Institute of Automation and Computer Control, Ruhr-Universität Bochum, Tech. Rep., 2010.

[8]   H. Yang, B. Jiang, and V. Cocquempot, "A fault tolerant control framework for periodic switched non-linear systems," *International Journal of Control*, vol. 82, no. 1, pp. 117–129, 2009.

[9]   N. Nayebpanah, L. Rodrigues, and Y. Zhang, "Fault-tolerant controller synthesis for piecewise-affine systems," in *Proceedings of the IEEE American Control Conference*, 2009, pp. 222–226.

[10] S. Tabatabaeipour, R. Izadi-Zamanabadi, T. Bak, and A. P. Ravn, "Passive fault-tolerant control of piecewise linear systems against actuator faults," *submitted to International Journal of Systems Science*, 2010.

[11] J. Löfberg, "YALMIP : A toolbox for modeling and optimization in MATLAB," in *Proceedings of the IEEE Conference on Computer Aided Control Systems Design*, 2004, pp. 284–289.

[12] F. Cuzzola and M. Morari, "A generalized approach for analysis and control of discrete-time piecewise affine and hybrid systems," *Hybrid Systems: Computation and Control*, vol. 2034, pp. 189–203, 2001.

[13] I. R. Petersen, "A stabilization algorithm for a class of uncertain linear systems," *System and Control Letters*, vol. 8, no. 4, pp. 351–357, 1987.

[14] M. Gholami, H. Shioler, and T. Soltani, M. Bak, "Multi-Zone Hybrid Model for Failure Detection of the Stable Ventialation System," in *Proceedings of Industrial Electronic Society*, 2010.

Paper F

Passive Fault Tolerant Control of Piecewise Affine Systems with Reference Tracking and Input Constraints

Mehdi Gholami, Vincent Cocquempot,Henrik Schioler and Thomas Bak

Abstract

A passive fault tolerant controller (PFTC) based on state feedback is proposed for discrete-time piecewise affine (PWA) systems. The controller is tolerant against actuator faults and is able to track the reference signal while the control inputs are bounded. The PFTC problem is transformed into feasibility of a set of linear matrix inequalities (LMIs). The method is applied on a large-scale live-stock ventilation model.

1 Introduction

In complex and industrial control systems, a large number of components are strongly interconnected, where abnormal behavior of a component may affect overall performance of the system or yield to the loss of system reliability or safety. In applications such as climate control systems of livestock buildings, this is unacceptable as it may lead to the loss of animal life. Therefore, it is desirable to develop control systems which are capable of tolerating component malfunctions while still maintaining desirable performances and stability properties. These control systems are known as fault tolerant control systems.

Fault tolerant control (FTC) approaches are divided generally into passive (PFTC) and active (AFTC) ones [1]. In AFTC, the control action is changed with respect to the information provided by a fault detection and isolation (FDI) scheme. As in [2] AFTC systems are classically divided into three layers. The first layer is related to the control loop, the second layer corresponds to the FDI and accommodation scheme and the last layer corresponds to the supervisor system. In PFTC, there is no FDI or supervisor layer. In this technique, the control laws are designed and fixed such that the control system is capable of tolerating a set of known faults. In fact, the fault is considered as a system disturbance or uncertainty and the control system is designed to be robust against such uncertainties, see [3], [4], and [5]. Many results which were reported in the literature are devoted to linear systems. However, complex industrial systems either show nonlinear behavior or contain both discrete and continuous components. One of the modeling frameworks which is relevant for such systems is piecewise affine (PWA) models. This framework has been applied in several areas, such as, switched production systems [6], aerospace systems [7], etc. For AFTC systems, the reader is referred to [8], where the authors design an output feedback controller against actuator failures for discrete-time switched linear systems. [9] presents a AFTC method for a class of periodic switched nonlinear systems subjected to both continuous and discrete faults. The continuous fault is diagnosed by a adaptive filter and discrete fault is diagnosed bye a sliding mode observer . In [10], an AFTC approach based on virtual sensors and actuators for continuous-time PWA system subject to actuator and sensor faults is proposed. A PFTC approach is presented in [11], where a controller is proposed for a class of continuous time switched nonlinear systems subject to actuator fault. The approach of [12] is based on a static output feedback controller for polytopic linear parameter varying systems . In [13], a state feedback controller is designed for continuous-time PWA systems while minimizing an upper bound of cost function. The controller is designed to be robust against actuator faults.

In [14], a PFTC for discrete time PWA systems is presented. The approach is based on a state feedback control that is tolerant against actuator faults. The considered PWA systems switch only due to state variables. In general, PWA systems may switch based on

both input and state trajectories, as in [15], where H_∞ analysis is used to design a state feedback controller against actuator faults. Most plants suffer from physical constraints, such as actuator saturation; however, such constraints are not taken into account in the above cited works.

In addition to the above discussions, we are motivated to design a PFTC approach for discrete-time PWA systems which switch due to the input and state of the system. In this work also physical constraints on the inputs of the system is also taken into account. The approach is based on a state feedback controller such that the closed-loop system is asymptotically stable and able to track the reference signal correctly in healthy and in actuator failure situations. A common Lyapunov function candidate is used to evaluate the stability of the system. The problem is cast as a set of linear matrix inequalities (LMI) and solved with YALMIP/ SeDumi solver, see [16]. The paper is organized as follows. Section II presents the piecewise affine model and actuator fault representation. Section III discusses control design for PWA systems. The extension of synthesis for fault tolerant control of piecewise affine systems is discussed in section IV. Section V is dedicated to the simulation results for the climate control system. The conclusion is presented in section VI.

2 Piecewise Affine Representation

2.1 Piecewise Affine Systems

Consider a discrete-time piecewise affine system, $\sum_i$ as:

$$x(k+1) = A_i x(k) + B_i u(k) + a_i \quad for \begin{bmatrix} x(k) \\ u(k) \end{bmatrix} \in \mathcal{X}_i, \tag{11.1}$$

$$y(k) = Cx(k) \tag{11.2}$$

where $x(k) \in \mathbb{R}^n$ is the state, $u(k) \in \mathbb{R}^m$ is the control input, $y(k) \in \mathcal{R}^p$ is the output. The set $\mathbb{X} \subseteq \mathbb{R}^{n+m}$ represents every possible vector $\begin{bmatrix} x(k)^T u(k)^T \end{bmatrix}^T$, $\{\mathcal{X}_i\}_{i=1}^s$ denotes polyhedral regions of $\mathbb{X}$ and $a_i \in \mathbb{R}^n$ is a constant vector. Each polyhedral region is represented by:

$$\mathcal{X}_i = \{ \begin{bmatrix} x(k)^T u(k)^T \end{bmatrix}^T \mid F_i^x x + F_i^u u \leq f_i^{xu} \} \tag{11.3}$$

It is assumed that the regions are defined with known matrices F_i^x, F_i^u, f_i^{xu}. $\mathscr{I} = \{1, \cdots, s\}$ is the set of indices of regions $\mathcal{X}_i$. All possible switchings from region $\mathcal{X}_i$ to $\mathcal{X}_j$ are defined by the set $\mathcal{S}$:

$$\mathcal{S} = \{(i,j) : i,j \in \mathscr{I} \ and \ \exists \begin{bmatrix} x(k) \\ u(k) \end{bmatrix}, \begin{bmatrix} x(k+1) \\ u(k+1) \end{bmatrix} \in \mathbb{X} \tag{11.4}$$

$$\mid \begin{bmatrix} x(k) \\ u(k) \end{bmatrix} \in \mathcal{X}_i \ and \ \begin{bmatrix} x(k+1) \\ u(k+1) \end{bmatrix} \in \mathcal{X}_j \}$$

$\mathscr{I}$ is divided in two partitions. First partition is $\mathscr{I}_0$, which is the index set of the regions that contain the origin and $a_i = 0$. The second partition is $\mathscr{I}_1$ which is the index set of the regions that do not contain the origin.

In order to cast the control problem as a set of LMIs, the polyhedral region $\mathcal{X}_i$ is over approximated with an ellipsoid when $i \in \mathscr{I}_1$.

Proposition 1. *([17]) Let $\mathfrak{X} \subseteq \mathbb{R}^n$ be a parallelepiped with non-empty interior.*

$$\mathfrak{X} = \{x \in \mathbb{R}^n \, || b_l^T x - \tilde{x_l}| \leq d_l, \ \ l = \{1, \cdots, n\}\} \tag{11.5}$$

and let

$$\widetilde{T} = \begin{bmatrix} b_1^T/d_1 & -\tilde{x_1}/d_1 \\ \vdots & \vdots \\ b_n^T/d_n & -\tilde{x_1}/d_n\} \end{bmatrix} \tag{11.6}$$

where b_l is a constant vector, $\tilde{x}_l$ and d_l are scalar which define the parallelepiped. Then, the ellipsoid of minimal volume that contains $\mathfrak{X}$ is given by

$$\tilde{x}^T \widetilde{T}^T \widetilde{T} \tilde{x} \leq n \tag{11.7}$$

where $\tilde{x} = [x^T \ \ 1]^T$, where 1 is scalar. The ellipsoid of minimal volume can be reformulated as

$$\xi = \{x | \ \| \ Ex + f \ \| \leq n\} \tag{11.8}$$

where E is a vector and f is a scalar which can be obtained from (7).

2.2 Fault Model

Actuator faults are considered. u_j is the actuator output. The partial loss of actuator can be formulated as

$$u_j^F = (1 - \alpha_j)u_j, \ \ 0 \leq \alpha_j \leq \alpha_{Mj}, \tag{11.9}$$

where α_j is the percentage of efficiency loss of the actuator j and α_{Mj} is the maximum loss. $\alpha_j = 0$ corresponds to the nominal system, $\alpha_j = 1$ corresponds to 100% loss of the actuator and $0 \leq \alpha_j \leq 1$ corresponds to partial loss. Let us define α as

$$\alpha = diag\{\alpha_1, \alpha_2, \ldots, \alpha_m\}. \tag{11.10}$$

Then

$$u^F = \Gamma u, \tag{11.11}$$

where $\Gamma = (I_{m \times m} - \alpha)$, I is a identity matrix. Thus u^F represents the control signal that is applied in normal or faulty situation. The PWA model of the system with the fault F_i is

$$x(k+1) = A_i x(k) + B_i \Gamma u(k) + a_i \ \ for \ \begin{bmatrix} x(k) \\ u(k) \end{bmatrix} \in \mathcal{X}_i \tag{11.12}$$

3 State Feedback Control Design

3.1 Reference Model

Here, the aim is to design a state feedback controller for piecewise affine system such that the closed loop system is able to track the reference $r(k)$. The control structure is displayed on Fig. 1. K_i and K_r are the controller to be designed. Σ_r is model of the reference r and its state space representation is given as :

$$x_r(k+1) = A_r x_r(k) + B_r(r(k) - Cx(k)) \tag{11.13}$$

where $x_r(k) \in \mathbb{R}^{n_r}$ is the state vector. A well known asymptotic tracking of a reference $r(k)$ is achieved by putting an integral action in the closed loop. i.e by fixing:

$A_r = I_{n_r \times n_r}$, $B_r = T_s \times I_{n_r \times p}$, where T_s is the sampling time of the system.

3.2 Controller Structure

Let a piecewise linear state feedback control be specified as:

$$u(k) = K_i x(k) + K_r x_r(k) \quad for \quad \begin{bmatrix} x(k) \\ u(k) \end{bmatrix} \in \mathcal{X}_i, \tag{11.14}$$

where K_i and K_r are controller gains which are designed to stabilize exponentially the closed loop PWA system. Since the index i is not a priori known, it is not possible to calculate $u(k)$. Hence, the problem is changed to the following structure

$$u(k) = K x(k) + K_r x_r(k) = \bar{K}\bar{x} \quad for \quad \begin{bmatrix} x(k) \\ u(k) \end{bmatrix} \in \mathcal{X}_i. \tag{11.15}$$

It means that we are positive; that we consider the same controller in all regions $\mathcal{X}_i$ with $i \in \mathscr{I}$.

With considering reference model (11.13) and piecewise affine model (11.2) and applying the control law (11.15) the following closed loop system is obtained:

$$\bar{x}(k+1) = \begin{bmatrix} x(k+1) \\ x_r(k+1) \end{bmatrix} = \mathcal{A}_i \bar{x}(k) + \bar{B}_r r(k) + \bar{a}_i \tag{11.16}$$

$$for \ \in \mathcal{X}_i,$$

where $\mathcal{A}_i = \bar{A}_i + \bar{B}_i \bar{K}$, $\bar{A}_i = \begin{bmatrix} A_i & 0_{n \times n_r} \\ -B_r C & A_r \end{bmatrix}$, $\bar{B}_i = \begin{bmatrix} B_i \\ 0_{n_r \times m} \end{bmatrix}$, $\bar{B}_r = \begin{bmatrix} 0_{n \times n_r} \\ B_r \end{bmatrix}$, $\bar{K} = [K \ K_r]$, and $\bar{a}_i = \begin{bmatrix} a_i \\ 0_{n_r \times 1} \end{bmatrix}$, 0 is a null matrix or vector.
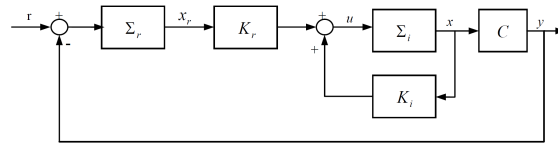

Figure 11.1: Control structure

Here, we describe how to over approximate the polyhedral regions $\mathcal{X}_i$ to a ellipsoid using Proposition 1. Let $\mathcal{X}_i$ be reformulated as

$$\mathcal{X}_i = \left\{ \left[\bar{x}^T u^T \right]^T \in \mathbb{R}^{n+n_r+m} | |b_l^T \bar{x} + c_l^T u - \tilde{x}_l| \leq d_l, \right. \tag{11.17}$$
$$l = \{1, 2\}\},$$

which is equivalent to

$$\mathcal{X}_i = \left\{ \left[\bar{x}^T \right]^T \in \mathbb{R}^{n+n_r} | |(b_l^T + c_l^T \bar{K}) \bar{x} - \tilde{x}_l| \leq d_l, \right. \tag{11.18}$$
$$l = \{1, 2\}\},$$

then

$$\widetilde{T}_i = \begin{bmatrix} (b_1^T + c_l^T)/d_1 & -\tilde{x}_1/d_1 \\ (b_2^T + c_2^T)/d_2 & -\tilde{x}_2/d_2 \} \end{bmatrix} \tag{11.19}$$

Then, the ellipsoid of minimal volume that contains $\mathcal{X}_i$ is given by

$$\xi_i = \{\bar{x} | \parallel (E_i + F_i \bar{K}) \bar{x} + f_i \parallel \leq 2\} \tag{11.20}$$

The following theorem gives the sufficient conditions for stability of a piecewise affine system.

Theorem 8. *([18]) System (11.16) is exponentially stable if there exist matrices $P_i = P_i^T > 0$, $\forall i \in \mathscr{I}$, such that the positive definite function $V(x(k)) = x^T(k)P_i x(k), \forall x \in \mathcal{X}_i$, satisfies $V(x(k+1)) - V(x(k)) < 0$.*

4 Passive Fault Tolerant Control of Piecewise Affine Systems

It is assumed that the control objective is to track the reference $r(k)$ when the system is subject to a fault F_i. The system (11.16) subject to the fault F_i is:

$$\bar{x}(k+1) = \begin{bmatrix} x(k+1) \\ x_r(k+1) \end{bmatrix} = \mathcal{A}_{if} \bar{x}(k) + \bar{B}_r r(k) + \bar{a}_i \tag{11.21}$$
$$for \ \in \mathcal{X}_i,$$

where $\mathcal{A}_{if} = \bar{A}_i + \bar{B}_i \Gamma \bar{K}, \xi_i = \{\bar{x} | \parallel (E_i + F_i \Gamma \bar{K}) \bar{x} + f_i \parallel \leq 2\}$.

4.1 Fault Tolerant Controller Without Input Constraints

Lemma 5. *([19]) Let M, N, H be real matrices. If $H^T H \leq I$, I is a identity matrix with an appropriate dimension, then for every scalar $\epsilon > 0$ the following inequality holds:*

$$MHN + N^T H^T M^T \leq \epsilon MM^T + \epsilon^{-1} N^T N \tag{11.22}$$

Definition 6. The control law (11.15) is a passive fault-tolerant control if the closed loop system (11.21), which is subject to fault F_i, is exponentially stable i.e. the following inequality for system (11.21) is satisfied: $V(x(k+1)) - V(x(k)) < 0 \ \forall (i, j) \in \mathcal{S}$. This definition is expressed in the following theorem.

Theorem 9. *The fault tolerant linear controller (11.15) stabilizes the system (11.21), if there exist symmetric matrices $Q = Q^T > 0$ and matrices Y and positive constants μ_i, ϵ_i such that:*

$$\begin{bmatrix} Q^{-1} & * & * & * \\ \bar{A}_i Q + \bar{B}_i \bar{Y} & Q + \frac{1}{2}\mu_i \bar{a}_i \bar{a}_i^T - \epsilon_i \bar{B}_i \bar{B}_i^T & * & * \\ E_i Q + F_i \bar{Y} & \frac{1}{2}\mu_i f_i \bar{a}_i^T - \epsilon_i F_i \bar{B}_i^T & \mu_i(\frac{1}{2}f_i f_i^T - I) - \epsilon_i F_i F_i^T & * \\ \alpha Y & 0 & 0 & \epsilon_i I \end{bmatrix} \tag{11.23}$$

$$> 0 \quad \forall (i,j) \in \mathcal{S}, i \in \mathscr{I}_1,$$

$$\begin{bmatrix} Q^{-1} & * & * \\ \bar{A}_i Q + \bar{B}_i \bar{Y} & Q - \epsilon_i \bar{B}_i \bar{B}_i^T & * \\ \alpha Y & 0 & \epsilon_i I \end{bmatrix} > 0, \tag{11.24}$$

$$\forall (i,j) \in \mathcal{S}, i \in \mathscr{I}_0$$

Then the linear feedback gains are given by:

$$\bar{K} = YQ^{-1}, \tag{11.25}$$

Proof. Let consider a common Lyapunov candidate function as $V(x(k) = x(k)^T P x(k), P > 0$ for $x(k) \in \mathcal{X}_i$. The sufficient stability condition is:

$$V(x(k+1)) - V(x(k)) < 0, \quad \forall (i,j) \in \mathcal{S}. \tag{11.26}$$

First, we assume those switchings with $i \in \mathscr{I}_1$. To treat with the affine term $\bar{a}_i$, the ellipsoidal approximation of regions as in (11.20) is considered . The equivalent form of (11.26) for the PWA system (11.21) is:

$$[(\bar{A}_i + \bar{B}_i \Gamma \bar{K})x(k) + \bar{a}_i]^T P[(\bar{A}_i + \bar{B}_i \Gamma \bar{K})x(k) + \bar{a}_i]$$
$$- x(k)^T P x(k) < 0, \quad \forall (i,j) \in \mathcal{S}, \tag{11.27}$$

which is equal to:

$$\begin{bmatrix} x(k) \\ 1 \end{bmatrix}^T \begin{bmatrix} \mathcal{A}_{if}^T P \mathcal{A}_{if} - P & * \\ \bar{a}_i^T P \mathcal{A}_{if} & \bar{a}_i^T P \bar{a}_i \end{bmatrix} \begin{bmatrix} x(k) \\ 1 \end{bmatrix} < 0, \tag{11.28}$$

where $\mathcal{A}_{if} = \bar{A}_i + \bar{B}_i \Gamma \bar{K}$ and 1 is scalar. The ellipsoidal approximation of $\mathcal{X}_i$ can be written as:

$$\begin{bmatrix} x(k) \\ 1 \end{bmatrix}^T \begin{bmatrix} \mathcal{E}_i^T \mathcal{E}_i & * \\ f_i^T \mathcal{E}_i & f_i^T f_i - 2 \end{bmatrix} \begin{bmatrix} x(k) \\ 1 \end{bmatrix} \leq 0, \tag{11.29}$$

where $\mathcal{E}_i = E_i + F_i \Gamma \bar{K}$. Using the S-procedure, see [20], the equation (11.28) is satisfied if there exist multipliers $\lambda_i > 0$ such that :

$$(11.28) - \lambda_i \begin{bmatrix} x(k) \\ 1 \end{bmatrix}^T \begin{bmatrix} \mathcal{E}_i^T \mathcal{E}_i & * \\ f_i^T \mathcal{E}_i & f_i^T f_i - 2 \end{bmatrix} \begin{bmatrix} x(k) \\ 1 \end{bmatrix} < 0 \tag{11.30}$$

The above inequality is equal to:

$$\begin{bmatrix} \mathcal{A}_{if}^T P \mathcal{A}_{if} - P & \mathcal{A}_{if}^T P \bar{b}_i \\ \bar{b}_i^T P \mathcal{A}_{if} & \bar{b}_i^T P \bar{b}_i \end{bmatrix} - \lambda_i \begin{bmatrix} \mathcal{E}_i^T \mathcal{E}_i & * \\ f_i^T \mathcal{E}_i & f_i^T f_i - 2 \end{bmatrix} < 0, \tag{11.31}$$

This is rearranged as:

$$\begin{bmatrix} P + \lambda_i \mathcal{E}_i^T \mathcal{E}_i & * \\ \lambda_i f_i^T \mathcal{E}_i & \lambda_i(f_i^T f_i - 2) \end{bmatrix} - \begin{bmatrix} \mathcal{A}_{if}^T \\ \bar{b}_i^T \end{bmatrix} P^{-1} \begin{bmatrix} \mathcal{A}_{if} & \bar{b}_i \end{bmatrix} > 0. \tag{11.32}$$

Applying Schur complement to the above equation yields to:

$$\begin{bmatrix} P + \lambda_i \mathcal{E}_i^T \mathcal{E}_i & * & * \\ \lambda_i f_i^T \mathcal{E}_i & \lambda_i(f_i^T f_i - 2) & * \\ \mathcal{A}_{if} & \bar{b}_i & P^{-1} \end{bmatrix} > 0. \tag{11.33}$$

By pre- and Post-multiplying the above equation with

diag $\left\{ I, \begin{bmatrix} 0 & * \\ I & 0 \end{bmatrix} \right\}$, I is a identity matrix with an appropriate dimension, it is obtained:

$$\begin{bmatrix} P + \lambda_i \mathcal{E}_i^T \mathcal{E}_i & * & * \\ \mathcal{A}_{if} & P^{-1} & * \\ \lambda_i f_i^T \mathcal{E}_i & \bar{b}_i^T & \lambda_i(f_i^T f_i - 2) \end{bmatrix} > 0. \tag{11.34}$$

By Schur complement, it is obtained that:

$$\begin{bmatrix} P + \lambda_i \mathcal{E}_i^T \mathcal{E}_i & * \\ \mathcal{A}_{if} & P^{-1} \end{bmatrix} - \tag{11.35}$$

$$\begin{bmatrix} \lambda_i \mathcal{E}_i^T f_i \\ \bar{b}_i \end{bmatrix} \lambda_i^{-1}(f_i^T f_i - 2)^{-1} \begin{bmatrix} \lambda_i f_i^T \mathcal{E}_i & \bar{b}_i^T \end{bmatrix} > 0,$$

Using the matrix inversion Lemma:

$$(A + BCD)^{-1} = A^{-1} - A^{-1}B(C^{-1} + DA^{-1}B)^{-1}DA^{-1} \tag{11.36}$$

, $Q = P^{-1}$ and $\mu_i = \lambda_i^{-1}$, the inequality (11.35) can be reformulated as:

$$\Delta + \mathbb{A}^T \mu_i (\frac{1}{2} + \frac{1}{4} f_i^T (I - \frac{1}{2} f_i f_i^T)^{-1} f_i) \mathbb{A} > 0 \tag{11.37}$$

where Δ is the first term of inequality (11.35) and $\mathbb{A} = [\mu_i^{-1} f_i f_i^T \mathcal{E}_i \quad f_i \bar{b}_i^T]$. The above inequality can be written as:

$$\Delta + \frac{1}{2} \mathbb{A}^T \mu_i \mathbb{A} + \frac{1}{4} \begin{bmatrix} \mathcal{E}_i^T f_i f_i^T \\ \mu_i \bar{b}_i f_i^T \end{bmatrix} (I - \frac{1}{2} f_i f_i^T)^{-1} \tag{11.38}$$

$$[\mu_i^{-1} f_i f_i^T \quad \mathcal{E}_i f_i \bar{b}_i^T] > 0.$$

Which is equal to:

$$\Delta + \frac{1}{2} \mathbb{A}^T \mu_i \mathbb{A} + \begin{bmatrix} \mathcal{E}_i^T - \mathcal{E}_i^T(I - \frac{1}{2} f_i f_i^T) \\ \frac{1}{2} \mu_i \bar{b}_i f_i^T \end{bmatrix} (I - \frac{1}{2} f_i f_i^T)^{-1} \tag{11.39}$$

$$\begin{bmatrix} \mu_i^{-1}(\mathcal{E}_i - (I - \frac{1}{2} f_i f_i^T) \mathcal{E}_i) & \frac{1}{2} f_i \bar{b}_i^T \end{bmatrix} > 0.$$

Let us define

$$\mathbb{A}_{11} = \mu_i^{-1}\mathcal{E}_i^T(I - \frac{1}{2}f_if_i^T)^{-1}\mathcal{E}_i - \mathcal{E}_i^T\mu_i^{-1}\mathcal{E}_i - \mathcal{E}_i^T\mu_i^{-1}\mathcal{E}_i$$

$$+\mu_i^{-1}\mathcal{E}_i^T(I - \frac{1}{2}f_if_i^T)\mathcal{E}_i,$$

$$\mathbb{A}_{12} = \frac{1}{2}\mathcal{E}_i^T(I - \frac{1}{2}f_if_i^T)^{-1}f_i\bar{b}_i^T - \frac{1}{2}\mathcal{E}_i^T f_i b_i^T,$$

$$\mathbb{A}_{21} = \frac{1}{2}\bar{b}_i f_i^T(I - \frac{1}{2}f_if_i^T)^{-1}\mathcal{E}_i - \frac{1}{2}b_i f_i^T\mathcal{E}_i,$$

$$\mathbb{A}_{22} = \frac{1}{4}\mu_i\bar{b}_i f_i^T(I - \frac{1}{2}f_if_i^T)^{-1}f_i\bar{b}_i^T.$$

Then, the equation (11.39) is rearranged as:

$$\begin{bmatrix} Q^{-1} + \mu_i^{-1}\mathcal{E}_i^T\mathcal{E}_i & \mathcal{A}_{if}^T \\ \mathcal{A}_{if} & Q \end{bmatrix} + \begin{bmatrix} \frac{1}{2}\mu_i^{-1}\mathcal{E}_i^T f_i f_i^T\mathcal{E}_i & \frac{1}{2}E_i^T f_i\bar{b}_i^T \\ \frac{1}{2}\bar{b}_i f_i^T\mathcal{E}_i & \frac{1}{2}\mu_i\bar{b}_i\bar{b}_i^T \end{bmatrix} \tag{11.40}$$

$$+\begin{bmatrix} \mathbb{A}_{11} & \mathbb{A}_{12} \\ \mathbb{A}_{21} & \mathbb{A}_{22} \end{bmatrix} > 0$$

Which can be rewritten as

$$\begin{bmatrix} Q^{-1} & * \\ \mathcal{A}_{if} & Q + \frac{1}{2}\mu_i\bar{b}_i\bar{b}_i^T \end{bmatrix} - \tag{11.41}$$

$$\begin{bmatrix} \mathcal{E}_i^T f_i \\ \frac{1}{2}\mu_i\bar{b}_i f_i^T \end{bmatrix} \mu_i^{-1}(I - \frac{1}{2}f_if_i^T)^{-1} \begin{bmatrix} \mathcal{E}_i & \frac{1}{2}\mu_i f_i\bar{b}_i^T \end{bmatrix} > 0.$$

By Schur complement, it is obtained that:

$$\begin{bmatrix} Q^{-1} & * & * \\ \bar{A}_i + \bar{B}_i\Gamma\bar{K} & Q + \frac{1}{2}\mu_i\bar{b}_i\bar{b}_i^T & * \\ E_i + F_i\Gamma\bar{K} & \frac{1}{2}\mu_i f_i\bar{b}_i^T & \mu_i(\frac{1}{2}f_if_i^T - I) \end{bmatrix} > 0, \tag{11.42}$$

which is equivalent to

$$\begin{bmatrix} Q^{-1} & * & * \\ \bar{A}_i + \bar{B}_i\bar{K} & Q + \frac{1}{2}\mu_i\bar{b}_i\bar{b}_i^T & * \\ E_i + F_i\bar{K} & \frac{1}{2}\mu_i f_i\bar{b}_i^T & \mu_i(\frac{1}{2}f_if_i^T - I) \end{bmatrix} > 0- \tag{11.43}$$

$$\begin{bmatrix} \bar{K}_i^T\alpha^T \\ 0 \\ 0 \end{bmatrix} \begin{bmatrix} 0 & \bar{B}_i^T & \bar{F}_i^T \end{bmatrix} - \begin{bmatrix} 0 \\ \bar{B}_i \\ \bar{F}_i \end{bmatrix} \begin{bmatrix} \alpha\bar{K} & 0 & 0 \end{bmatrix} > 0.$$

Using Lemma 2 in [14] with $H = -I$, it is obtained:

$$(11.43) \geq \Delta - \epsilon_i^{-1} \begin{bmatrix} \bar{K}^T\alpha^T \\ 0 \\ 0 \end{bmatrix} \begin{bmatrix} \alpha\bar{K} & 0 & 0 \end{bmatrix} - \begin{bmatrix} 0 \\ \bar{B}_i \\ \bar{F}_i \end{bmatrix} \begin{bmatrix} 0 & \bar{B}_i^T & \bar{F}_i^T \end{bmatrix}$$

$$> 0. \tag{11.44}$$

We have $\alpha \leq \alpha_M$, therefore it holds that:

$$(11.44) \geq \begin{bmatrix} Q^{-1} - \epsilon_i^{-1}\bar{K}^T\alpha^T\alpha\bar{K} & * & * \\ \bar{A}_i + \bar{B}_i\bar{K} & Q + \frac{1}{2}\mu_i\bar{b}_i\bar{b}_i^T - \epsilon_i\bar{B}_i\bar{B}_i^T & * \\ E_i + F_i\bar{K} & \frac{1}{2}\mu_i f_i\bar{b}_i^T - \epsilon_i F_i\bar{B}_i^T & \Lambda \end{bmatrix} > 0, \tag{11.45}$$

where $\Lambda = \mu_i(\frac{1}{2}f_i f_i^T - I) - \epsilon_i F_i F_i^T$.

Applying Schur complement we obtain the LMI (11.23).

For regions that contain the origin i.e. $i \in \mathcal{I}_0$, we have $\frac{1}{2}f_i f_i^T - I < 0$ which means that the LMI (11.23) is not feasible. For these regions the LMI (11.24) is considered and there is no need to include the region information. Therefore, the following matrix inequality must be satisfied:

$$
[(\bar{A}_i + \bar{B}_i \Gamma_i \bar{K}_i)]^T P_j [(\bar{A}_i + \bar{B}_i \Gamma_i \bar{K}_i)]
$$
$$
-P_i < 0, \ \ \forall (i,j) \in \mathcal{S}, \tag{11.46}
$$

which can be shown that it is equivalent to (11.24). The proof is similar to the previous part. □

4.2 Fault Tolerant Controller with input constraints

Here we develop the previous results to deal with the input constraints.

Theorem 10. *Assume that there exist symmetric matrices $Q = Q^T > 0$, and matrices Y and positive constants $\mu_i > 0, \epsilon_i > 0$, such that the LMIs (11.23) and (11.24) are satisfied and*

$$
\begin{bmatrix} 1 & * \\ x(0) & -Q \end{bmatrix} < 0 \tag{11.47}
$$

$$
\begin{bmatrix} -u_{v,max}^2 Q & * & * & * \\ X_F^T Y & -I & * & * \\ E_i + F_i Y & 0 & \mu_i(\frac{1}{2}f_i f_i^T - I) & * \\ \alpha Y & 0 & 0 & -\epsilon_i I \end{bmatrix} \leq 0 \ \forall i \in \mathscr{I}_1, \tag{11.48}
$$

$$
\begin{bmatrix} -u_{v,max}^2 Q & * \\ X_F^T Y & -I \end{bmatrix} < 0 \ \forall i \in \mathscr{I}_0, \ v = 1, 2, \dots, m \tag{11.49}
$$

where $u_{v,max}$ is a known control input boundary and m is the number of the inputs, then the fault tolerant controller gain is obtained as $\bar{K} = YQ^{-1}$, and the closed loop system (11.21) subject to fault F_i has these properties:

(i) It is exponentially stable

(ii)The input constraints are satisfied, i.e.

$$
|u_v| \leq u_{v,max} \ \ v = 1, 2, \dots, m \tag{11.50}
$$

Proof. Property (i) can be proved following the same way as in proof of Theorem 2. We just focus on the proof of property (ii). In order to treat the norm constraints on the input $u = \bar{K}\bar{x}$, the stabilizability is specified in terms of holdable ellipsoids i.e. the ellipsoid $\Omega = \{x \in \mathcal{R}^n | x^T Q^{-1} x \leq 1\}$ is holdable for the system (11.21) if there exist a state feedback gain $\bar{K}$ and LMIs (11.23) and (11.24) such that Ω is invariant for the system (11.21) [20]. Using (11.50), the S-procedure, with multipliers $\lambda_i = \mu_i^{-1} > 0$ for approximated ellipsoids for each region $\mathcal{X}_i$ and $\lambda_{ie} = u_{v,max}^2 > 0$ for holdable ellipsoids,

we can obtain that:

$$(u_v^T u_v - u_{v,max}^2) - u_{v,max}^2 (x^T Q^{-1} x - 1) \tag{11.51}$$

$$-\lambda_i \begin{bmatrix} x(k) \\ 1 \end{bmatrix}^T \begin{bmatrix} \mathcal{E}_i^T & * \\ f_i^T \mathcal{E}_i & f_i^T f_i - 2 \end{bmatrix} \begin{bmatrix} x(k) \\ 1 \end{bmatrix} \le 0,$$

which is equivalent to

$$\begin{bmatrix} \bar{K}^T X_F X_F^T \bar{K} - u_{v,max}^2 Q^{-1} - \lambda_i \mathcal{E}_i^T \mathcal{E}_i & * \\ -\lambda_i f_i^T \mathcal{E}_i & -\lambda_i(f_i^T f_i - 2) \end{bmatrix} \le 0. \tag{11.52}$$

As in proof of Theorem 2, by using Schur complement, the following LMI is achieved:

$$\begin{bmatrix} -u_{v,max}^2 Q^{-1} & * & * \\ X_F^T \bar{K} & -I & * \\ \mathcal{E}_i & 0 & -\lambda_i^{-1}(\frac{1}{2} f_i f_i^T - I) \end{bmatrix} \le 0. \tag{11.53}$$

Which is the same as:

$$\begin{bmatrix} -u_{v,max}^2 Q & * & * \\ X_F^T Y & -I & * \\ \bar{E}_i Q + F_i \Gamma Y & 0 & -\lambda_i^{-1}(\frac{1}{2} f_i f_i^T - I) \end{bmatrix} \le 0. \tag{11.54}$$

As for the previous proof and using Lemma 2 and $H = -I$, we can obtain the LMI (11.48). In the same way we can obtain the LMI (11.49) for $x \in \mathcal{X}_i$ with $i \in \mathscr{I}_0$. $\qquad\square$

5 Example

The method is applied to a climate control systems of a live-stock building, whose model was obtained during previous research. The general scheme of the large scale live-stock building equipped with hybrid climate control system is illustrated in Fig. 11.2. In a large scale stable, the indoor airspace is incompletely mixed; therefore it is divided into fictive homogeneous parts called zones. In our model, there are three zones which are not similar in size. Zone 1, the one on the left, is the biggest and Zone 2, the middle one, is the smallest. Due to the indoor and outdoor conditions, the airflow direction varies between adjacent zones. Therefore, the system behavior is represented by a finite number of different dynamic equations. The model is divided into subsystems as follows: Inlet model for both windward and leeward, outlet model, and stable heating system, and finally the dynamic model of temperature based on the heat balance equation. The nonlinear model of the system is approximated by a discrete-time PWA system with 4 regions based on the airflow direction. The model of the system is derived for the following polyhedral regions:

$$\mathcal{X}_1 = \{[x^T \; u^T]^T | F_1^x x + F_1^u \ge f_1, F_2^x x + F_2^u \ge f_2\}, \tag{11.55}$$

$$\mathcal{X}_2 = \{[x^T \; u^T]^T | F_1^x x + F_1^u < f_1, F_2^x x + F_2^u < f_2\}, \tag{11.56}$$

$$\mathcal{X}_3 = \{[x^T \; u^T]^T | F_1^x x + F_1^u < f_1, F_2^x x + F_2^u \ge f_2\}, \tag{11.57}$$

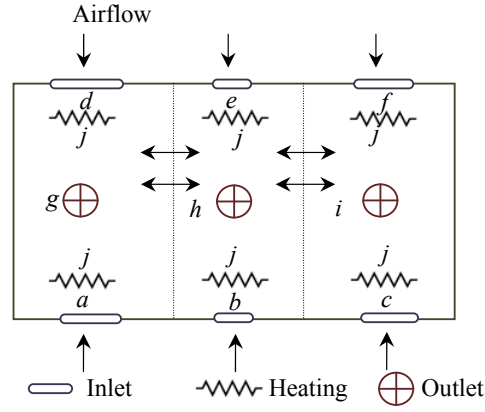$$\mathcal{X}_4 = \{[x^T \; u^T]^T | F_1^x x + F_1^u \ge f_1, F_2^x x + F_2^u < f_2\}, \tag{11.58}$$

Figure 11.2: The top view of the test stable

where

$$F_1^x = \begin{bmatrix} 1.0817 & -0.0457 & -0.9938 \end{bmatrix}$$
$$F_2^x = \begin{bmatrix} -1.1144 & 0.0490 & 1.0187 \end{bmatrix}$$
$$F_1^u = \begin{bmatrix} 0.2323 & -0.0072 & 0.2323 & 0.2323 & -0.0072 \\ 0.2323 & -0.072 & 0.1349 & -0.0719 & -0.0064 \end{bmatrix},$$
$$F_2^u = \begin{bmatrix} -0.2558 & 0.0074 & -0.2558 & -0.2558 & 0.0074 \\ -0.2558 & 0.0742 & -0.12 & 0.0742 & 0.0074 \end{bmatrix},$$
$$f_1 = 0.4058, f_2 = -0.4575 \tag{11.59}$$

The discrete-time PWA model is described by:

$$A_1 = \begin{bmatrix} 1.6361 & 0.0480 & -0.7716 \\ 1.5782 & 0.5522 & -0.9983 \\ 0.7747 & 0.0462 & 0.0990 \end{bmatrix}, \tag{11.60}$$

$$A_2 = \begin{bmatrix} 1.1145 & -0.0300 & -1.0590 \\ 1.6452 & 0.1010 & -1.4342 \\ 0.3008 & 0.0191 & -0.2324 \end{bmatrix}, \tag{11.61}$$

$$A_3 = \begin{bmatrix} 1.6340 & 0.0259 & -0.7150 \\ 1.5474 & 0.8335 & -1.4790 \\ 0.7674 & 0.0314 & 0.1456 \end{bmatrix}, \tag{11.62}$$

$$A_4 = \begin{bmatrix} 1.6274 & 0.0049 & -0.6987 \\ 1.6242 & 0.8163 & -1.4751 \\ 0.7623 & 0.0051 & 0.1640 \end{bmatrix}, \tag{11.63}$$

$$
B_1 = \begin{bmatrix}
-0.1163 & 0.0459 & -0.1163 & -0.1163 & 0.0459 \\
0.5718 & -0.3768 & 0.5718 & 0.5718 & -0.3768 \\
-0.1147 & 0.0353 & -0.1147 & -0.1147 & 0.0353
\end{bmatrix}
$$

$$
\left. \begin{matrix}
-0.1163 & 0.0018 & -0.0567 & 0.0018 & 0.0070 \\
0.5718 & -0.1518 & 0.2724 & -0.1518 & -0.0056 \\
-0.1147 & 0.0022 & -0.0553 & 0.0022 & 0.0071
\end{matrix} \right], \qquad (11.64)
$$

$$
B_2 = \begin{bmatrix}
0.1137 & -0.0044 & 0.1137 & 0.1137 & -0.0044 \\
-0.0104 & 0.1057 & -0.0104 & -0.0104 & 0.1057 \\
0.0581 & 0.0258 & 0.0581 & 0.0581 & 0.0258
\end{bmatrix}
$$

$$
\left. \begin{matrix}
0.1137 & -0.0697 & 0.2883 & -0.0697 & 0.0023 \\
-0.0104 & 0.0183 & 0.8276 & 0.0183 & 0.1275 \\
0.0581 & 0.0097 & 0.0939 & 0.0097 & 0.0273
\end{matrix} \right], \qquad (11.65)
$$

$$
B_3 = \begin{bmatrix}
-0.0677 & -0.0127 & -0.0677 & -0.0677 & -0.0127 \\
0.2031 & 0.0778 & 0.2031 & 0.2031 & 0.0778 \\
-0.0697 & -0.0188 & -0.0697 & -0.0697 & -0.0188
\end{bmatrix}
$$

$$
\left. \begin{matrix}
-0.0677 & -0.0103 & -0.0080 & -0.0103 & 0.0078 \\
0.2031 & -0.0594 & -0.0506 & -0.0594 & -0.0012 \\
-0.0697 & -0.0098 & -0.0087 & -0.0098 & 0.0075
\end{matrix} \right], \qquad (11.66)
$$

$$
B_4 = \begin{bmatrix}
-0.0393 & -0.0380 & -0.0393 & -0.0393 & -0.0380 \\
0.0851 & 0.1683 & 0.0851 & 0.0851 & 0.1683 \\
-0.0414 & -0.0434 & -0.0414 & -0.0414 & -0.0434
\end{bmatrix}
$$

$$
\left. \begin{matrix}
-0.0393 & -0.0133 & -0.0234 & -0.0133 & 0.0086 \\
0.0851 & -0.0568 & 0.0160 & -0.0568 & 0.0029 \\
-0.0414 & -0.0130 & -0.0241 & -0.0130 & 0.0085
\end{matrix} \right], \qquad (11.67)
$$

$$
b_1 = \begin{bmatrix} 0.4749 \\ -0.9236 \\ 0.4214 \end{bmatrix}, \; b_2 = \begin{bmatrix} -0.0676 \\ 2.2442 \\ 0.3784 \end{bmatrix}, \qquad (11.68)
$$

$$
b_3 = \begin{bmatrix} 0.2356 \\ 0.3694 \\ 0.2500 \end{bmatrix}, \; b_4 = \begin{bmatrix} 0.3510 \\ -0.5021 \\ 0.3682 \end{bmatrix}. \qquad (11.69)
$$

Here, the PFTC objective is to tolerate actuator faults. The climate control system contains 10 actuators, 6 inlets, 3 fans and a heating system. Each of inlets consists of 6 or 12 connected inlets. In order to show the performance of the PFTC, 3 of the 6 inlets and 1 of the 3 fans are assumed to be faulty with 95% efficiency loss. $x(0) = 20°C$ and the aim is to regulate the temperature of each zone around $10°C$. The PFTC based on Theorem 3 is designed for temperature regulation while the control inputs due to the physical restrictions are bounded. Here $\mathscr{I}_0 = 1$ and $\mathscr{I}_1 = 2, 3, 4$. The LMIs problem is solved with YALMIP/SeDuMi solver. The linear controller and common Lyapunov function are obtained as:

$$\bar{K} = \begin{bmatrix} -0.0520 & -0.0058 & 0.0558 & 0.0000 & 0.0001 & 0.0000 \\ -0.0082 & -0.0029 & 0.0106 & 0.0000 & 0.0001 & 0.0000 \\ -0.0520 & -0.0058 & 0.0559 & 0.0000 & 0.0001 & 0.0000 \\ -0.2620 & -0.0256 & 0.3088 & 0.0030 & 0.0030 & -0.0051 \\ -0.0493 & 0.0040 & 0.0038 & -0.0011 & 0.0038 & -0.0032 \\ -0.1817 & -0.0248 & 0.2241 & -0.0066 & 0.0033 & 0.0042 \\ 4.4924 & 0.1510 & -4.2053 & -0.0287 & -0.0443 & -0.0264 \\ 1.8256 & 0.2009 & -2.0118 & -0.0048 & -0.0027 & -0.0044 \\ 0.0202 & 0.0023 & -0.0207 & -0.0000 & -0.0000 & -0.0000 \\ -3.8247 & -0.3018 & 0.3386 & 0.0454 & 0.1155 & 0.0499 \end{bmatrix}.$$

$$(11.70)$$

$$\bar{P} = \begin{bmatrix} 0.1534 & -0.0006 & -0.1480 & -0.0001 & -0.0002 & 0.0001 \\ -0.0006 & 0.0007 & -0.0003 & -0.0000 & -0.0000 & -0.0000 \\ -0.1480 & -0.0003 & 0.1461 & 0.0001 & 0.0002 & -0.0001 \\ -0.0001 & -0.0000 & 0.0001 & 0.0000 & 0.0000 & -0.0000 \\ -0.0002 & -0.0000 & 0.0002 & 0.0000 & 0.0000 & 0.0000 \\ 0.0001 & -0.0000 & -0.0001 & -0.0000 & 0.0000 & 0.0000 \end{bmatrix}.$$

$$(11.71)$$

Fig. 11.3 shows the temperature of each zone, the fault tolerant controller is able to track the reference signal after $1500\ s$ when there is no fault in the system. 3 of 6 inlets and 1 of 3 fans lose 95% of their efficiency at time 900 second. Fig. 11.4 shows that the controller with a small oscillation is still able to track precisely the reference signal after $2000\ s$. The bounded control signal for the faulty system is illustrated in Fig. 11.5. Due to the physical limitation the control inputs can not exceed a boundary. The boundary is assumed as follows; angle of the inlets is $-1 \leq \mathfrak{a}_{inlet} \leq 1$, voltage of the fan is
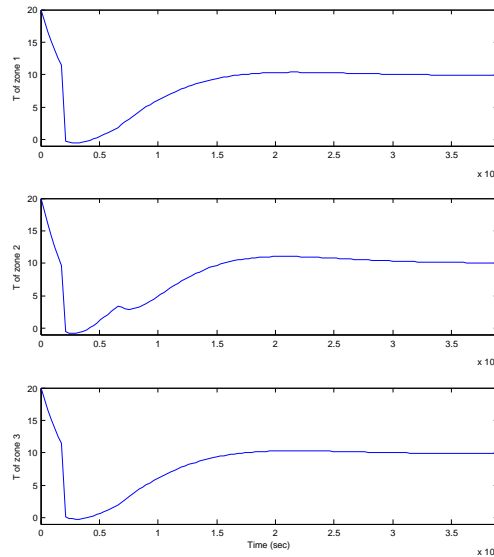

Figure 11.3: Simulation results with a controller designed to tolerate 95% actuator failure for the fault-free system
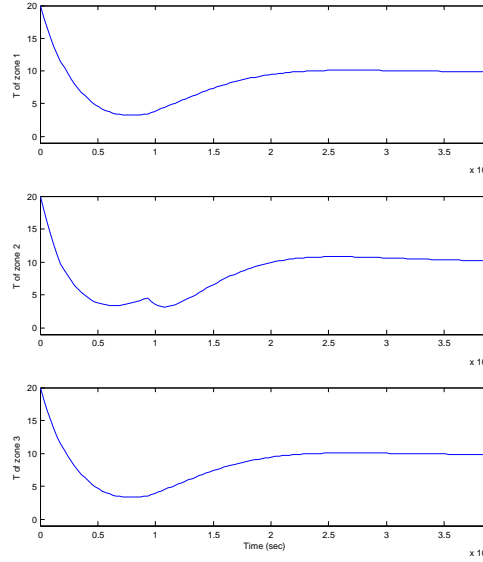
Figure 11.4: Simulation results with a controller designed to tolerate 95% actuator failure for the faulty system

$-10 \leq V_{fan} \leq 10$, and temperature of heating system is $-50 \leq T_{heating} \leq 50$. The illustration confirms that these restrictions on the input do not degrade the performance of the system. Fig. 11.6 shows the control input of the system when the physical constraints are not considered at the PFTC problem. The illustration shows that the value of the inputs growth substantially when a fault happen in the system, this value of the inputs are not acceptable in the practical systems.

6   Conclusion and Future Works

In the paper, a passive fault tolerant controller is proposed to deal with actuator loss for a discrete-time PWA model of a piecewise nonlinear system. The PWA model switches not only due to the state but also due to the control input. By using a common Lyapunov function for stability analysis, a state feedback controller is design such that the closed-loop system is able to track the reference signal in healthy situation as well as in the faulty case. In many industrial systems, the control inputs can not take any value and they should be less than a threshold. Here, the input limitations are also integrated in the control design. The results show that the closed-loop system with a PFTC scheme tracks the reference signal precisely while the actuators are subject to 95% efficiency loss.
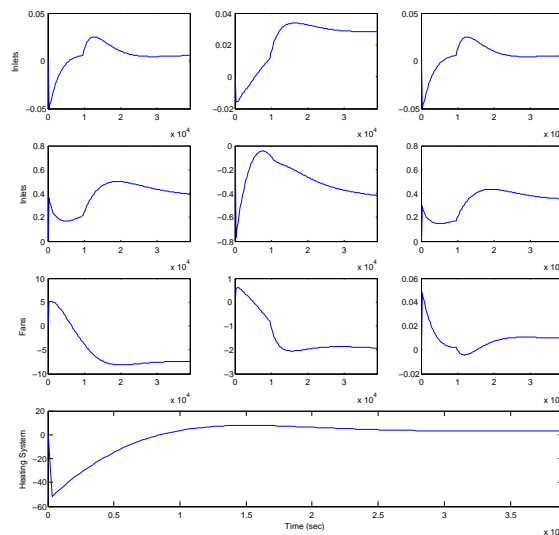
7   Acknowledgments

Figure 11.5: Angle of the inlets, voltages of the fans and temperature of the heating system. The inlet 1 to 3 and fan 3 lose 95% of their efficiency

References

[1] Y. Zhang and J. Jiang, "Bibliographical review on reconfigurable fault-tolerant control systems," *Annual Reviews in Control*, vol. 32, no. 2, pp. 229–252, 2008.

[2] M. Blanke, M. Kinnaert, J. Lunze, and M. Staroswiecki, *Diagnosis and Fault-Tolerant Control*. Springer-Verlag, 2006.

[3] J. Chen, R. Patton, and Z. Chen, "An linear matrix inequality (lmi) approach to fault-tolerant control of uncertain systems," in *Intelligent Control (ISIC), 1998. Held jointly with IEEE International Symposium on Computational Intelligence in Robotics and Automation (CIRA), Intelligent Systems and Semiotics (ISAS), Proceedings of Intelligent Control (ISIC)*, Sept. 1998, pp. 175 –180.

[4] Z. Qu, C. Ihlefeld, J. Yufang, and A. Saengdeejing, "Robust control of a class of nonlinear uncertain systems. fault tolerance against sensor failures and subsequent self recovery," in *Decision and Control, 2001. Proceedings of Decision and Control, the 40th IEEE Conference*, vol. 2, 2001, pp. 1472 –1478.

[5] Z. Qu, C. M. Ihlefeld, Y. Jin, and A. Saengdeejing, "Robust fault-tolerant self-recovering control of nonlinear uncertain systems," *Automatica*, vol. 39, no. 10, pp. 1763 – 1771, 2003.

[6] L. Rodrigues and E.-K. Boukas, "Piecewise linear h_∞ controller synthesis with application to inventory control of switched production systems," *Automatica*, vol. 42, pp. 1245–1254, 2006.
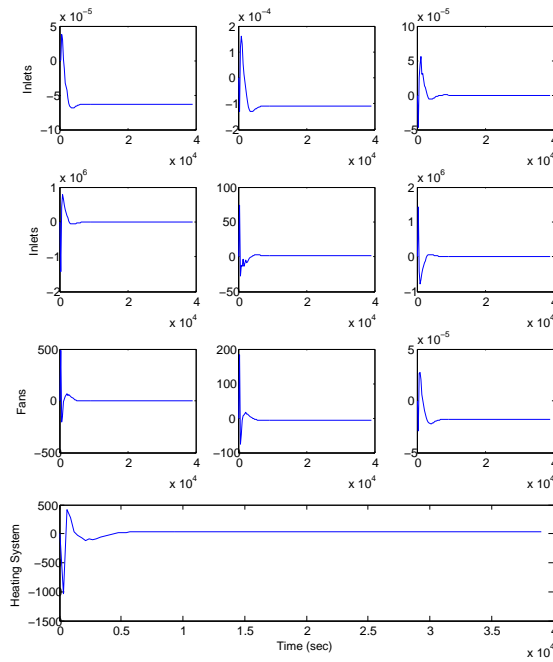
Figure 11.6: Angle of the inlets, voltages of the fans and temperature of the heating system. The inlet 1 to 3 and fan 3 lose 95% of their efficiency. Here, no input constraints are considered in the PFTC problem

[7] B. Samadi and L. Rodrigues, "Stability of sampled-data piecewise affine systems: A time-delay approach," *Automatica*, vol. 45, no. 9, pp. 1995–2001, 2009.

[8] M. Rodrigues, D. Theilliol, and D. Sauter, "Fault tolerant control design for switched systems," in *2nd IFAC Conference on Analysis and design of hybrid systems, Alghero Sardinia, Italy*, 2006, 10.3182/20060607-3-IT-3902.00041.

[9] H. Yang, B. Jiang, and V. Cocquempot, "A fault tolerant control framework for periodic switched non-linear systems," *International Journal of Control*, vol. 82, no. 1, pp. 117–129, 2009.

[10] J. H. Richter, W. Heemels, N. van de Wouw, and J. Lunze, "Reconfigurable control of piecewise affine systems with actuator and sensor faults: stability and tracking1," Institute of Automation and Computer Control, Ruhr-Universität Bochum, Tech. Rep., 2010.

[11] R. Wang, M. Liu, and J. Zhao, "Reliable H_∞ control for a class of switched non-linear systems with actuator failures," *Nonlinear Analysis: Hybrid Systems*, vol. 1, no. 3, pp. 317–325, 2007.

[12] M. Rodrigues, D. Theilliol, S. Aberkane, and D. Sauter, "Fault tolerant control design for polytopic LPV systems," *International Journal of Applied Mathematics and Computer Science*, vol. 17, no. 1, pp. 27–37, 2007.

[13] N. Nayebpanah, L. Rodrigues, and Y. Zhang, "Fault-tolerant controller synthesis for piecewise-affine systems," in *Proceedings of the IEEE American Control Conference*, 2009, pp. 222–226.

[14] S. Tabatabaeipour, R. Izadi-Zamanabadi, T. Bak, and A. P. Ravn, "Passive fault-tolerant control of piecewise linear systems against actuator faults," *submitted to International Journal of Systems Science*, 2010.

[15] M. Gholami, V. Cocquempot, H. Schiler, and T. Bak, "Passive fault tolerant control of piecewise affine systems based on h infinity synthesis," in *Submitted to IFAC 18th World Congress*, 2011.

[16] J. Löfberg, "YALMIP : A toolbox for modeling and optimization in MATLAB," in *Proceedings of the IEEE Conference on Computer Aided Control Systems Design*, 2004, pp. 284–289.

[17] M. Johansson, *Piecewise linear control systems*. Springer-Verlag, 2003.

[18] F. Cuzzola and M. Morari, "A generalized approach for analysis and control of discrete-time piecewise affine and hybrid systems," *Hybrid Systems: Computation and Control*, vol. 2034, pp. 189–203, 2001.

[19] I. R. Petersen, "A stabilization algorithm for a class of uncertain linear systems," *System and Control Letters*, vol. 8, no. 4, pp. 351–357, 1987.

[20] S. Boyd, L. E. Ghaoui, E. Feron, and V. Balakrishnan, *Linear Matrix Inequalities in System and Control Theory*. Society for Industrial Mathematics, 1994.